AD-777 496

PREDICTION OF GEAR-MESH-INDUCED HIGH-
FREQUENCY VIBRATION SPECTRA IN GEARED
POWER TRAINS

Alston L. Gu, et al
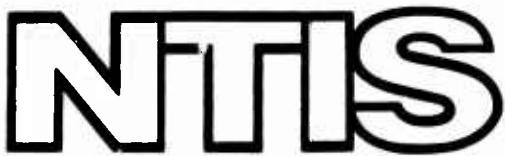
Mechanical Technology, Incorporated

Prepared for:

Army Air Mobility Research and Development
Laboratory

January 1974

AD 777496

DOCUMENT CONTROL DATA - R & D		
(Security classification of title, body of abstract and indexing annotation must be entered when the overall report is classified)		
1. ORIGINATING ACTIVITY *(Corporate author)* Mechanical Technology Incorporated 968 Albany-Shaker Road Latham, New York 12110	2a. REPORT SECURITY CLASSIFICATION Unclassified	
	2b. GROUP	

3. REPORT TITLE

PREDICTION OF GEAR-MESH-INDUCED HIGH-FREQUENCY
VIBRATION SPECTRA IN GEARED POWER TRAINS

4. DESCRIPTIVE NOTES *(Type of report and inclusive dates)*
Technical Report

5. AUTHOR(S) *(First name, middle initial, last name)*

Alston L. Gu
Robert H. Badgley

6. REPORT DATE January 1974	7a. TOTAL NO. OF PAGES 92	7b. NO. OF REFS 13
8a. CONTRACT OR GRANT NO. DAAJ02-72-C-0040 b. PROJECT NO. 1G162207AA72 c. d.	9a. ORIGINATOR'S REPORT NUMBER(S) USAAMRDL Technical Report 74-5 9b. OTHER REPORT NO(S) *(Any other numbers that may be assigned this report)* MTI Report 73TR28	

10. DISTRIBUTION STATEMENT

Approved for public release; distribution unlimited.

11. SUPPLEMENTARY NOTES	12. SPONSORING MILITARY ACTIVITY Eustis Directorate U.S. Army Air Mobility Research and Development Laboratory, Fort Eustis, Va.

13. ABSTRACT Characteristics of vibration spectra induced by gear meshes in both single gear reductions and planetary gear reductions have been investigated. Methods have been developed to analyze the planet-pass induced vibrations which exist in normal planetary gear reduction systems. It is found that the planet-pass vibration sideband frequencies occur both below and above the base signal at integer multiples of planet-pass frequency and that the sideband amplitudes may exceed that of the base signal. The effect of planet pair phasing on the vibration sideband spectra has been determined for the CH-47 helicopter forward rotor drive transmission first-stage planetary reduction. A computer-implemented analysis has been established for predicting vibration sidebands produced by variations in centerline distance, tooth transmitted force, and tooth support discontinuities for single gear mesh systems. The sidebands are normally found at mesh frequency harmonics plus and minus integer multiples of the frequency of variation of the gear parameters. The sideband amplitudes depend on the magnitude of variation of the gear parameters. The vibration sideband spectra produced by spiral bevel gear shaft runout, externally-imposed tooth mesh force variation, and a decrease in support stiffness over a number of consecutive ring gear teeth have been obtained for gear meshes in the CH-47 helicopter forward rotor drive transmission. The sideband analysis is useful both for designing low-vibration gear systems by properly controlling various gear parameters, and for identifying the existence of several types of gear problems such as gear runout, high dynamic tooth force, and tooth cracks.

DD FORM 1473 REPLACES DD FORM 1473, 1 JAN 64, WHICH IS OBSOLETE FOR ARMY USE.

14. KEY WORDS	LINK A		LINK B		LINK C	
	ROLE	WT	ROLE	WT	ROLE	WT
GEAR-MESH-INDUCED VIBRATIONS						
PLANET-PASS EXCITATION IN REDUCTION GEARS						
VIBRATION SPECTRA OF GEAR SYSTEMS						
DESIGN OF GEAR SYSTEMS						
DIAGNOSIS OF GEAR SYSTEMS						

The research described herein was conducted by Mechanical Technology Incorporated under the terms of Contract DAAJ02-72-C-0040. The work was performed under the technical management of Mr. Leroy T. Burrows, Technology Applications Division, Eustis Directorate.

During the past decade, vibration and noise measurements and data reduction procedures have improved to the point where it can be (and has been) clearly shown that noise and vibration are directly relatable to each other. Moreover, many noise components have been shown to be directly relatable to the gear mesh frequencies in such drive trains, and analytical methods have been formulated to help understand and control them. These methods deal with the mechanical vibrations of the gearbox components. Other significant signals that are present, however, are not directly relatable to the mesh frequencies. Some of these signals, called "sidebands", have been found to occur in tests of helicopter rotor-drive gearboxes.

The major aims of this study were as follows:

1. Using existing measured and calculated CH-47 ring gear acceleration data together with sideband amplitude prediction methods presently under development, the contractor was (a) to investigate CH-47 lower planetary mesh planet-pass sideband amplitudes for several lower planet-to-ring gear mesh relationships in order to determine sensitivity of sidebands to planet phasing, (b) to identify other design parameters expected to be useful in controlling planet-pass sidebands and describe their effects and importance, and (c) to draw conclusions concerning mechanisms producing planet-pass sidebands.

2. The computer program entitled GEARO, which is in the possession of the contractor and the Government, was to be modified and extended.

Appropriate technical personnel of this directorate have reviewed this report and concur with the conclusions contained herein.

ib

PREDICTION OF GEAR-MESH-INDUCED HIGH-FREQUENCY VIBRATION SPECTRA IN GEARED POWER TRAINS

MTI Report 73TR28

By

Alston L. Gu
Robert H. Badgley

Prepared by

Mechanical Technology Incorporated
Latham, New York

for

EUSTIS DIRECTORATE
U.S. ARMY AIR MOBILITY RESEARCH AND DEVELOPMENT LABORATORY
FORT EUSTIS, VIRGINIA

SUMMARY

Users of geared power trains have begun to recognize the importance of the
high-frequency vibrations which are present in virtually all operating gear-
boxes: these vibrations are the key to understanding the gearbox condition
in real time, a problem of considerable current importance. An immediate
outward indication of the presence of such vibrations is the noise produced
by a gearbox. Even the untrained ear can distinguish the presence of
signals which arise in the gearbox. (Sensors are of course required to
obtain information of the quality required for engineering purposes.)

During the past decade, vibration and noise measurements and data reduction
procedures have improved to the point where it can be (and has been) clearly
shown that noise and vibration are directly relatable to each other. More-
over, many noise components have been shown to be directly relatable to the
gear mesh frequencies in such drive trains, and analytical methods have been
formulated to help understand and control them. These methods deal with the
mechanical vibrations of the gearbox components.

Other significant signals which are present, however, are not directly re-
latable to the mesh frequencies. Some of these signals, called "sidebands",
have been found to occur in tests of helicopter rotor-drive gearboxes. As
originally conceived, this investigation had the rather limited objective
of providing the designer of geared power trains with an analytical tool
which could be used to predict, and thus control, the frequencies and
amplitudes at which vibration sidebands are produced by operating gearboxes.
As the work progressed, however, it became apparent that the analyses and
associated understanding could also have a significant and far-reaching
impact on the more general problem of on-line monitoring. It is important,
therefore, that the results of this study be viewed in the context of their
potential impact on this technology area, as well as upon the area of gear-
box noise reduction.

The major aims of this study were as follows:

1. Development of an engineering understanding of, and methods for
    predicting, geometrically-induced planet-pass vibration sidebands
    which accompany normal planetary gear reduction operation; and

2. Development of an engineering understanding of, and new analytical
    methods for treating, the vibration sidebands which are produced
    by undesirable gear characteristics, such as tooth support dis-
    continuities (cracks), gear runout, and variations in tooth
    transmitted forces.

These objectives have been achieved. Sidebands as a second major category
of geared drive train vibration signals can now be described and discussed
directly in terms of hardware condition. An engineering understanding of
the mechanisms which cause many of the kinds of vibrations produced by
gear meshes thus exists.

The payoffs from such an understanding can be enormous. First, gear train

designers now have important vibration analysis tools for minimizing, at the time of design, the disturbances produced by gear meshes. This will not only make gear trains quieter, but will also reduce their internal forces, with significant improvements in lifetimes of all components.

Second, when properly exploited by joint technologist/manufacturer teams, the high-frequency vibration analysis tools will permit real-time condition monitoring to be approached on an individual signal component basis in which the precise meaning of each component is well understood, rather than on the multiple component basis associated with usual signature analysis techniques. The engineering application of the vibration analysis tools permits specific signal components to be explained on a detailed basis. This removes the uncertainty associated with the use of signal level ratio techniques and the need for lengthy test-bed study programs involving failure implants.

Extension of the gear mesh analysis techniques to high-contact-ratio gearing is now in order, as is an extension of the torsional response analysis to coupled torsional-lateral-axial vibrations.

FOREWORD

Dr. Robert H. Badgley of Mechanical Technology Incorporated served as Program Manager for the efforts reported herein. The contract was carried out under the technical cognizance of Mr. R. Burrows, Eustis Directorate, U. S. Army Air Mobility Research and Development Laboratory, Fort Eustis, Virginia.

Special credit is due to Mrs. L. Cziglenyi of MTI, who programmed the computer program modifications and who conducted the calculations.

TABLE OF CONTENTS

LIST OF ILLUSTRATIONS

x

LIST OF TABLES

INTRODUCTION

Geared power train vibrations can occur at many different frequencies. The most common of these vibrations may be found at the mesh frequencies, and their integer multiples, of particular gear meshes in the train. These are known to be caused by the mesh properties of the gear teeth. Less well understood are vibrations which occur at the foregoing frequencies plus and minus integer multiples of other frequencies. Such components are called sidebands. While methods had been developed for predicting the levels of the vibration components at the mesh frequency and its integer multiples [1 through 7],* these methods were not capable of treating the sideband components. Unfortunately, high acoustic noise levels can be produced by both types of components.

In addition, there is increasing recognition of the fact that vibrations which produce noise also carry information about the dynamic behavior of the drive train [8 through 11], in effect, information from which the condition of the drive train components may be inferred. Such vibrations are known to be present in virtually all geared systems, and they have been recorded and monitored for diagnostic purposes for many years by many people. However, a detailed engineering understanding of the meanings of the shapes and amplitudes of the measured spectra has not proceeded in company with the development of methods for sensing and displaying these spectra.

Sidebands are produced during normal operation of gearboxes which employ planetary reductions. Such sidebands normally occur at the planetary mesh frequency plus and minus the planet-pass frequency. (They may also be similarly distributed about twice mesh frequency, three times mesh frequency, etc.) It must be stressed that their presence is due simply to the kinematics of the planetary reduction, wherein the planets physically pass any stationary point. The presence of each planet in turn changes the vibration properties of the gearbox structure, both from an impedance viewpoint and also more importantly from the amount of excitation applied to the structure by the moving mesh. This change is periodic at planet-pass frequency.

Sidebands are also produced during normal operation of gearboxes with gear meshes at more than one frequency. These sidebands are normally found at one mesh frequency plus and minus integer multiples of the other mesh frequencies (and of course at other frequency combinations as mentioned above). Such sidebands are caused primarily by the dynamic properties of the drive train components (i.e., coupled torsional-lateral-axial vibrations), which permit dynamic tooth force variations to occur in one mesh at frequencies of other meshes.

Other sources of sidebands do, of course, exist, but these are for the most part associated with the presence of undesirable component behavior. Perhaps the best-known sideband source is that due to runout of a gear because of machining or assembly inaccuracies. This type of sideband, which the

---

*Numbers in brackets refer to literature cited at the end of this report.

1

analysis described herein can predict, is typically found at mesh frequency plus and minus shaft rotation frequency. It can be produced by runout not only of pinion or gear in a simple mesh, but also of a planet gear relative to its bearings on a planet carrier.

Other undesirable effects can also produce sidebands. For instance, variation of tooth support stiffness around the circumference of a gear can alter the mesh properties in a manner which repeats at gear running speed, and which can have many forms depending on the circumferential distribution of the stiffness variation. A typical cause of such sidebands would be a cracked gear web, which the analysis described herein can treat.

DESCRIPTION OF PROGRAM

In this study, the characteristics of vibration sidebands produced by gear meshes in both single gear meshes and planetary gear reductions were investigated. The study was conducted in two tasks, the details of which are described below.

During the course of earlier test efforts, it became obvious that gearbox vibration and noise signal components were being produced at frequencies which corresponded to those at which various sideband signals were expected. It was recognized that these signals would have to be explained analytically before they could be dealt with properly. Hence the decision was made to treat the signals at their sources, i.e., the gear mesh itself.

Since earlier analytical efforts had yielded a computer-implemented analysis for predicting the vibration excitation properties of normal gear meshes, the decision was made to upgrade this computer program to incorporate the new analyses. The upgraded computer program was modularized so as to permit future inclusion of other gear types and effects. A schematic diagram of the computer program's capabilities is presented and discussed later in the report (as Figure 11). The analyses described herein have been included in this program.

TASK I — INVESTIGATION OF PLANETARY MESH PLANET-PASS SIDEBANDS

As a result of earlier studies, predicted dynamic behavior of the CH-47 forward rotor drive gearbox ring gear was available. This predicted data was used to study the complex vibrations existing at a preselected point on the ring gear (corresponding to a location where measured data had been taken).

These studies produced radial vibration levels versus time, and corresponding vibration spectra, for various planet phasing relationships in the lower stage planetary reduction. Planet phasing is under the control of the gear designer, and thus it can be altered to modify and thus reduce mesh frequency vibration sidebands.

TASK II — ANALYSIS OF GEAR-MESH-INDUCED HIGH-FREQUENCY VIBRATION SPECTRA AND CALCULATIONS

This phase of the study treated both the spiral bevel and lower stage planetary planet-to-ring gear meshes. Spiral bevel gear shaft runout and externally-imposed tooth mesh force variations were studied, and gear mesh excitation spectra produced by these effects were predicted.

In the case of the planet-to-ring mesh, planet runout and externally-imposed tooth mesh force variations were considered, and excitation spectra caused by these effects were predicted. In addition, the mesh excitation spectrum resulting from the condition where a number of consecutive ring gear teeth have relatively soft support stiffness (such as could be caused by a local crack) was predicted.

INVESTIGATION OF PLANETARY MESH PLANET-PASS SIDEBANDS

ANALYSIS OF PLANET-PASS INDUCED VIBRATION

A schematic of the planetary gear system to be analyzed is shown in Figure 1. The ring gear is stationary and the sun gear rotates with speed ω_s. The four planets rotate about their own centers with a speed of ω_o (relative to the planet carrier), and the planet carrier rotates with speed ω_b (planet orbiting speed). Depending on the numbers of teeth on the component gears, the four planets are, in general, not equally spaced. In the particular case considered herein, δ is the angular offset of the pair (C,D) with respect to the pair (A,B).

In this analysis the ring gear is considered as an elastic shell-type structure. At a given location, the ring gear experiences a dynamic tooth mesh force each time a planet passes. This mesh force is associated with the tooth mesh frequency resulting from the transfer of load from one pair of teeth to the other. In this calculation, it is assumed that the dynamic tooth mesh force has a rectangular pulse form whose magnitude varies sinusoidally with the mesh frequency (see below). This oscillating force produces an oscillating deformation. It is this planet-pass induced vibration of the ring gear that is treated in this analysis.

In a coordinate frame fixed with the planet carrier, both sun and ring gears rotate as shown in the upper diagram of Figure 2. The sun gear rotates with a speed of $\omega_s - \omega_b$, while the ring gear moves in the opposite direction with the planet orbiting speed ω_b. In this reference frame, the forces acting on the ring gear due to the planet-ring gear meshes occur at fixed angular locations of $\theta = 0$, $\pi/2 - \delta$, π, $3\pi/(2) - \delta$, corresponding to the locations of planets A, D, B and C respectively.

Since planets A and B are in phase, the dynamic force per unit area due to gear meshes at these two locations can be approximately expressed as

$$F_{AB}(\theta,t) = P_{AB}(\theta) \cos f_M t \tag{1}$$

where t is the time, P_{AB} the normal pressure due to normal tooth mesh forces, and f_M the tooth mesh frequency defined by

$$f_M = \omega_o N_p = \omega_b N_r \tag{2}$$

In the above, N_p and N_r are the numbers of teeth on the planet and ring gear respectively. It may be assumed that P consists of two identical rectangular pulses occurring at the locations of planets A and B, and that the width of each pulse is one tooth spacing, as shown in the lower diagram of Figure 2. The magnitude of the rectangular pulse P_o is related to common gear parameters as follows:

4
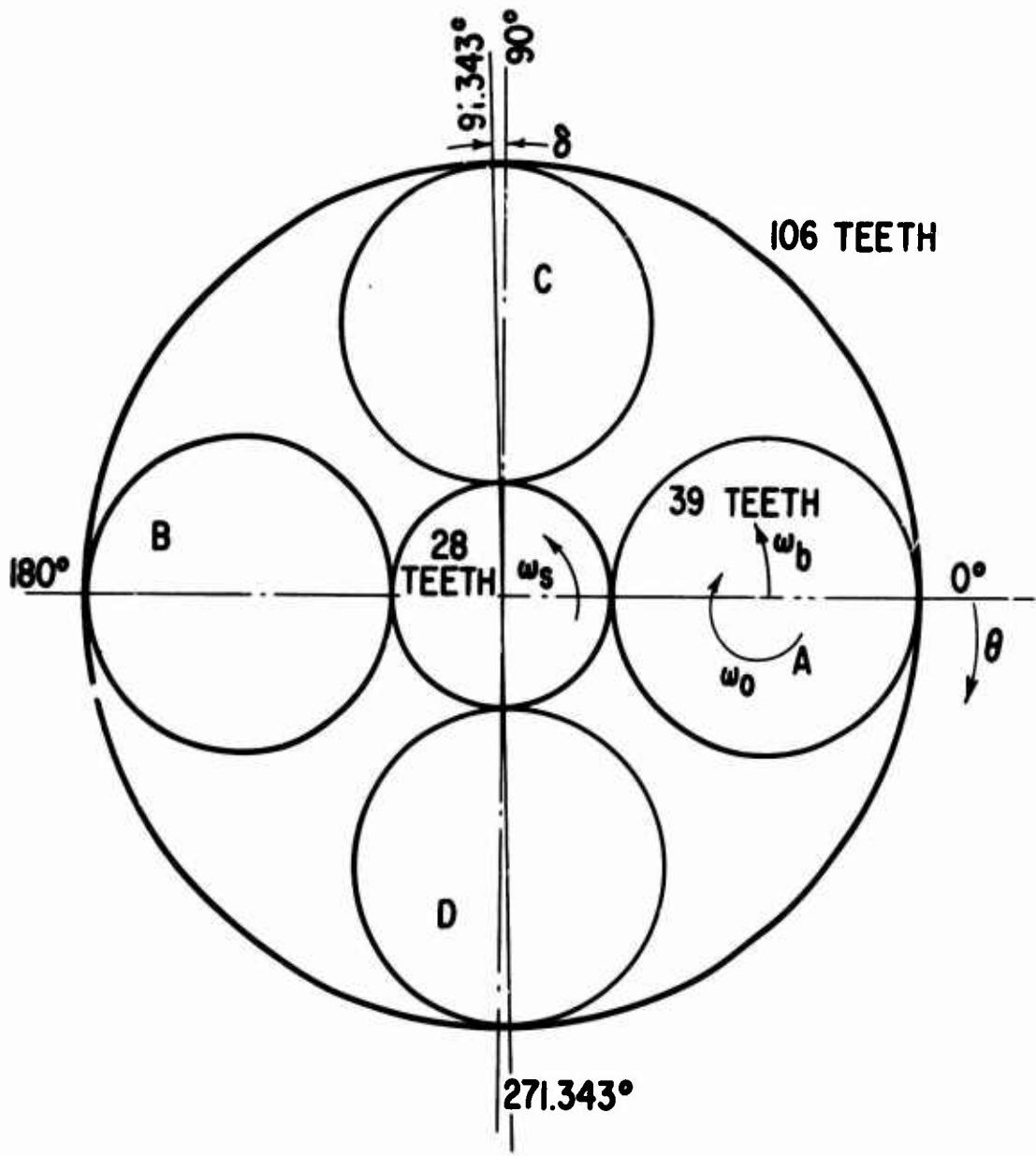
Figure 1. CH-47 Forward Rotor-Drive Gearbox
Lower Planetary Gear System.

5
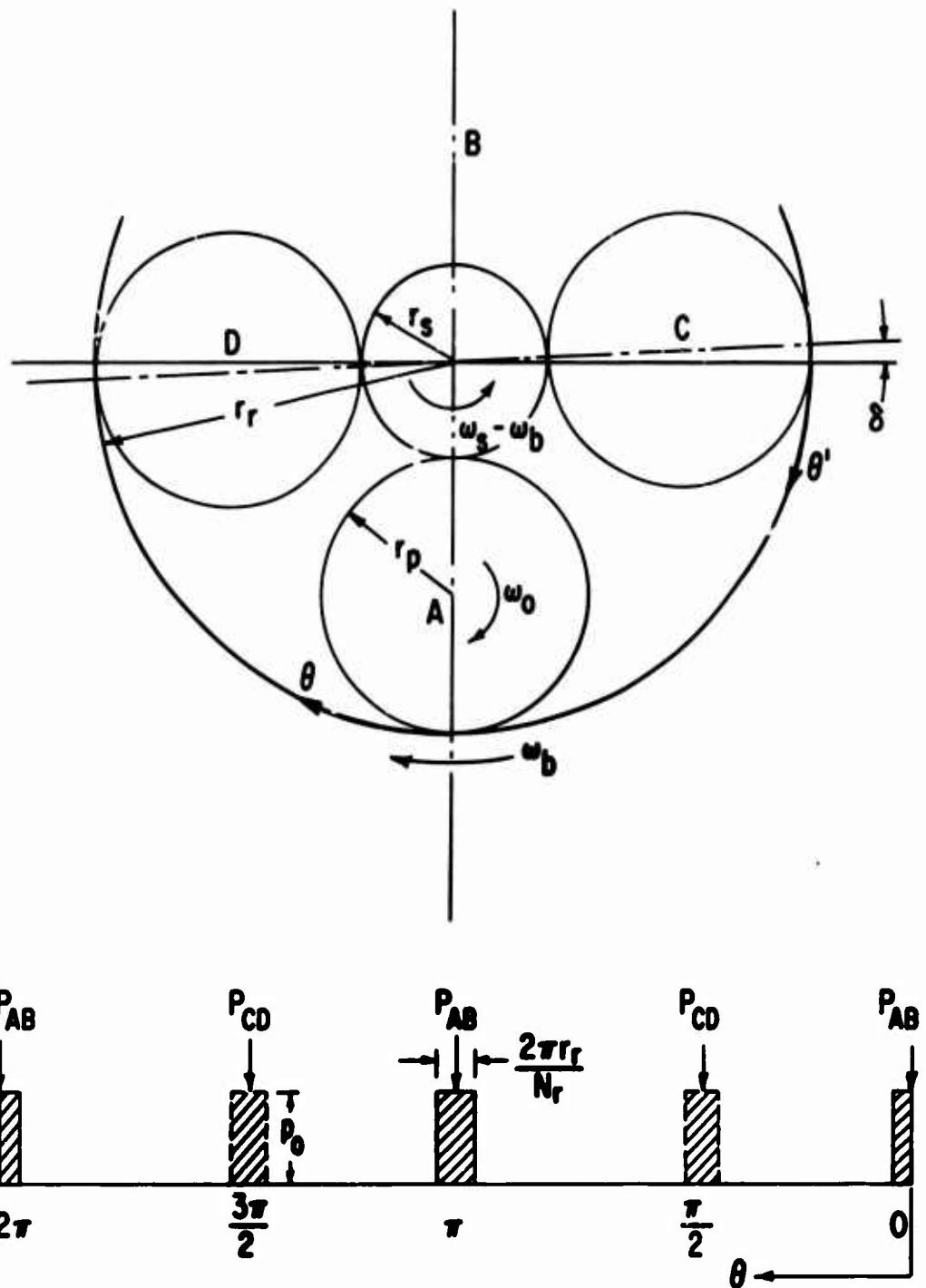
Figure 2. Gear System in a Planet-Fixed Frame and
Corresponding Force Diagram.

$$P_o = \frac{F_t \tan \emptyset}{\frac{2\pi r_r}{N_r} L} \tag{3}$$

where F_t is the tangential tooth force, $\emptyset$ the pressure angle, r_r the pitch radius of ring gear, and L the tooth face width.

As a result of the angular offset δ, there exists a temporal phase difference between the dynamic forces at planets C and D and those at A and B. Since rotation of the sun gear over one tooth spacing corresponds to one full cycle in gear meshing, it can be shown that the temporal phase lag of the tooth meshes of planets C and D relative to those of A and B is

$$\Psi = \delta \cdot N_s \tag{4}$$

where N_s is the number of teeth of the sun gear. The dynamic forces at planets C and D can be thus expressed as

$$F_{CD}(\theta, t) = P_{CD}(\theta) \cos(f_M t - \Psi) \tag{5}$$

where P_{CD} is similar to P_{AB} and is shown in the lower diagram of Figure 2.

There exist radial displacement response functions for the ring gear shell due to the dynamic forces F_{AB} and F_{CD}. These response functions depend on the elastic characteristics of the shell-type ring gear structure. Neglecting ring gear inertia (valid for shell-type structures), the response function due to the meshing of planets A and B is in phase with its forcing function F_{AB}. It may in general be written as

$$b_{AB}(\theta, z) \cos f_M t \tag{6}$$

where z is the axial coordinate, designated for the general case that the ring gear shell is nonuniform axially. Similarly, the response function due to the meshing of planets C and D is

$$b_{CD}(\theta, z) \cos(f_M t - \Psi) \tag{7}$$

The total response function for the ring gear shell is the sum of Equations (6) and (7), i.e.,

$$w(\theta, z, t) = b_{AB} \cos f_M t + b_{CD} \cos(f_M t - \Psi) \tag{8}$$

where w represents the dynamic radial response at a location whose coordinates are (θ, z) on the ring gear casing.

7

After some manipulations, Equation (8) becomes

$$w(\theta, z, t) = A(\theta, z) \cos f_M t + B(\theta, z) \sin f_M t \qquad (9)$$

where

$$A(\theta, z) = b_{AB} + b_{CD} \cos \Psi \qquad (10)$$

$$B(\theta, z) = b_{CD} \sin \Psi \qquad (11)$$

If the ring gear is axially symmetric, both b_{AB} and b_{CD} are even functions in θ and have a periodicity of π in θ, and so do the functions $A(\theta, z)$ and $B(\theta, z)$. Therefore, the latter may be expanded in terms of Fourier series, i.e.,

$$A(\theta, z) = \frac{a_o(z)}{2} + \sum_{n=1}^{\infty} a_{2n}(z) \cos 2n\theta \qquad (12)$$

and

$$B(\theta, z) = \frac{b_o(z)}{2} + \sum_{n=1}^{\infty} b_{2n}(z) \cos 2n\theta \qquad (13)$$

Let θ_o be the angular coordinate of a fixed point on the ring gear. Since the ring gear rotates clockwise with speed ω_b (see Figure 2),

$$\theta_o(t) = \theta_i + \omega_b t \qquad (14)$$

where θ_i is the coordinate of the fixed point at $t = 0$. Setting $\theta_i = 0$,

$$\theta_o(t) = \omega_b t \qquad (15)$$

Thus, the fixed point on the ring gear travels clockwise starting from the position of $\theta = 0$ in the frame fixed with the planet carrier.

To calculate the vibration at a fixed point on the ring gear, Equation (15) is substituted for θ into the total response function, Equation (9). This yields

$$w_o(t) = w(\omega_b t, z_o, t) = A(\omega_b t, z_o) \cos f_M t$$
$$+ B(\omega_b t, z_o) \sin f_M t \qquad (16)$$

where z_o is the axial coordinate of the fixed point.

Using the Fourier representations of Equations (12) and (13),

8

$$w_o(t) = \frac{a_o}{2} \cos f_M t + \frac{b_o}{2} \sin f_M t$$

$$+ \frac{1}{2} \sum_{n=1}^{\infty} a_{2n} \left[\cos (f_M + 2n\, \omega_b)\, t + \cos (f_M - 2n\, \omega_b)\, t \right]$$

$$+ \frac{1}{2} \sum_{n=1}^{\infty} b_{2n} \left[\sin (f_M + 2n\, \omega_b)\, t + \sin (f_M - 2n\, \omega_b)\, t \right] \qquad (17)$$

The above equation represents the planet-pass induced vibration amplitude history at a fixed point on the ring gear. At $t = 0$, planet A is at the location of this fixed point; and as time goes on, planets D, B, and C pass the point in sequence.

From Equation (17), the vibration amplitude at gear tooth mesh frequency is

$$M_o = \frac{1}{2} \left(a_o{}^2 + b_o{}^2 \right)^{1/2} \qquad (18)$$

The amplitudes at various sidebands about the mesh frequency are

$$M_n = \frac{1}{2} \left(a_{2n}{}^2 + b_{2n}{}^2 \right)^{1/2} \quad \text{for } n = 1,2,3\ldots \qquad (19)$$

Since there are four planets, the planet-pass frequency is

$$f_p = 4\, \omega_b \qquad (20)$$

The sidebands occur at $f_M \pm n\, \dfrac{f_p}{2}$ with $n = 1,2,3,\ldots$. In the case of zero offset ($\delta = 0$), sidebands would appear only at $f_M \pm n\, f_p$, because the function A and B would have a periodicity of $\pi/2$ instead of π. Physically it means that at the fixed observation point, the pass of planets C and D is identical to that of planets A and B.

Equation (17) gives the amplitude-time relationship of the planet-pass induced vibration as observed at a fixed point on the ring gear. The amplitude-frequency spectrum of the vibration is presented by Equations (18) and (19).

PLANET-PASS INDUCED VIBRATION AND SIDEBAND AMPLITUDE CALCULATIONS

The gear parameters for the CH-47 lower planetary gear system and the operating conditions used in the calculations are as follows:

Number of sun gear teeth $N_s = 28$

Number of planet gear teeth $N_p = 39$

9

Number of ring gear teeth N_r = 106

Pitch radius of sun gear r_s = 2.8 in.

Pitch radius of planet gear r_p = 3.9 in.

Pitch radius of ring gear r_r = 10.6 in.

Pressure angle φ = 25°

Ring gear tooth face width L = 1.25 in.

Angular offset of planets C and D δ = 1.343°

Planet-ring mesh frequency f_M = 1482 Hz

Tangential tooth force at planet-ring mesh = 159.2 lb

The planet orbiting speed ω_b is 14 Hz, and the planet-pass frequency is therefore 56 Hz. Due to the angular offset δ, the temporal phase lag of planets C and D relative to A and B is 37.6 degrees.

The cross section of the ring gear casing, which is considered as the vibrating elastic body, is depicted in Figure 3. In the dynamic response calculation, this ring gear casing is modeled as a composite cylindrical shell with variable thickness (see Figure 3). Both ends of the casing are assumed to be "simply supported," i.e., no linear translation but free to rotate. The MTI general shell dynamic response computer program was used to obtain the response functions b_{AB} (θ,z) and b_{CD} (θ,z) [4].

Let the vibration observation point on the ring gear be located at z_o = 1.5 inches. The response functions at this point for the specified tooth load are plotted in Figure 4. The small angular offset of 1.343° for planets C and D is neglected. It is noted that both b_{AB} and b_{CD} are periodic with a periodicity of 180°. Due to the axial symmetry of the ring-gear casing, b_{AB} and b_{CD} are completely similar but have a phase difference of 90°.

The vibration induced by planet-pass as observed at a fixed point located at z_o = 1.5 inches on the ring gear was calculated by using Equation (17) and is plotted in Figure 5. The first half bump corresponds to the pass of planet A, and the next three bumps correspond to the passes of planets D, B and C, respectively. The pattern repeats itself after one full revolution of all planets. The period is 0.0714 sec, which is the reciprocal of ω_b.

The frequency spectrum of this planet-pass induced vibration is shown in the lower diagram of Figure 6. The amplitude at the mesh frequency has the largest value. However, the amplitude at the second pair of sidebands, at $f_M \pm f_p$, is quite large.

To see the effect of planet phasing on the vibration amplitudes at the selected point, the vibrations produced at three different temporal phase

10
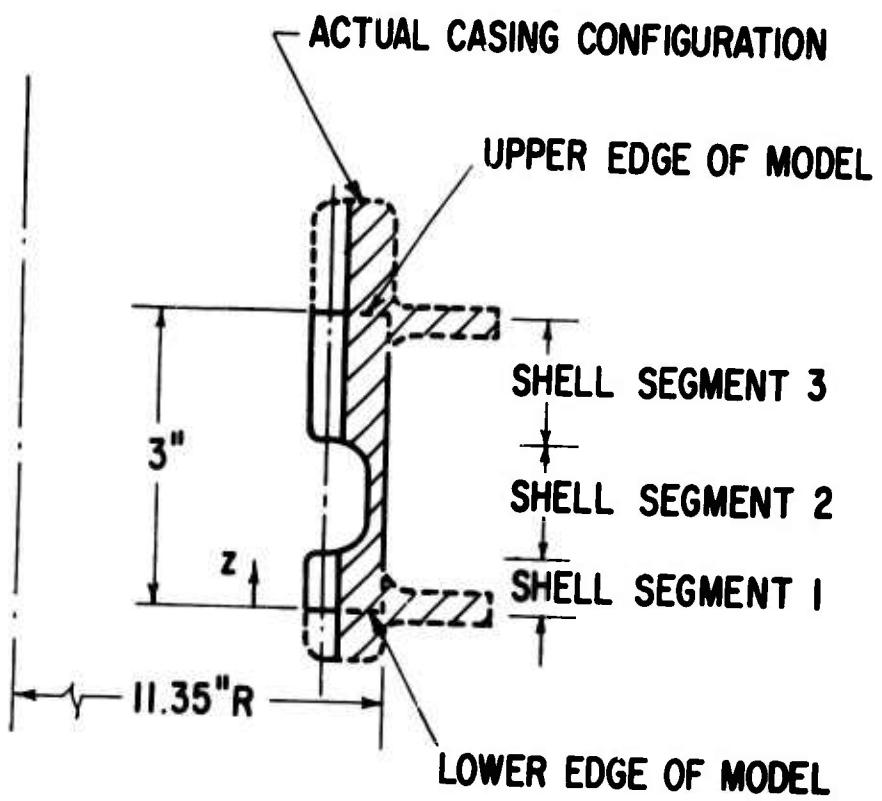
Figure 3.   Dynamic Model of CH-47 Lower Planetary
Ring-Gear Casing.

11
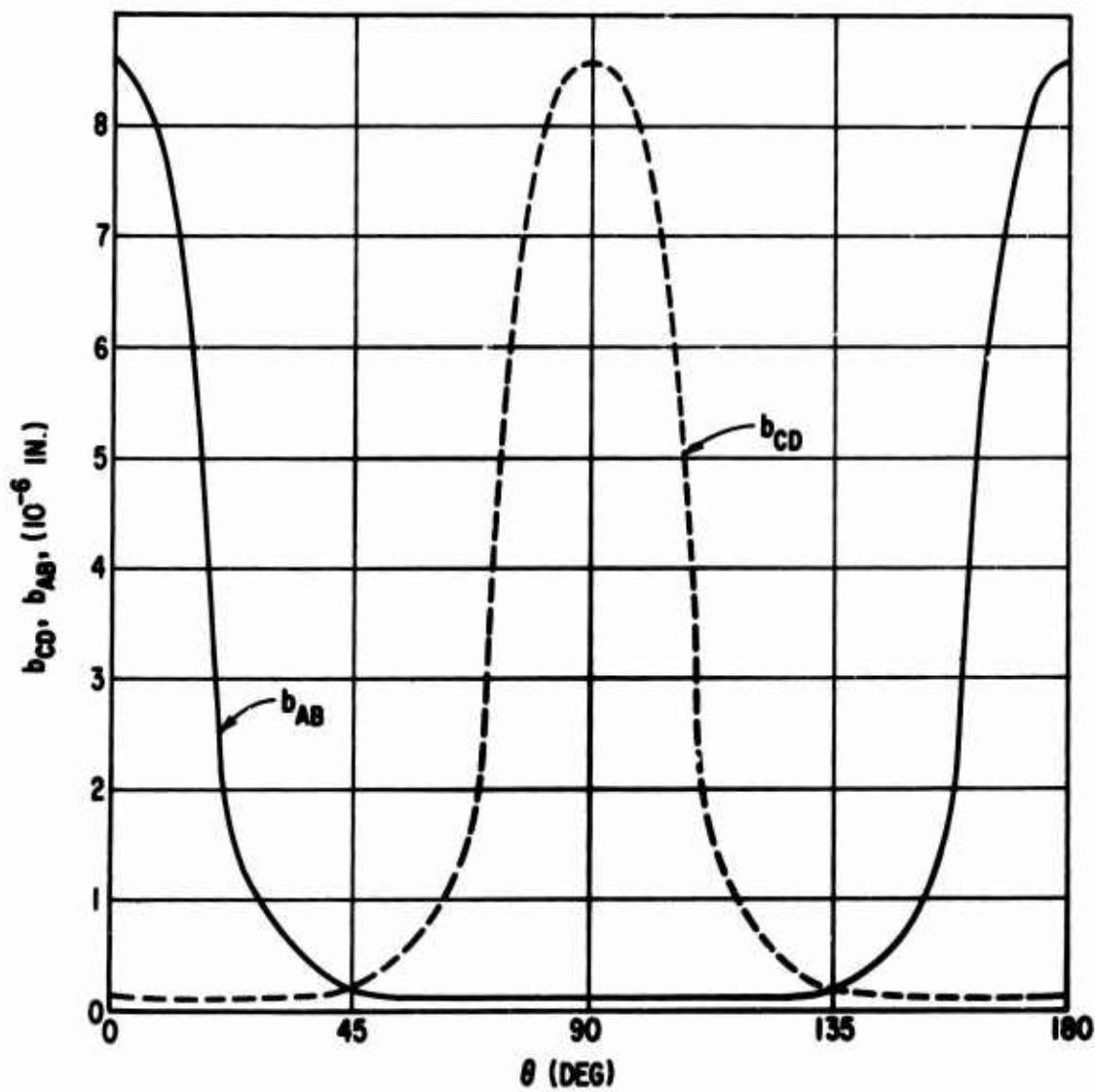
Figure 4. Ring-Gear Casing Response Functions.

12
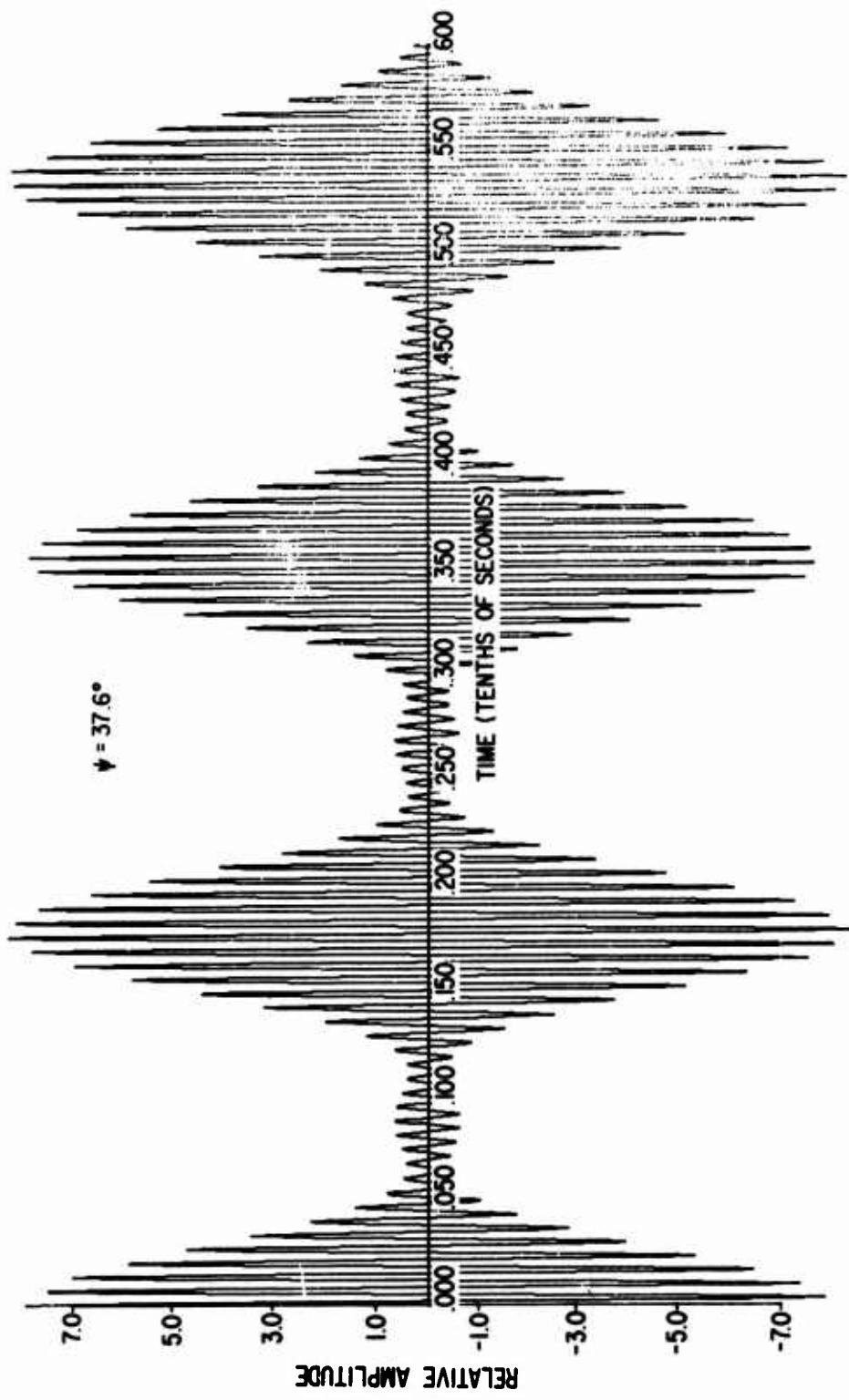
Figure 5. Radial Vibration Amplitude vs. Time at Fixed Location on CH-47 Forward Rotor-Drive Gearbox Ring Gear for ψ = 37.6°.

13
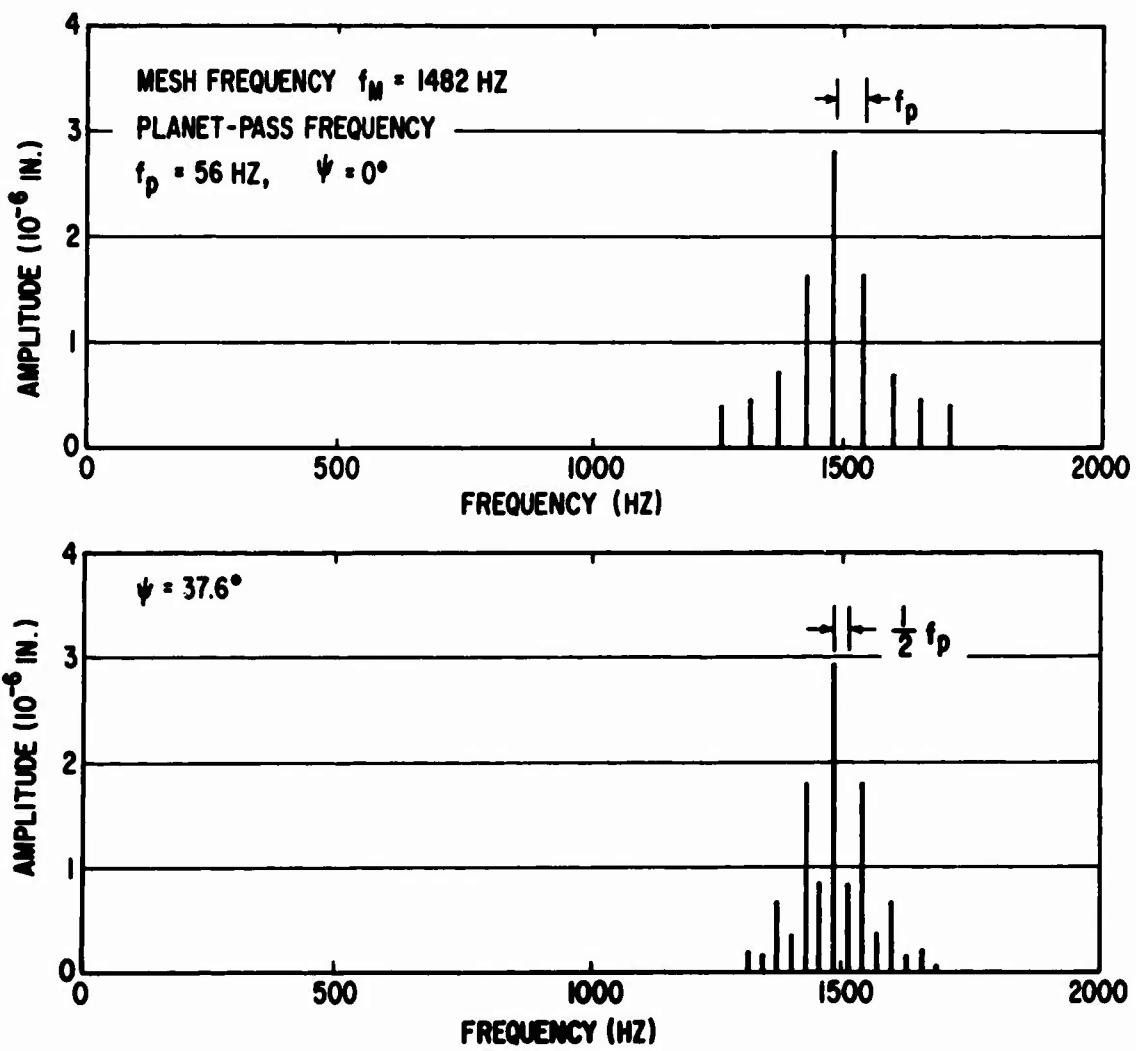
Figure 6. Frequency Spectra for $\psi = 0^\circ$ and 37.6°.

14

angles ($\Psi = 0^O$, 90° and 142.4^O) were investigated. The amplitude-time plots of these cases are shown in Figures 7, 8 and 9. In a gross sense, they appear to be similar. However, the frequency spectra for these three cases are quite different. They are shown in the upper diagram of Figure 6 and the upper and lower diagrams of Figure 10 for $\Psi = 0^O$, 90° and 142.4^O, respectively. It is noted that for $\Psi = 0^O$, sidebands occur only at frequencies of $f_M \pm n \; \dot{r}_p$.
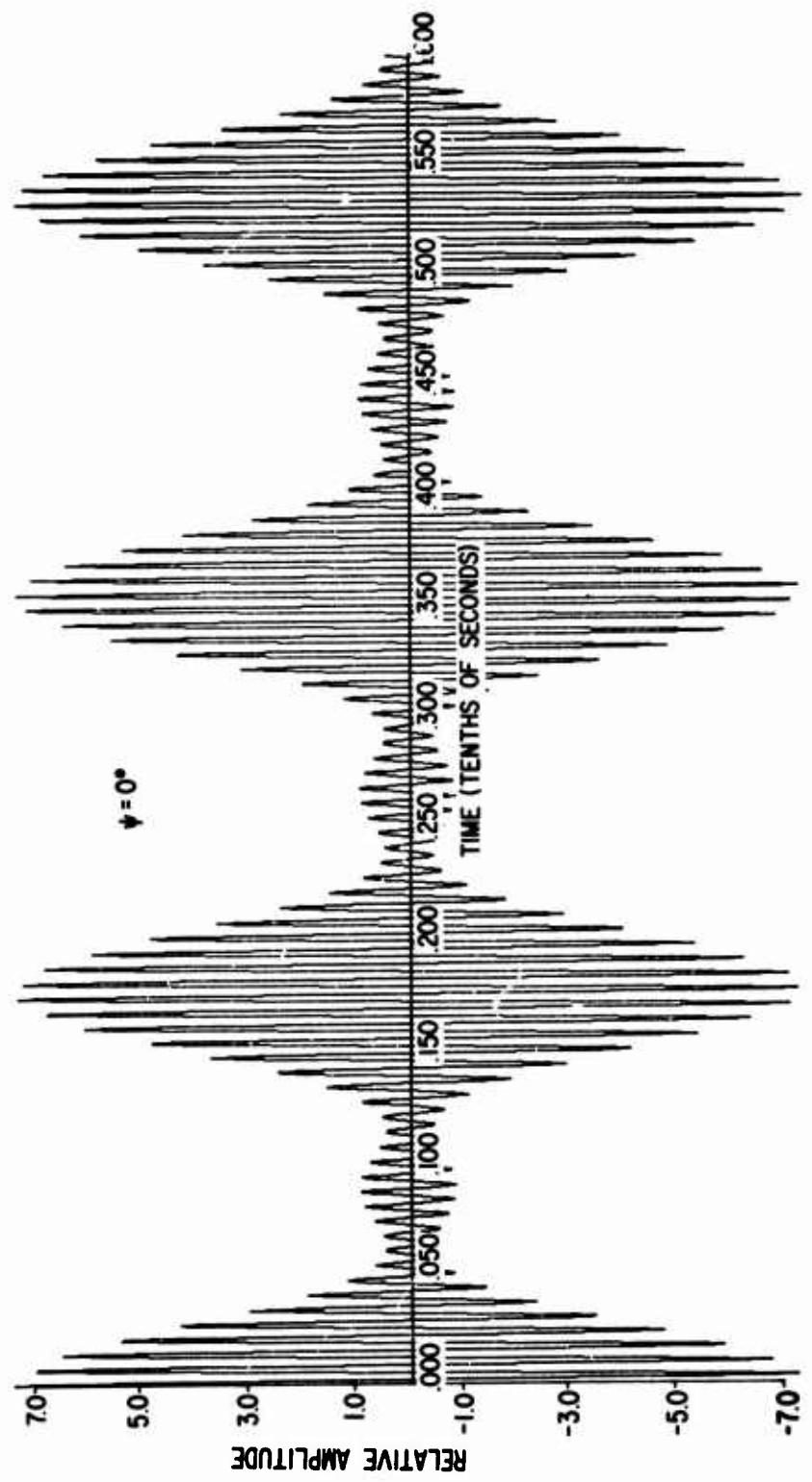
Figure 7. Radial Vibration Amplitude vs. Time at Fixed Location on CH-47 Forward Rotor-Drive Gearbox Ring Gear for $\psi = 0^\circ$.

16
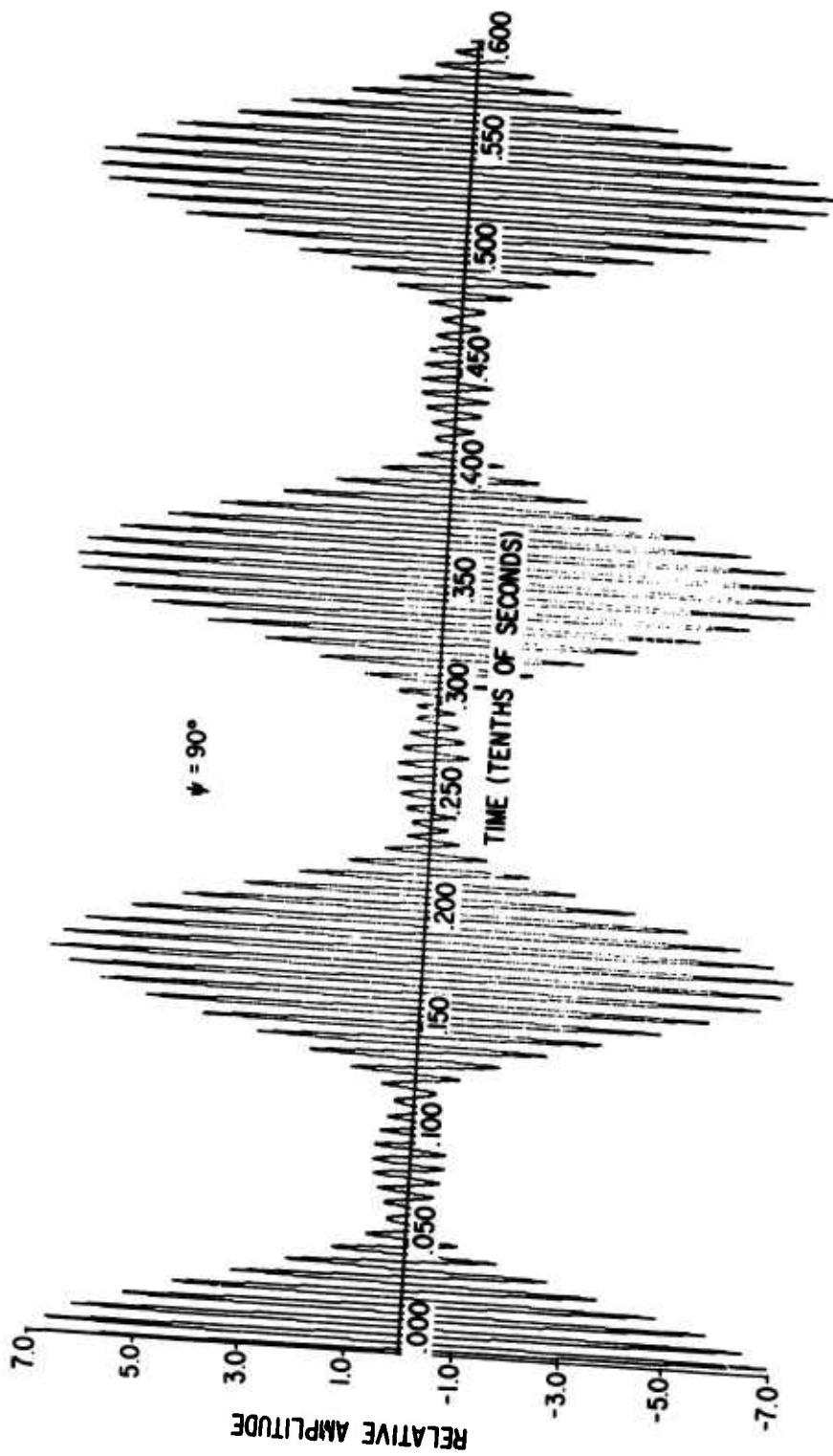
Figure 8. Radial Vibration Amplitude vs. Time at Fixed Location on CH-47 Forward Rotor-Drive Gearbox Ring Gear for $\psi = 90°$.

17
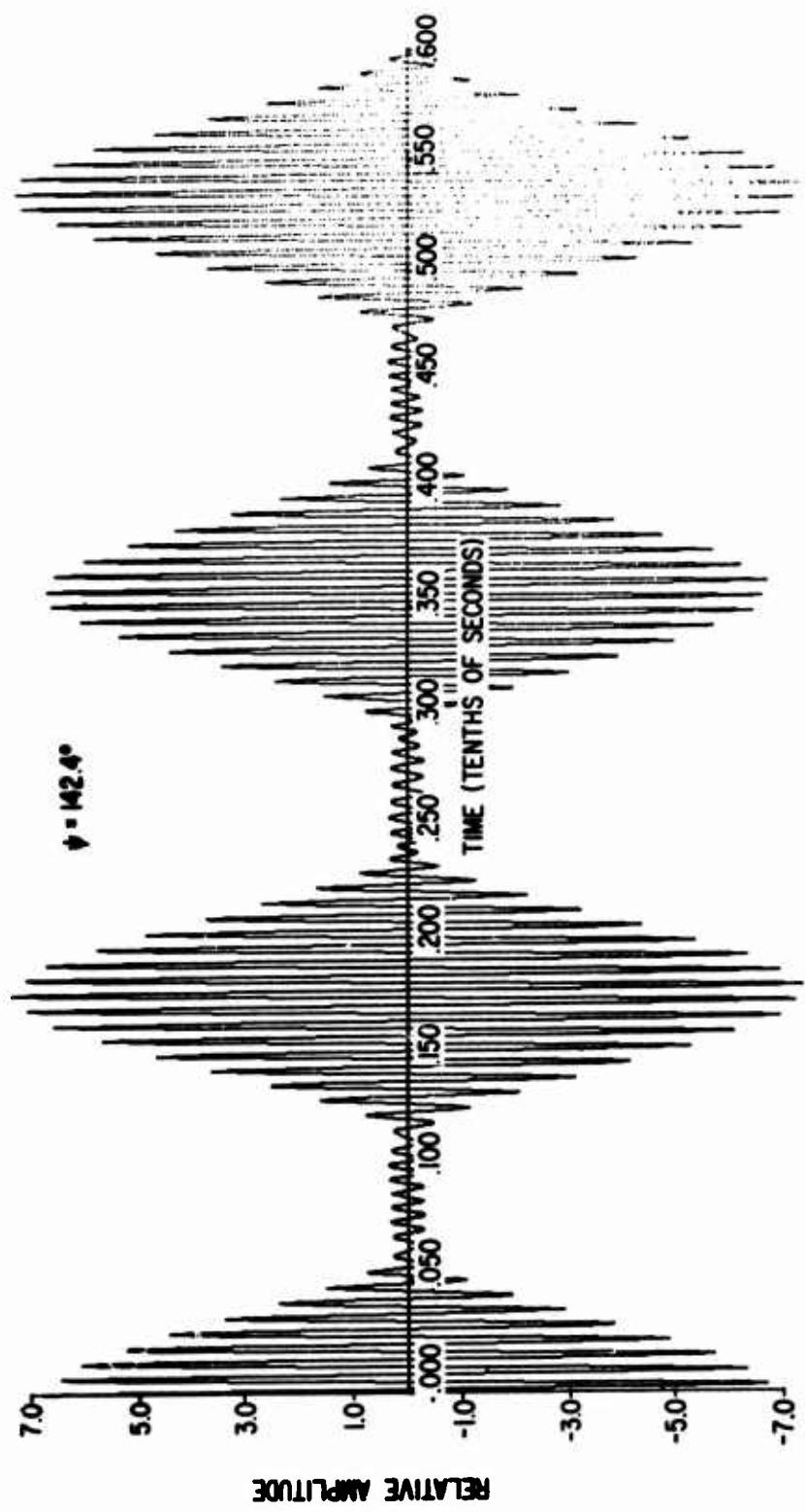
Figure 9. Radial Vibration Amplitude vs. Time at Fixed Location on CH-47 Forward Rotor-Drive Gearbox Ring Gear for ψ = 142.4°.

18
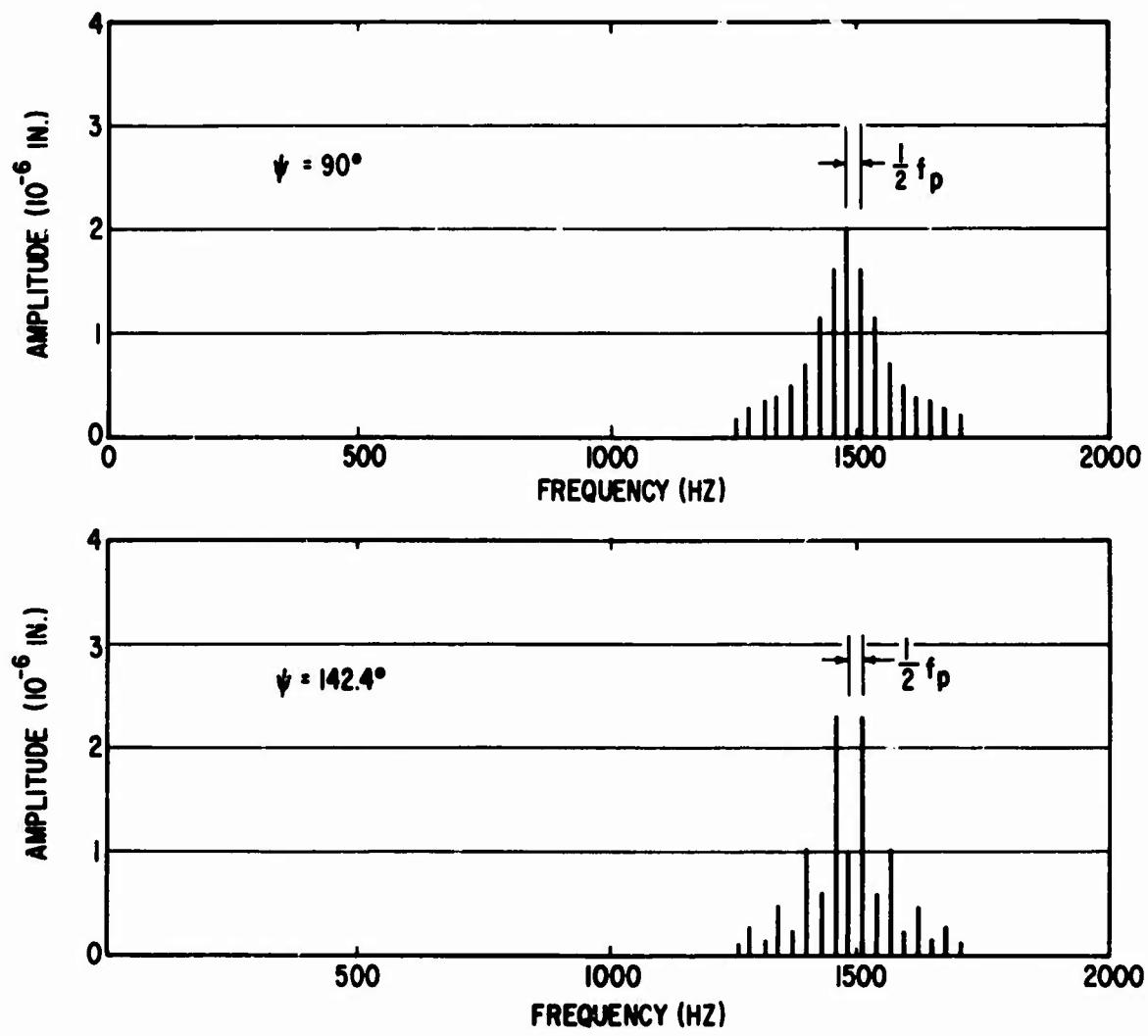
Figure 10. Frequency Spectra for $\psi = 90°$ and $142.4°$.

ANALYSIS OF GEAR-MESH-INDUCED
HIGH-FREQUENCY VIBRATION SPECTRA AND CALCULATIONS

ANALYSIS OF GEAR MESH EXCITATION

The mesh of gears with perfect involute profiles can induce vibration, simply because of the nonuniform deflection resulting from varying tooth compliance along the length of the tooth. The nonuniform deflection or displacement deviation introduces irregular motion superimposed on the uniform rotation of the gears. This irregularity of motion becomes one of the major sources of vibration in the drive system, especially of the vibration associated with noise production. Manufacturing errors in tooth shape or spacing can further increase the magnitude of the motion irregularity and thus the excited vibration amplitude. If all the teeth in each of the meshing gears are identical, and if the mesh is otherwise ideal (i.e., no runout, etc.), then the spectrum of the vibration induced by the gear mesh contains signals at only the mesh frequency and its higher harmonics. The analysis of this gear mesh excitation was performed by Laskin, Orcutt and Shipley [1].

However, if the gear mesh deviates from the ideal (e.g., gear runout, dynamic torque, etc.), or if there is deviation in tooth profiles as the gear mesh continues from one set of mating teeth to the other, the tooth deflection pattern will, in general, vary from tooth pair to tooth pair. The associated vibration will then contain signal components at other than the mesh frequency and its harmonics. These components are the so-called gear mesh excitation sidebands. It is the purpose of this work to study the gear-mesh-induced vibration spectra considering three gear parameters as variables between mesh cycles. These three parameters are:

1. Center-Line Distance

This variation, in most cases, is due to shaft or gear runout. The center-line distance is treated to be constant within a tooth mesh, but it can vary between mesh cycles. This simplifying approximation is possible because the variation in center-line distance due to shaft or gear runout is slow with respect to tooth mesh frequency.

2. Tooth Load

This variation may be caused, for instance, by the dynamic effects of other gear meshes in the drive system. The tooth load can also be variable between calculation points within one mesh cycle. This accommodates high-frequency dynamic forces.

3. Tooth Support Compliance

This is the compliance in addition to the compliance due to tooth bending, shearing, rotation, and contact deformation normally existing during gear mesh. It may be produced by elastic nonuniformity in the gear structure supporting the gear teeth. This compliance can also be variable at all calculation points within one mesh cycle.

Each of these three variations is in general periodic with a definite

frequency. For example, the center distance variation caused by shaft run-out has a frequency equal to the rotational speed of the shaft. In each of the cases, there exists a base period for the tooth deflection pattern which is equal to the reciprocal of the largest common factor between the mesh frequency and the frequency (or frequencies) of variation of the gear parameter (or parameters). During one base period, integer multiples of gear mesh cycles and of parameter variation cycles occur. The spectrum of the associated vibration is thus discrete, with the fundamental frequency equal to the reciprocal of the base period. The frequency spectrum is obtained by a Fourier analysis of the tooth deflection profile over one base period.

However, if the variation of the gear parameter is random, the spectrum of the gear-mesh-induced vibration will be continuous. It may be obtained by calculating the power spectral density function of the tooth deflection data over a long period of time. The method of power spectra calculation is included in Appendix I.

Within one mesh cycle, the method of calculating the tooth deflection is directly similar to that in [1]. The limitations and assumptions in the calculation are listed below:

1. Only spur gears are treated, and these are treated only for the two cases of (a) an external gear driving an external gear and (b) an external gear driving an internal gear. Straight bevel gears may be treated in an approximate manner by replacing them with equivalent spur gears by Tregold's Approximation [13].

2. The working portions of the tooth profiles are essentially involute. Design and manufacturing profile deviations are small enough so as not to affect load location, load direction, or tooth stiffness.

3. There is no tip interference, either due to excessive addendum length or due to tooth deflection under load.

4. In any single interval between the pitch points of two successive pairs of teeth, contact and load carrying are limited to the two successive pairs of teeth. In the same interval, there must be at all times at least one pair of teeth in contact and carrying load. This prevents consideration of cases where the contact ratio is less than one or more than two; it may in some unusual designs also eliminate cases where the contact ratio has certain intermediate values.

5. The load is assumed to be transmitted uniformly across the face of the gear except for normal end effects in stress distribution. This excludes any consideration of face crowning, lead modification, lead manufacturing error, gear windup, or nonuniform deflection of gear supports.

6. All variations in tooth deflection as the load point moves along the tooth profile either are confined to elastic effects on the

21

tooth alone or can be supplied as point-by-point compliances as part of the input data. This means that variations such as might result from the deflection of thin rims are not calculated directly by the analysis.

7. The contact deformation is assumed to be independent of the tooth surface lubricating film.

The above analysis is incorporated in the computer program GGEAR. It is obtained by modifying and extending the program GEARO reported in [1]. The overall structure of the modified program is shown in Figure 11. The modifications consist of the creation of the main program GGEAR and the subroutine SPECT, and some changes in subroutines GEARO, FOUR and PLT to accommodate the extension of computation over multiple mesh cycles. GGEAR accepts those items of gear data that are constant over all mesh cycles. Subroutine GEARO, on the other hand, reads in variable gear data and, together with subroutines AJCDH and CALCJ, calculates the tooth deflection over one mesh cycle. In the computation, the mesh cycle is divided into a number of calculation points as is done in the program GEARO. Tooth deflections at all the calculation points over the prescribed number of mesh cycles are stored and printed out in GGEAR.

With reference to Figure 11, it may be noted that provision is being made for eventual incorporation of other subroutines similar to GEARO for the calculation of excitation levels in high-contact-ratio spur gears, helical gears, and eventually spiral-bevel gears. While such calculation capabilities were not included in the computer program during the present contract, the modified program was prepared on a modular basis for their later inclusion.

According to the user's instruction, either the calculated tangential deflection data can be plotted by subroutine PLT, or it can be analyzed to obtain the Fourier representation of the deflection pattern via the subroutine FOUR, as is now done in program GEARO. The data can also be analyzed by using SPECT to produce the power spectral density function. A description of the computer program is given in Appendix II.

CH-47 SPIRAL BEVEL GEAR MESH CALCULATIONS

The CH-47 forward rotor-drive gearbox spiral bevel gear mesh is analyzed in terms of its equivalent spur gear mesh [2]. The equivalent spur gears will be equivalent to the spiral bevel gears only in the sense that their physical proportions, those likely to influence deflection under load, approximate the mean proportions of the actual spiral bevel gear teeth. The use of the equivalent spur gears is sufficiently adequate for the present purpose of studying the effects of shaft runout and load variation to produce high-frequency-vibration sidebands. The gear mesh parameters and the conversion of the CH-47 spiral bevel gears into equivalent spur gears are summarized in Table I, which has been taken from [2]. The gear mesh tangential load is taken to be 2760 lb, and the gearbox input shaft speed is 7059 rpm. This yields a gear tooth mesh frequency of 3412 Hz. Variations in center distance and in tooth load as the source for generating tooth displacement deviations at sideband frequencies have been studied.

22
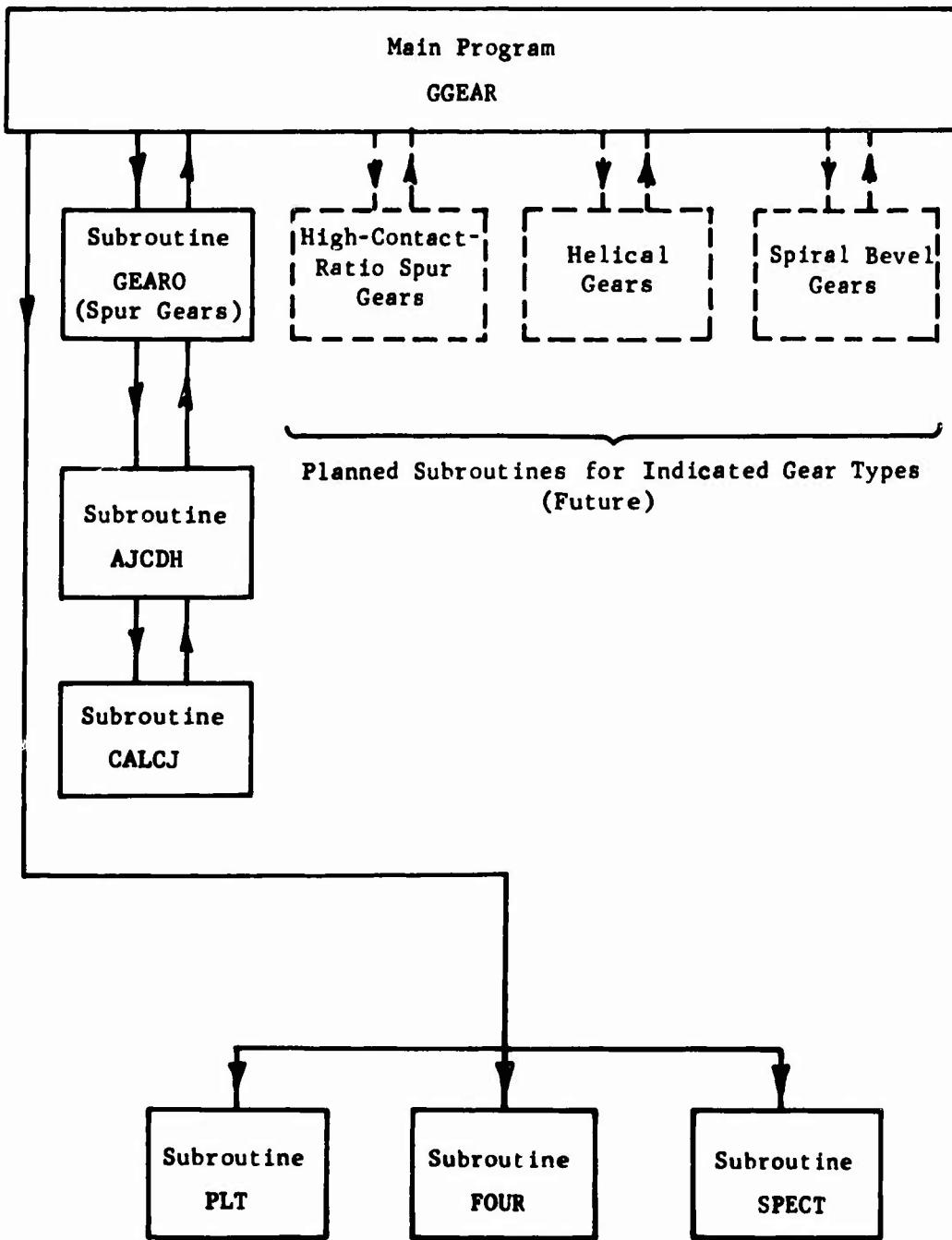
Figure 11. Computer Program Structure.

23

TABLE 1. COMPARISON OF SPIRAL BEVEL GEARS INTO EQUIVALENT SPUR GEARS FOR CH-47 FORWARD ROTOR TRANSMISSION (FROM REFERENCE 2)

SYMBOL	DEFINITION	UNITS	PINION [114D1044(12)]			GEAR [114D1053(13)]		
			SPIRAL BEVEL	HELICAL	SPUR	SPIRAL BEVEL	HELICAL	SPUR
N	NUMBER OF TEETH OF SPIRAL BEVEL	---	29			51		
Y	PITCH CONE ANGLE OF SPIRAL BEVEL	DEGREES	31° 39'			67° 21'		
	COS Y	---	.85127			.38510		
	SIN Y	---	.52473			.92287		
ϕ	SPIRAL ANGLE OF SPIRAL BEVEL - HELIX ANGLE OF EQUIVALENT HELICAL	DEGREES	25°	25°		25°	25°	
	COS ϕ	---	.90631	.90631		.90631	.90631	
	COS²ϕ	---	.82140	.82140		.82140	.82140	
	COS³ϕ	---	.74444	.74444		.74444	.74444	
N_V	NUMBER OF TEETH OF EQUIVALENT HELICAL = $N/\cos^3 Y$			34.0655	45.7623		132.4331	177.9058
N_S	NUMBER OF TEETH OF EQUIVALENT SPUR = $N_V/\cos^3\phi$							
F	FACE WIDTH OF SPIRAL BEVEL	INCHES	2.188			2.188		
F_V	FACE WIDTH OF EQUIVALENT HELICAL = F	INCHES		2.188			2.188	
F_S	FACE WIDTH OF EQUIVALENT SPUR = $F_V/\cos\phi$	INCHES			2.4142			2.4142
R	PITCH RADIUS OF SPIRAL BEVEL AT LARGE END	INCHES	3.775			6.639		
R_M	MEAN PITCH RADIUS OF SPIRAL BEVEL = $R - (F/2)\sin Y$	INCHES	3.2010			5.6294		
R_V	PITCH RADIUS OF EQUIVALENT HELICAL = $R_M/\cos Y$	INCHES		3.7601			14.6180	
R_S	PITCH RADIUS OF EQUIVALENT SPUR = $R_V/\cos^2\phi$	INCHES			4.5776			17.7964
σ	RATIO OR RADII OF SPIRAL BEVEL = R_M/R	INCHES	.8479			.8479		
a	ADDENDUM OF SPIRAL BEVEL AT LARGE END	INCHES	.297			.146		
a_V	ADDENDUM OF EQUIVALENT HELICAL = a	INCHES		.2518	.2518		.1237	.1237
R_{OV}	OUTER RADIUS OF EQUIVALENT HELICAL = $R_V + a_V$	INCHES		4.0119			14.7417	
R_{OS}	OUTER RADIUS OF EQUIVALENT SPUR = $R_S + a_S$	INCHES			4.8294			17.9201
b	DEDENDUM OF SPIRAL BEVEL AT LARGE END	INCHES	.195			.346		
b_V	DEDENDUM OF EQUIVALENT HELICAL = b	INCHES		.1653	.1653		.2933	.2933
R_{RV}	ROOT RADIUS OF EQUIVALENT HELICAL = $R_V - b_V$	INCHES		3.5948			14.3247	
R_{RS}	ROOT RADIUS OF EQUIVALENT SPUR = $R_S - b_S$	INCHES			4.4123			17.5031
d	WORKING DEPTH OF SPIRAL BEVEL AT LARGE END	INCHES	.443			.443		
d_H	MEAN WORKING DEPTH OF SPIRAL BEVEL = d	INCHES	.3756			.3756		
d_V	WORKING DEPTH OF EQUIVALENT HELICAL = d_H	INCHES		.3756	.3756		.3756	.3756
d_S	WORKING DEPTH OF EQUIVALENT SPUR = d_V	INCHES						
$TIFR_V$	TRUE INVOLUTE FORM RADIUS OF EQUIVALENT HELICAL = $R_{OV} - d_V$	INCHES		3.6363			14.3661	
$TIFR_S$	TRUE INVOLUTE FORM RADIUS OF EQUIVALENT SPUR = $R_{OS} - d_S$	INCHES			4.4538			17.5445
T_H	MEAN CIRCULAR TOOTH THICKNESS OF SPIRAL BEVEL = $\sigma T \cos$	INCHES	.506			.312		
T_V	CIRCULAR TOOTH THICKNESS OF EQUIVALENT HELICAL = T_H	INCHES	.3888	.3888	.3888	.2397	.2397	.2397
T_S	CIRCULAR TOOTH THICKNESS OF EQUIVALENT SPUR = T_V	INCHES						
C_V	RADIAL CLEARANCE OF EQUIVALENT HELICAL = $TIFR_V - R_{RV}$	INCHES		.0415	.0415		.0414	.0414
C_S	RADIAL CLEARANCE OF EQUIVALENT SPUR = $TIFR_S - R_{RS}$	INCHES						
r_V	TOOTH FILLET RADIUS OF EQUIVALENT HELICAL = $(.75)C_V$	INCHES		.0311	.0311		.0310	.0310
r_S	TOOTH FILLET RADIUS OF EQUIVALENT SPUR = $(.75)C_S$	INCHES						

24

1. Center Distance Variation

Center distance variation resulting from a 0.001-in. (peak) input shaft runout is chosen to be the representative case. The runout is assumed to be a sine wave in form. The expression for the center distance is

$$C \text{ (in.)} = 22.3735 + 0.001 \sin \frac{2\pi f_M}{29} t \qquad (21)$$

where the number 22.3735 is the nominal center distance in inches, t the time in seconds, and f_M the mesh frequency in Hz. The input pinion has 29 teeth, and therefore $f_M/29$ is the shaft rotational speed.

Using the computer program, tooth displacement deviation is calculated over 29 mesh cycles covering one period of variation in center distance (one complete shaft rotation). The tooth deviation is periodic with a period equal to one shaft rotation. This periodic tooth deviation pattern is analyzed by using the extended subroutine FOUR to obtain the amplitude-frequency relationship. This relationship is shown in Figure 12. Amplitude is the magnitude of tangential deviation over and above the mean tooth deflection. The frequency is expressed in multiples of mesh frequency f_M. Since the tooth deviation is periodic, the amplitude distribution is discrete and is nonzero only at the multiples of reciprocal of the base period, which is the shaft speed ($f_M/29$). It is seen from Figure 12 that mesh frequency is still the most dominant frequency. However, the sideband amplitudes close to the harmonic frequencies are seen to be comparable to the high harmonic components.

It is expected that a larger shaft runout would produce higher sideband amplitudes. This is indeed shown in Figure 13, which is a frequency-amplitude plot for a 0.002-in. (peak) shaft runout. It is seen that the amplitudes at $f_M/29$ and at sidebands around the higher harmonics are approximately doubled in magnitude.

2. Transmitted Load Variation

A sinusoidal dynamic load of 500 lb at half mesh frequency is assumed to be superimposed on the nominal tooth load of 2760 lb. The total tangential tooth load is therefore

$$W \text{ (lb)} = 2760 + 500 \sin \frac{2\pi f_M}{2} t \qquad (22)$$

The calculated tooth displacement deviation has a periodicity of two mesh cycles. The resulting amplitude-frequency plot of this periodic tooth deviation pattern is shown in Figure 14. It is seen that the first sideband amplitude, which is at $f_M/2$, is larger than all the high harmonic components. Also, all other sideband amplitudes are relatively small. This large first sideband amplitude may be attributed to the large maximum dynamic load (500 lb) relative to the nominal load.

25
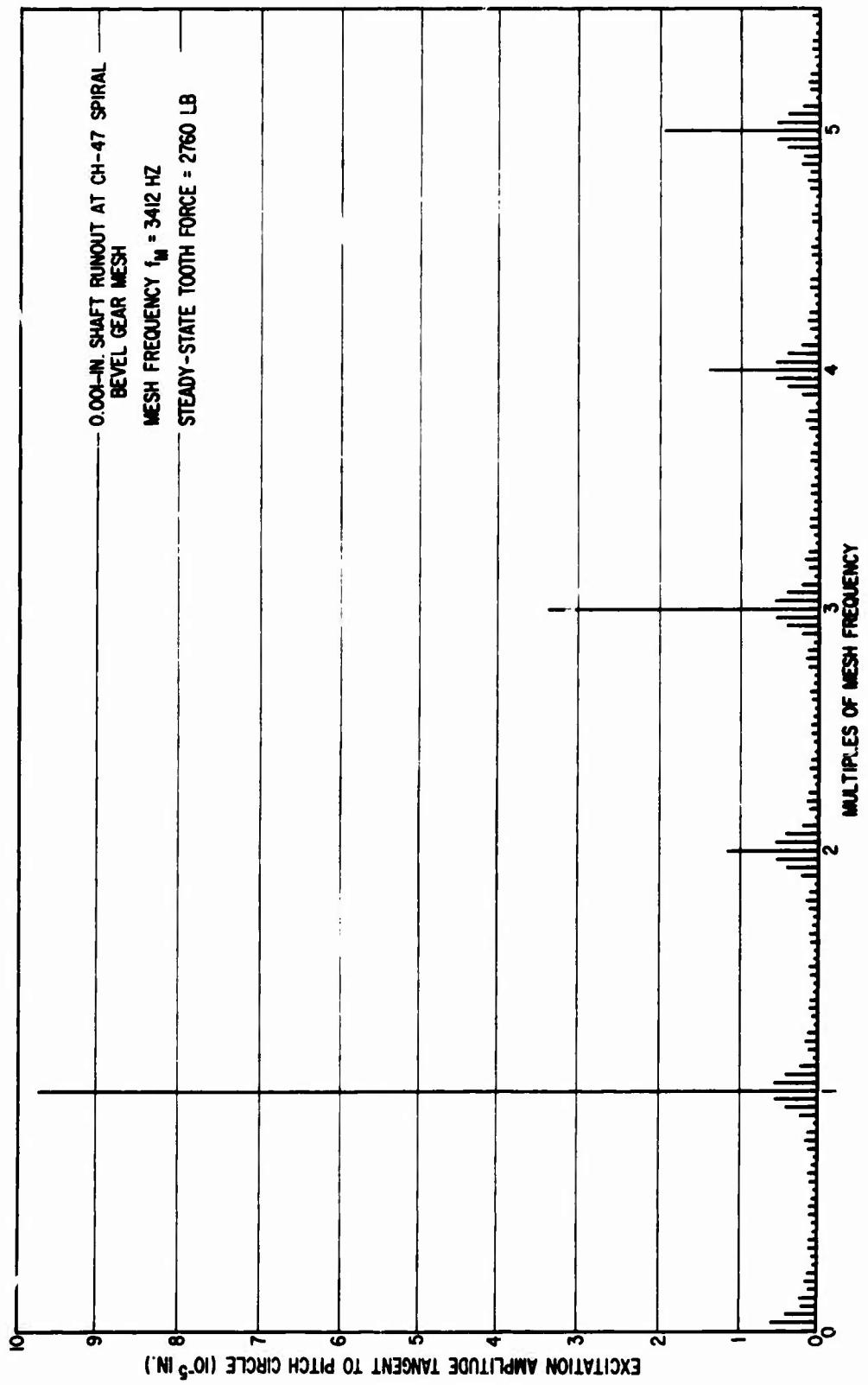
Figure 12. Frequency vs. Excitation Amplitude for Pinion Shaft Runout, CH-47 Spiral Bevel Gear Mesh.
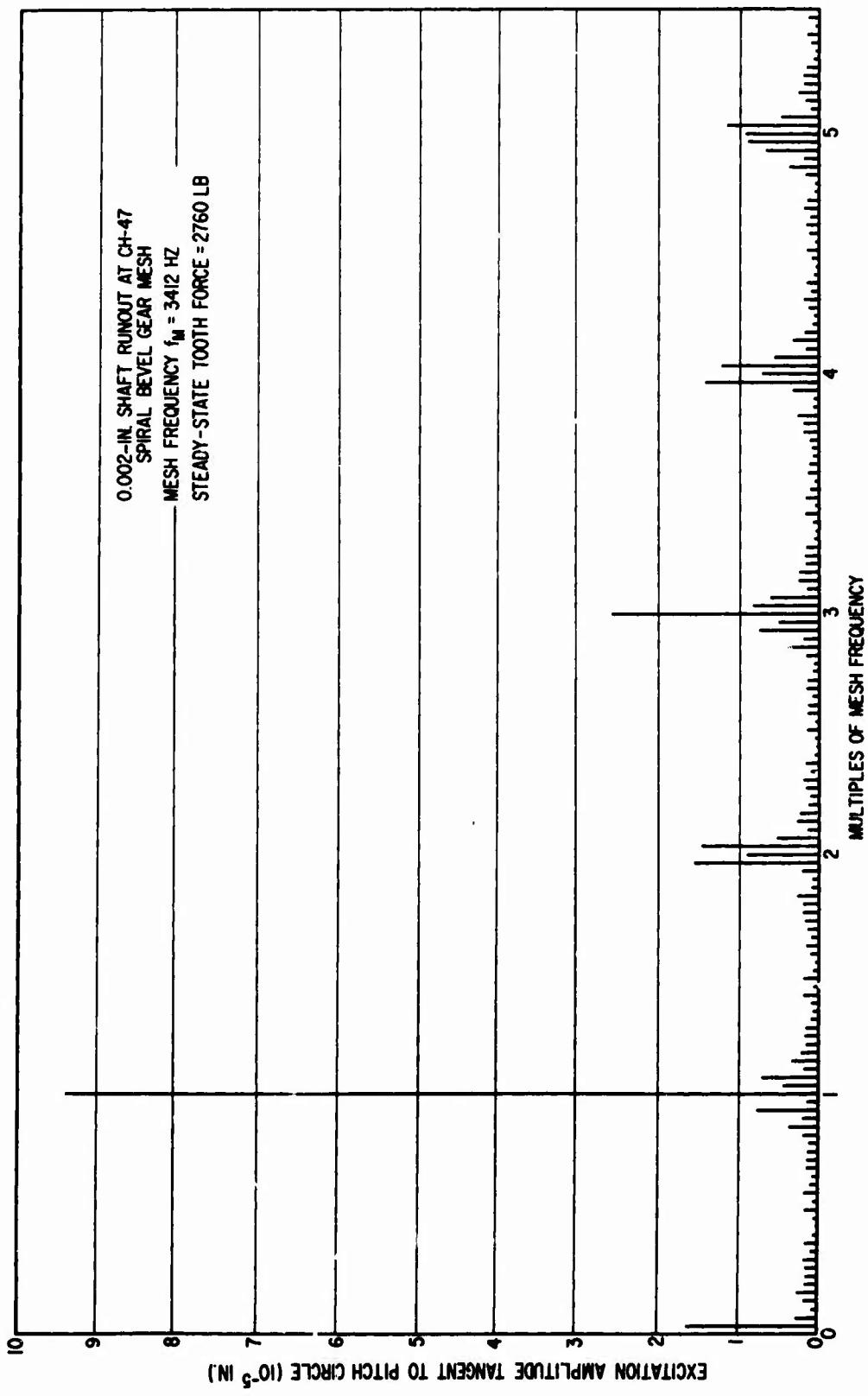
Figure 13. Frequency vs. Excitation Amplitude for Pinion Shaft Runout, CH-47 Spiral Bevel Gear Mesh.

0.002-IN. SHAFT RUNOUT AT CH-47 SPIRAL BEVEL GEAR MESH

MESH FREQUENCY f_M = 3412 HZ

STEADY-STATE TOOTH FORCE = 2760 LB

MULTIPLES OF MESH FREQUENCY

EXCITATION AMPLITUDE TANGENT TO PITCH CIRCLE (10^{-5} IN.)

27
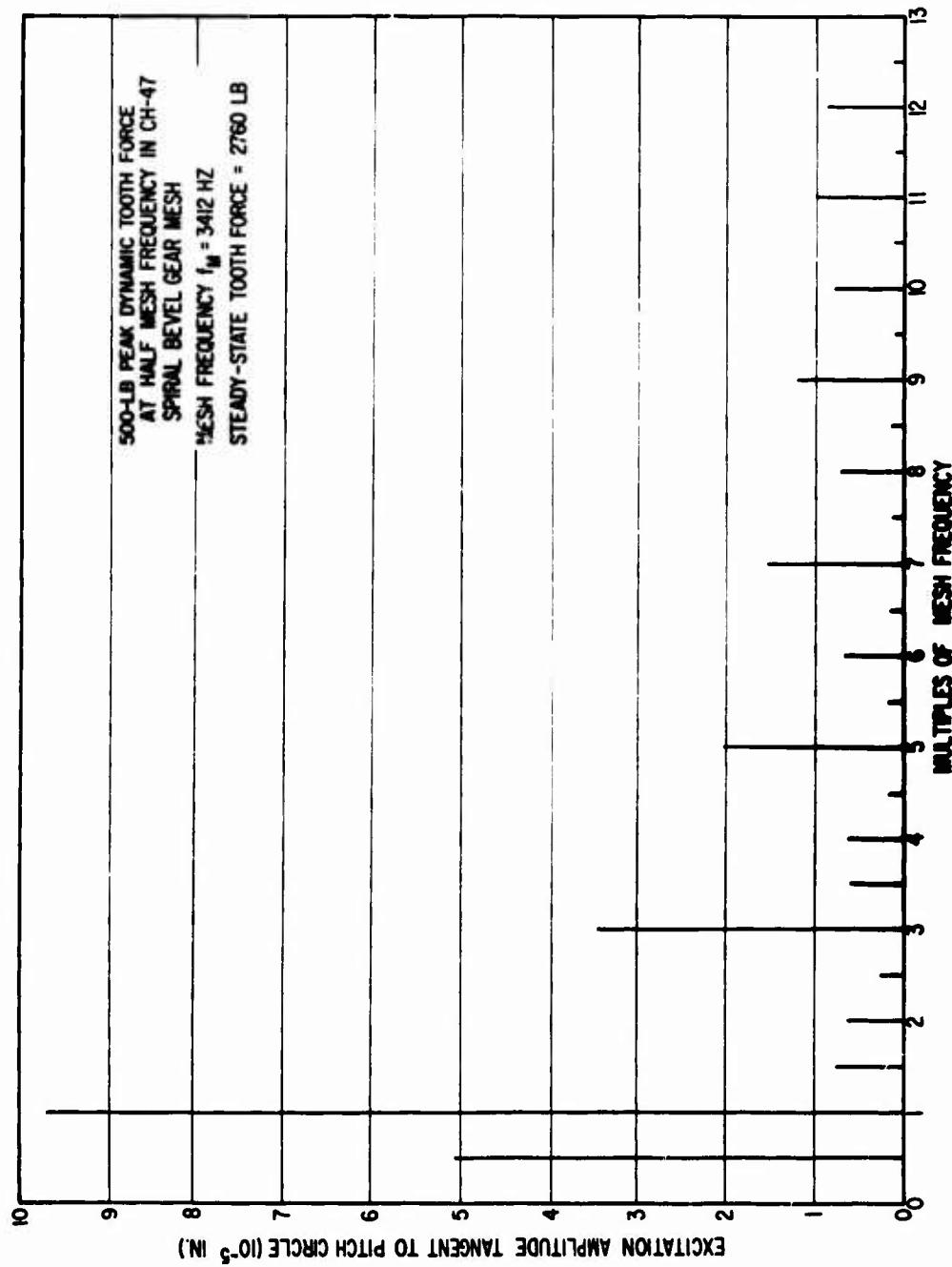
Figure 14. Frequency vs. Excitation Amplitude for Tooth Force Variation, CH-47 Spiral Bevel Gear Mesh.

28

CH-47 LOWER PLANETARY PLANET-TO-RING GEAR MESH CALCULATIONS

The CH-47 lower planetary planet and ring gear parameters are summarized in Table II. The tangential tooth load at the planet-to-ring gear mesh is taken to be 2103 lb. The planet rotational speed is 2280 rpm. The corresponding mesh frequency is 1482 Hz. Effects of variation in center distances, tooth load, and tooth support compliance to produce vibration sideband frequencies have been investigated.

1. Center Distance Variation

A planet runout of 0.001 in. (peak) in sine wave form is assumed. With a nominal center distance of 6.7 in., the expression for center distance is

$$C \text{ (in.)} = 6.7 + 0.001 \sin \frac{2\pi f_M}{39} t \qquad (23)$$

Tooth displacement deviation is calculated using the computer program, over 39 mesh cycles, to cover a full rotation of the planet. The frequency spectrum of the tooth-mesh-induced vibration, obtained by Fourier analyzing the displacement deviation, is plotted in Figure 15. The mesh frequency is still the dominating frequency. The largest sideband amplitudes occur at the sidebands closest to and on each side of the mesh frequency.

TABLE II. CH-47 LOWER PLANETARY PLANET AND RING GEAR PARAMETERS		
	Planet	Ring
Number of Teeth	39	106
Face Width	1.55 in.	1.25 in.
Pitch Radius	3.9 in.	10.6 in.
Outer Radius	4.0845 in.	—
Inner Radius	—	10.43 in.
Root Radius	3.69 in.	10.845 in.
Radius to the Beginning of Involute Profile	3.738 in.	10.7935 in.
Circular Tooth Thickness at Pitch Circle	0.3462 in.	0.276 in.
Tooth Fillet Radius	0.075 in.	0.094 in.
Pressure Angle	25 deg	25 deg
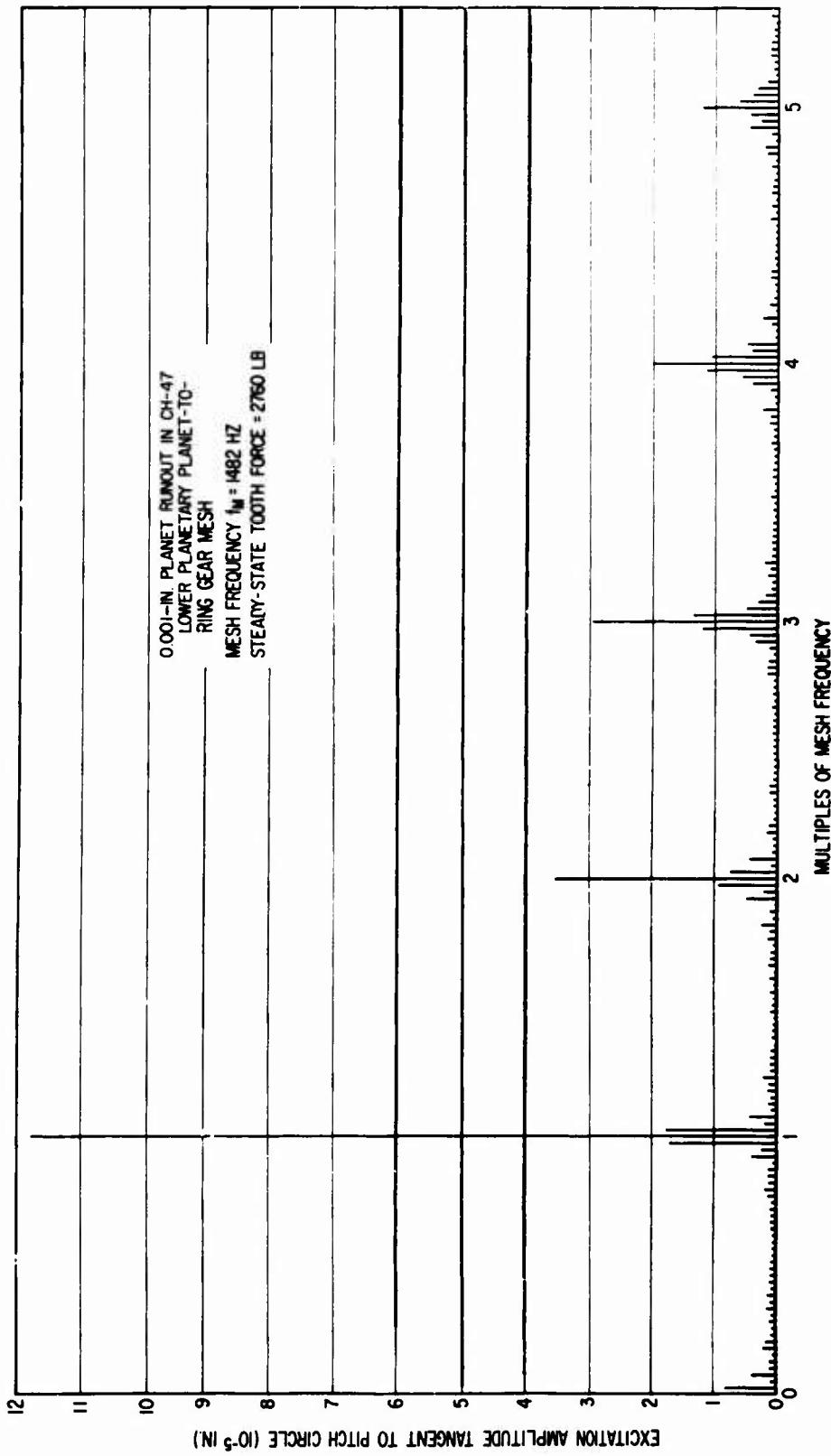
Figure 15. Frequency vs. Excitation Amplitude for Planet Runout, CH-47 Lower Planetary Planet-to-Ring Gear Mesh.

30

2. Transmitted Load Variation

A dynamic load of 400 lb varying sinusoidally at one-third of the mesh frequency is assumed to be superimposed on the nominal transmitted load of 2103 lb. The total tooth load is therefore

$$W \text{ (lb)} = 2103 + 400 \sin \frac{2\pi f_M}{3} t \tag{24}$$

The vibration induced by this load variation at gear tooth mesh has a fundamental frequency of $f_M/3$. The frequency spectrum is shown in Figure 16, which is obtained by the computer program calculating the tooth displacement deviation over three mesh cycles. It is seen that the amplitude at $f_M/2$ is higher than those at high harmonics of the mesh frequency.

3. Tooth Support Compliance Variations

Five consecutive ring gear teeth (out of a total of 106 teeth) are assumed to have a finite (tangential) tooth support compliance of 10^{-6} in./lb. This compliance is in addition to the tooth bending, tooth shear, tooth rotation, and contact deformation compliances calculated by the computer program in terms of gear tooth geometry and elastic properties.

The amplitude-frequency plot of the vibration induced by this compliance variation is shown in Figure 17. The information shown in this figure may be interpreted as follows: Assume first that the planets are fixed and the ring gear rotates. The frequency of mesh between a fixed planet and the ring gear is equal to the number of teeth on the ring gear multiplied by the relative rotational speed between them. This speed is actually the orbiting speed of the planet with respect to a fixed body, since the ring gear is stationary. The periodicity of the tooth deflection excitation caused by an assumed local ring gear compliance variation is equal to the time for one full relative rotation of the ring gear with respect to the planet. Since there are 106 teeth on the ring gear, this periodicity is 106 times the tooth mesh time; that is, the reciprocal of the tooth mesh frequency. Therefore, in the amplitude-frequency plot shown in Figure 17, there appear 105 equally-spaced sideband frequencies between two successive harmonics of mesh frequency. Any two neighboring sidebands are separated by the planet orbiting frequency.

It is seen from the figure that the sideband amplitudes are in general quite large and that the amplitudes of the low-frequency sidebands are even larger than the amplitude at the mesh frequency. The compliance due to tooth bending, tooth shear, tooth rotation and contact deformation is about 10^{-7} in./lb calculated by the computer program. The large sideband amplitudes are therefore due to the large tooth support compliance variation relative to the normal compliance existing during tooth mesh.

31
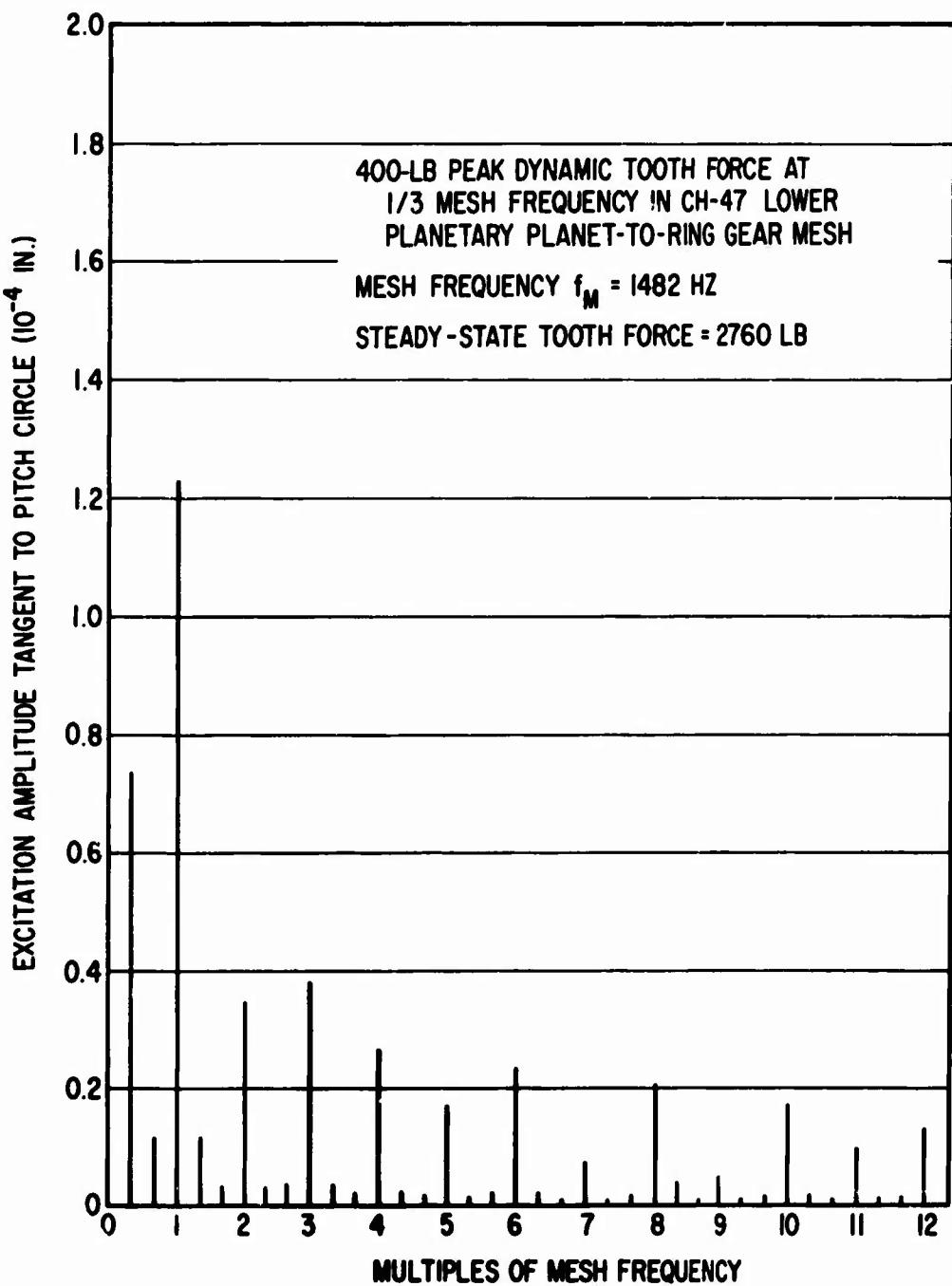
Figure 16. Frequency vs. Excitation Amplitude for Tooth
Force Variation, CH-47 Lower Planetary Planet-
to-Ring Gear Mesh.

32
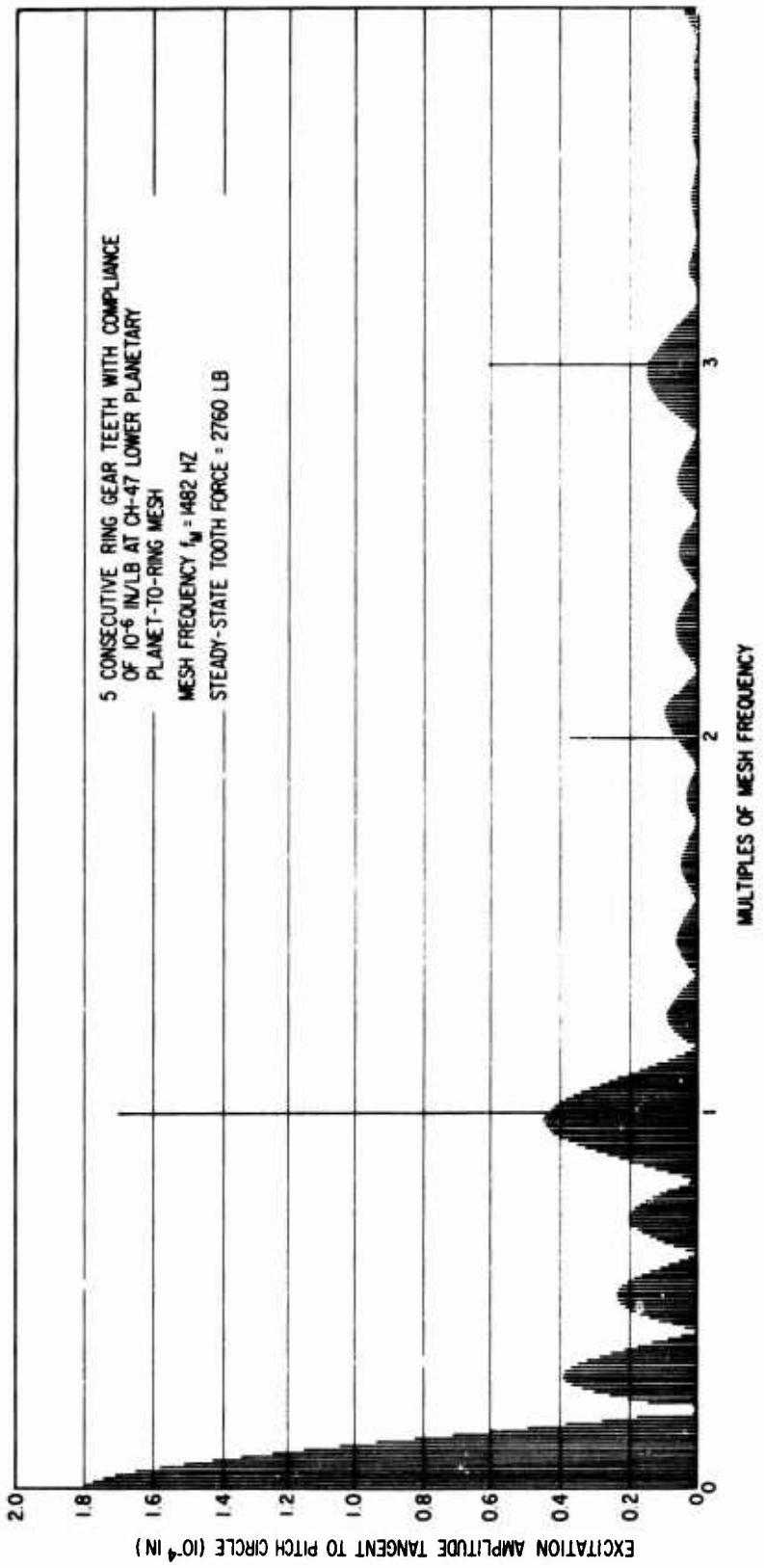
Figure 17. Frequency vs. Excitation Amplitude for Tooth Support Compliance Variation, CH-47 Lower Planetary Planet-to-Ring Gear Mesh.

33

It is also seen from Figure 17 that sidebands are grouped into a series
of bumps, and there are about five bumps between two adjacent harmonic
frequencies. This is attributed to the fact that the finite tooth sup-
port compliance variation occurs in only five consecutive teeth and
that the compliance variation is much larger than the normal tooth mesh
compliance. Tooth deflection patterns over one period (106 mesh cycles)
may be considered as the sum of two separate deflection profiles. One
is the normal tooth mesh deflection profile consisting of 106 identical
segments representing deflections for the 106 mesh cycles. The other
is the deflection due to the tooth support compliance variation, which
is nonzero only in the first five mesh cycles and is much larger in
magnitude than the former. The frequency content of the first deflec-
tion profile consists of only the mesh frequency and its harmonics,
while the frequency spectrum of the latter is roughly periodic with
declining amplitude and the period is about one-fifth of the mesh fre-
quency. Therefore, the frequency spectrum of the total tooth deflection
pattern appears to be a series of bumps superimposed on the mesh fre-
quency harmonics.

CH-47 SPIRAL BEVEL GEAR SYSTEM RESPONSE CALCULATIONS

In order to demonstrate the manner in which the gear excitation sidebands
may be applied in the vibration analysis of geared power trains, and to
illustrate the type of response which is produced by gear excitation spec-
tra which include sidebands, a sample calculation has been made using com-
puter program TORRP [2].

In this calculation, the excitation spectrum obtained under the assumption
of 0.002-in. runout in the CH-47 spiral bevel mesh was used. Mesh fre-
quency is 3412 Hz, and a steady-state tangential tooth force of 2760 lb
was used. The gearbox drive train components were represented dynamically
by the torsional response model reported in [2].

Results of the calculations are shown in Table III and Figures 18 and 19.
From these results it is apparent that significant torsional response occurs
in the gearbox components as a result of the sideband disturbances. It is
worth mentioning that essentially zero response occurs at frequencies
between the peaks shown because there are no sources of excitation at these
frequencies.

34

TABLE III. CH-47 SPIRAL BEVEL MESH EXCITATION AMPLITUDES AND CORRESPONDING PREDICTED PEAK DYNAMIC TOOTH FORCES AT INDICATED FREQUENCIES

Frequency (Hz)	Tangential Excitation Amplitude (10^{-6} in.)	Peak Dynamic Tooth Force (lb)	
		Spiral Bevel Mesh	Ring-Planet Mesh
117	16.35	0.71	0.21
2941	3.65	7.37	48.46
3059	1.82	196.46	165.61
3177	7.44	282.61	132.62
3294	1.11	26.01	9.78
3412	93.88	1672.19	606.54
3530	4.27	60.80	25.49
3647	6.99	73.38	48.42
3765	1.66	1.99	21.81
3883	3.18	119.34	61.66
6589	1.97	32.84	0.15
6707	15.52	230.07	0.94
6824	8.87	122.31	0.46
7059	4.02	50.49	0.16
10,001	7.33	71.74	0.08
10,118	4.99	48.67	0.05
10,236	25.53	247.61	0.26
10,354	8.22	79.43	0.08
10,471	6.04	58.16	0.06

		Peak Dynamic Tooth Force	
	Tangential Excitation	(lb)	
Frequency	Amplitude		
(Hz)	(10^{-6} in.)	Spiral Bevel Mesh	Ring-Planet Mesh
13,413	3.11	27.98	0.09
13,530	14.15	121.36	0.61
13,648	7.00	51.97	0.58
13,765	12.23	1044.30	33.84
13,883	5.51	64.10	0.40
16,825	6.66	61.93	0.01
16,942	8.95	83.11	0.01
17,060	9.17	85.10	0.01
17,178	11.64	107.88	0.01
17,295	4.67	43.25	0.005

TABLE III - Continued
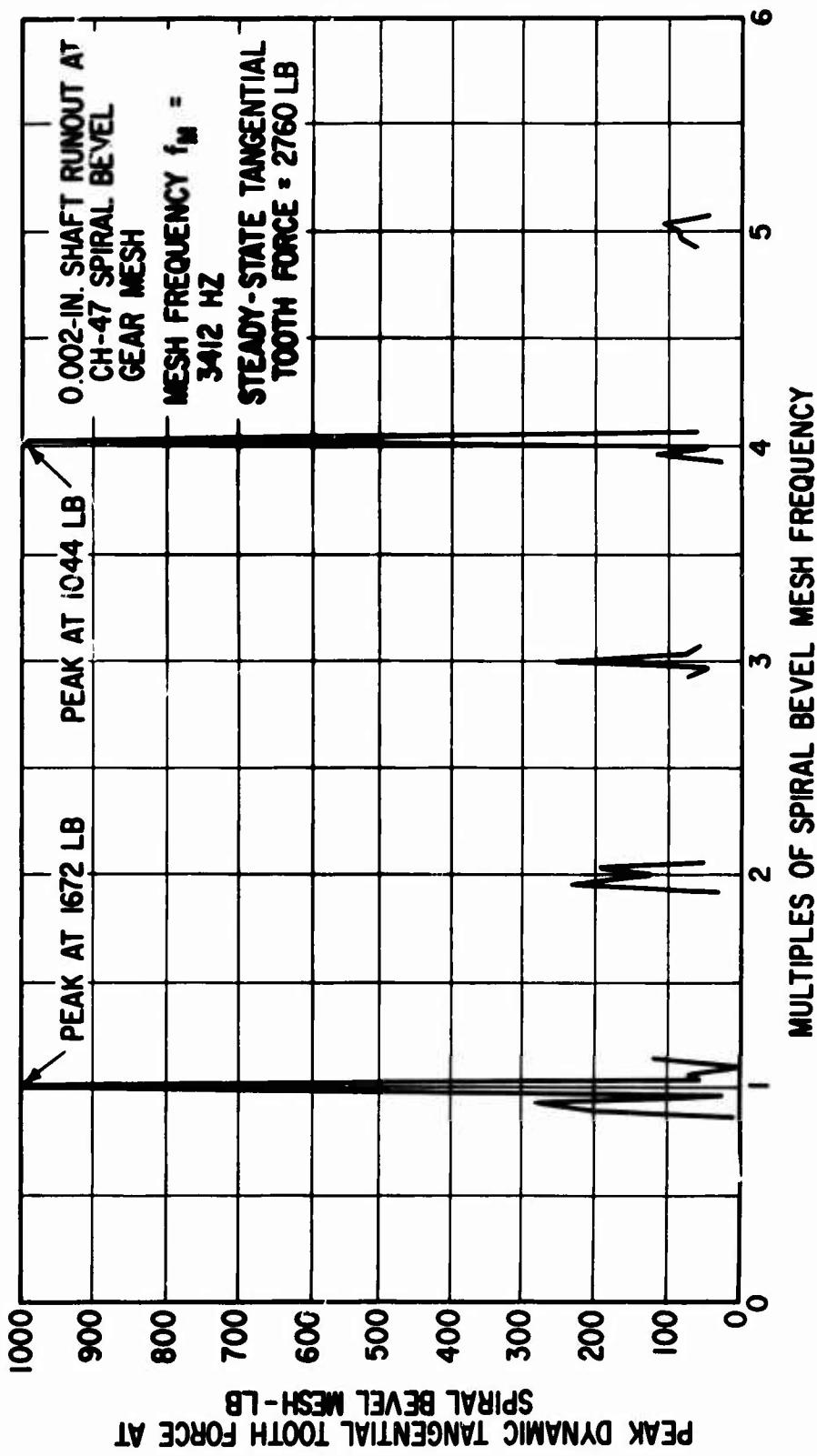
Figure 18. Calculated Dynamic Tooth Force at CH-47 Spiral Bevel Gear Mesh.
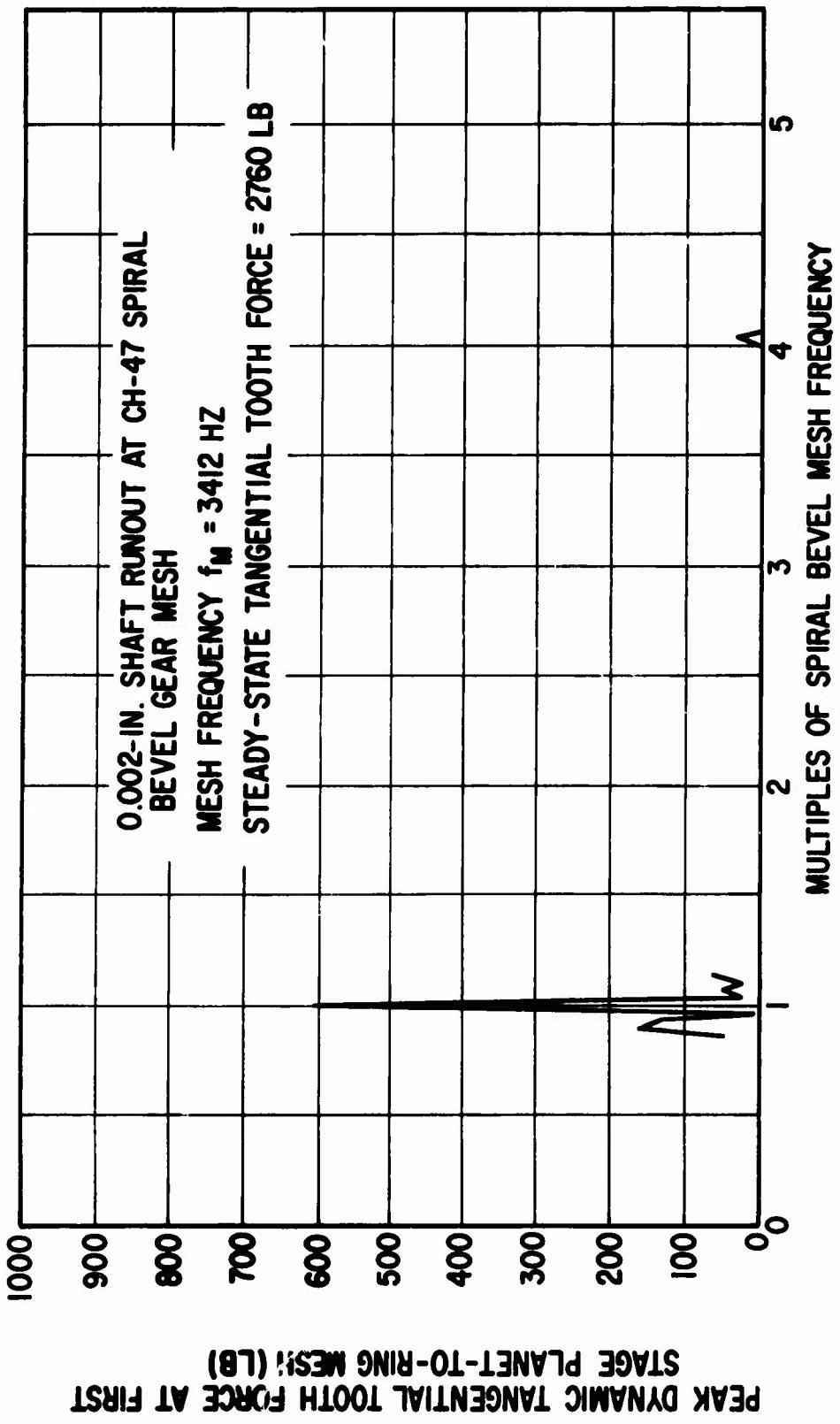
Figure 19. Calculated Dynamic Tooth Force at CH-47 Planet-Ring Gear Mesh.

38

DISCUSSION OF RESULTS

DISCUSSION OF TASK I RESULTS

The planet-pass induced vibration given by Equation (17) is the amplitude-time history of radial displacement at a fixed point on the ring gear casing. The zero time is arbitrarily chosen to be the moment when planet A (see Figure 2) is at the observation point. As time progresses, planets D, B and C pass the observation point in sequence. This sequence repeats with a frequency equal to the planet orbiting speed ω_b.

Since ring gear radial vibration results from the planet-ring gear mesh dynamic tooth force, the vibration amplitude is large when the planet is close to the observation point and smaller when the planet is more distant. This is seen from the calculated results in Figures 5, 7, 8 and 9, which are for phase angles $\psi = 37.6^o$, 0°, 90° and 142.4^o (between opposite pairs of planets), respectively. The four major large-vibration-amplitude areas in each of the figures correspond to the passage of the four planets past the fixed observation point.

In general, it appears that the shape and magnitude of the vibration data in Figures 5 through 9 are quite similar, and that only the amplitude between planet passes varies appreciably with the phase angle ψ. This is because the two components of the total response function, b_{AB} and b_{CD}, are quite localized (i.e., peaked at 0° and 90°, respectively). Also, they are identical in shape due to the axisymmetry of the ring gear casing, but with 90° phase difference (see Figure 4). This 90° phase difference corresponds to the time spacing between the passes of adjacent planets. Using the first two bumps as examples, the vibration amplitude around the passes of planets A and D (around $\theta = 0^o$ and 90°) are dominantly determined by b_{AB} and b_{CD}, respectively, without much interference between them. Only between planet passes (around $\theta = 45^o$) does appreciable interference exist, and therefore the local amplitude depends on the temporal phase difference ψ between the two response functions (see Equations (6) and (7)).

The vibration of the ring gear casing is induced by the passing of the planet gears and originates in the dynamic tooth forces which exist in the planet-ring gear tooth meshes. The vibration occurs, therefore, at the gear tooth mesh frequency, f_M, modulated by the planet-pass frequency.

This is shown in the frequency spectrum plots of Figures 6 and 10. It is seen that the mesh frequency is the center frequency and that around it, there are a number of sidebands which are found at mesh frequency plus or minus (in general) integer multiples of half of the planet-pass frequency f_p. In the special case of $\psi = 0$, four equally spaced planets (small positional offset δ has been neglected) pass the observation point with orbiting speed ω_b. Dynamically, this is equivalent to one planet passing this point with planet-pass frequency f_p (where $f_p = 4\omega_b$). Therefore, sidebands occur only at $f_M \pm n f_p$, where n is an integer. In the more

general case where $\psi \neq 0$, there is some phase difference between the planet pairs (A,B) and (C,D). Each pair passes the observation point with a frequency of $f_p/2$. Therefore, sidebands in general appear at

$$f_M \pm n \frac{f_p}{2}.$$

Comparison of the four spectrum diagrams shown in Figures 6 and 10 reveals that the effect of the phase angle ψ is to increase the sideband amplitude at mesh frequency plus and minus integer multiples of $f_p/2$. For $\psi = 0$, the amplitudes at these sidebands are zero, while for $\psi = 142.4°$, the corresponding amplitudes are even greater than those at the neighboring frequencies of $f_M \pm n\, f_p$.

Under some circumstances, it may be desirable to control the vibration amplitudes at certain sidebands. For the CH-47 lower planetary gear system, the phase angle ψ is a major controlling parameter of sideband amplitudes for the planet-pass induced vibration. The angle in turn is determined by other gear parameters including the numbers of teeth of component gears. For example, Equation (4) indicates that the greater the number of teeth on the sun gear, the larger the phase angle. However, other gear performance characteristics such as speed ratio, load distribution, etc., must be considered when gear parameters are altered to control the value of ψ.

Finally, it should be noted that the analysis used herein assumes that the normal components of the planet gear dynamic tooth forces vary sinusoidally with time. This variation occurs about the nominal steady-state normal tooth force component which accompanies the transfer of torque. Passage of this nominal steady-state force itself causes quasi-static ring gear deflections, which are ignored in the vibration calculations.

DISCUSSION OF TASK II RESULTS

Vibration can be excited by nonuniform tooth deflection and tooth profile characteristics during the mesh of even precisely machined gears. If the center distance and nominal tooth load are constant and all other gear parameters are the same from one pair of teeth to the next, the nonuniform tooth deflection pattern in one mesh cycle will repeat in all successive cycles. The frequency content of this tooth-mesh-induced vibration will consist, therefore, of only the mesh frequency and its harmonics. However, if there is any variation in center distance or tooth load, or any change of any other gear parameters from mesh to mesh, other vibration frequencies (the so-called sidebands) are introduced. The results of this investigation have clearly shown this point.

From the frequency spectra shown in Figures 12, 13, and 15, it is seen that major sidebands due to variation in center distance occur around the mesh frequency and its harmonics. In all cases the mesh frequency is still the most dominating frequency. A comparison of Figures 12 and 13 reveals that the sideband amplitudes depend quite strongly on the

40

magnitude of the center distance variation. The general shape and magnitude of the harmonic components in Figure 13 (0.002-in. runout) are similar to those shown in Figure 12 (0.001-in. runout). However, the amplitudes at major sidebands in Figure 13 are about twice those at corresponding sidebands shown in Figure 12. Furthermore, in the 0.002-in. runout case, the sideband amplitudes around the fourth and fifth harmonics are even larger than the harmonic amplitudes.

Actual vibration frequency spectrum measurements [8] taken from an accelerometer mounted on the CH-47 rotor-drive gearbox bear some similarity to those in Figures 12, 13, and 15. Output from this accelerometer, located on the outside of the gearbox near the spiral bevel gear shaft support bearings, is reproduced in Figure 20. It should be noted that the noise signals shown in Figure 20 are generated not only by the spiral bevel gear mesh but also by a number of other possible vibration sources, such as gear runout, planet-pass, etc., occurring in the drive system. The signal is strongest at the spiral bevel mesh frequency because the accelerometer is located near the spiral bevel gears' shaft support bearings. The sideband with large amplitude near the spiral bevel gear mesh fundamental is separated by 118 Hz from the mesh frequency. This difference is the rotational speed of the input pinion. Therefore, this sideband is clearly due to input shaft runout, and it is equivalent to the relatively large-amplitude sidebands around the mesh frequency shown in Figures 12 and 13.

The sideband amplitudes produced by tooth load variations as shown in Figures 14 and 16 are quite large in comparison with the harmonic components. In both cases the amplitude of the first sideband is greater than the amplitudes at high harmonics of the mesh frequency. These large sideband amplitudes may be attributed to the large load variation relative to the nominal tooth load (500 lb vs. 2760 lb for spiral bevel gear mesh and 400 lb vs. 2103 lb for lower planetary planet-to-ring gear mesh).

In the example of tooth support compliance variation, five consecutive teeth were assumed to have a finite compliance of 10^{-6} in./lb in the tangential direction. This represents a case in which the lower planetary ring gear casing has a relatively weak local elastic stiffness. This finite support compliance produces tangential tooth displacement in addition to that due to normal tooth bending, shear, rotation and contact deformation during mesh. Figure 17 shows that the sideband amplitudes resulting from this compliance consist of a number of bumps superimposed on the harmonic components. The amplitudes at small sideband frequencies are large, and those at the first few sidebands are even greater than the amplitude at the gear mesh frequency. This is because the nominal compliance with respect to tooth deflection during gear mesh is only on the order of

10^{-7} in./lb, which is one order of magnitude smaller than the assumed local tooth support compliance.

In all of the cases studied in this investigation, the frequency spectrum is discrete (i.e., the amplitudes are nonzero only at discrete frequencies), because the frequency of variation of the gear

41
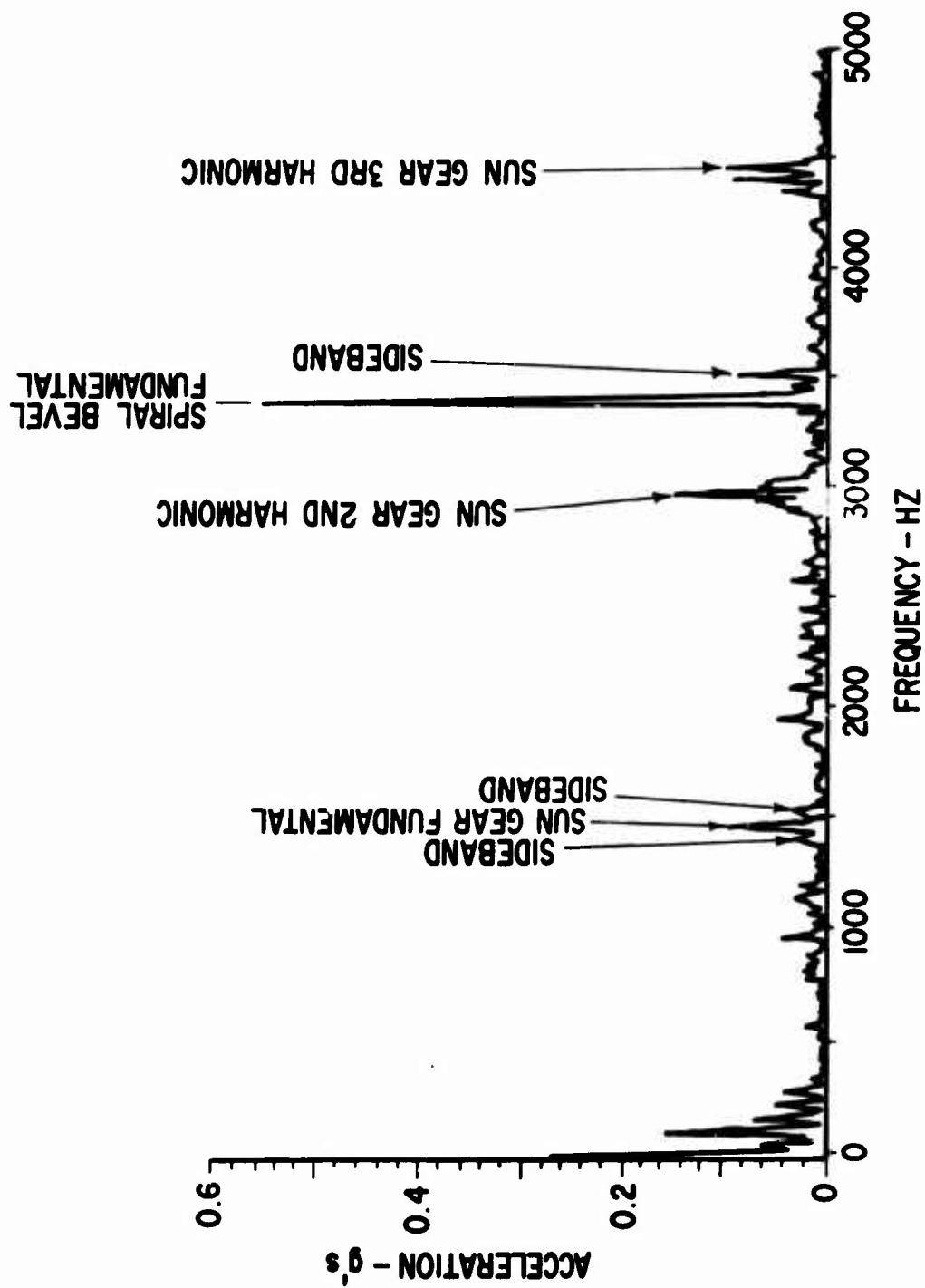
Figure 20. Vibration Spectrum Measured Near the Spiral Bevel Gears (From Reference 8).

42

parameter selected for study is in all cases a rational fraction of the gear mesh frequency. There thus always exists a base period over which the tooth displacement pattern repeats itself. This base period is an integer multiple of the gear mesh time, which is the reciprocal of the mesh frequency. Therefore, the vibration frequencies are integer multiples of the reciprocal of the base period, and the frequency spectrum is thus discrete. The frequency spectrum is obtained by performing a Fourier analysis of the periodic tooth deflection pattern.

If the variation of the gear parameter is random, or if its frequency is an irrational fraction of the mesh frequency, the corresponding frequency spectrum of the gear-mesh-induced vibration will be continuous. The subroutine SPECT may be used to compute the power spectral density function based on the tooth deflection data over a large number of mesh cycles in such cases.

43

CONCLUSIONS

The following conclusions are drawn as a result of the studies reported herein:

With respect to planet-pass vibration sidebands:

1. Methods have been developed for predicting geometrically-induced planet-pass vibration sidebands which accompany normal planetary gear reduction operation.

2. Planet-pass vibration sideband amplitudes may exceed that of the base signal, and plans for dealing with them must be part of any vibration and noise reduction program.

3. Planet-pass vibration sideband frequencies exist both below and above the base signal at integer multiples of one-half planet-pass frequency in four-planet systems with opposite pairs of planets in phase.

4. Planet-pass vibration sideband spectra are affected by the phase relationships of the planets, and spectra for several such relationships have been determined for the CH-47 forward rotor drive gearbox first-stage planetary reduction.

With respect to vibration sidebands in single gear meshes:

1. Methods have been developed for predicting vibration sidebands which are produced by gear runout, dynamic variations in tooth transmitted force, and tooth support discontinuities.

2. Shaft runout vibration sideband amplitudes may exist with significant amplitudes. They must therefore be considered in vibration and noise reduction efforts. Conversely, such sidebands if detectable could be used for the diagnosis of improperly assembled shafts and bearings.

3. Dynamic transmitted tooth force variations can produce vibration sidebands with significant amplitudes. While the presence of such signals is important from the vibration and noise reduction standpoint, the most important aspects of this type of sideband are as follows:

   a) This type of disturbance implies the presence of additional dynamic loads on gear teeth and bearings, with resulting degradation of component lifetimes. The importance of this type of dynamic force on gear and bearing life has yet to be assessed.

   b) A major source of vibration signals within operating gearboxes has been explained, thereby reducing the number of unknown

44

signals which must be explained in any diagnostic exercise. Likewise, the dynamic interactions between gear meshes in multiple-mesh gear trains have been explained.

4. Vibration sidebands of a very distinctive character are predicted herein to be produced by gear meshes with tooth support discontinuities, such as cracks. Consequently, a very important diagnostic method has been identified for identifying gear structural integrity problems which may be introduced during manufacture or which may appear in service.

In summary, methods have been devised both for designing low-vibration and noise gear reductions and for identifying the existence of several types of gear problems. It is felt that the diagnostic potential of the vibration analysis methods described herein is of considerable importance.

45

RECOMMENDATIONS

The results reported herein strengthen considerably an already valuable body of technology which relates gear train component condition to measurable symptoms. The most important aspect of this technology is that much of it appears as computer-implemented analytical procedures which can be utilized by the gearbox designer.

Recommendations for future efforts in this important area fall into three specific areas:

1. It is recommended that the analytical procedures next be extended to include high-contact-ratio gearing and coupled response of gear train components.

2. It is recommended that the high-frequency vibration analysis tools be utilized in their present form, where applicable, in the design of future gearboxes; further, that the results of this usage be documented in specific instances, particularly where comparative testing accompanies this usage, for feedback to this technology program.

3. It is recommended that the use of high-frequency gearbox vibration technology be included as an integral part of future efforts directed at drive train condition monitoring and diagnosis, and at component life and/or failure prognosis.

LITERATURE CITED

1. Laskin, I., Orcutt, F. K., and Shipley, E. E., ANALYSIS OF NOISE GENERATED BY UH-1 HELICOPTER TRANSMISSION, Mechanical Technology Incorporated; USAAVLABS Technical Report 68-41, U.S. Army Aviation Materiel Laboratories, Fort Eustis, Virginia, June 1968, AD 675 457.

2. Badgley, R. H., and Laskin, I., PROGRAM FOR HELICOPTER GEARBOX NOISE PREDICTION AND REDUCTION, Mechanical Technology Incorporated; USAAVLABS Technical Report 70-12, U.S. Army Aviation Materiel Laboratories, Fort Eustis, Virginia, March 1970, AD 869 822.

3. Badgley, R. H., MECHANICAL ASPECTS OF GEAR-INDUCED NOISE IN COMPLETE POWER TRAIN SYSTEMS, ASME Paper No. 70-WA/DGP-1, presented at the ASME Winter Annual Meeting, New York, December 1970.

4. Badgley, R. H., and Chiang, T., INVESTIGATION OF GEARBOX DESIGN MODIFICATIONS FOR REDUCING HELICOPTER GEARBOX NOISE, Mechanical Technology Incorporated; USAAMRDL Technical Report 72-6, Eustis Directorate, U.S. Army Air Mobility Res & Dev Lab, Ft. Eustis, Va, March 1972, AD 742 735.

5. Badgley, R.H., GEARBOX DYNAMICS — THE KEY TO UNDERSTANDING AND REDUCING ACOUSTIC-FREQUENCY ENERGY IN GEARED POWER TRAINS, presented at the Meeting of the Aerospace Gearing Committee of the American Gear Manufacturers Association, Cleveland, Ohio, January 17-18, 1972.

6. Chiang, T., and Badgley, R.H., REDUCTION OF VIBRATION AND NOISE GENERATED BY PLANETARY RING GEARS IN HELICOPTER AIRCRAFT TRANSMISSIONS, ASME Paper No. 72-PTG-11, presented at ASME Mechanisms Conference & International Symposium on Gearing and Transmissions, San Francisco, California, October 8-12, 1972.

7. Badgley, R.H., REDUCTION OF NOISE AND ACOUSTIC-FREQUENCY VIBRATIONS IN AIRCRAFT TRANSMISSIONS, AHS Paper No. 661, presented at the 28th Annual National Forum of the American Helicopter Society, Washington, D C., May 1972.

8. Sternfeld, H., Schairer, J., and Spencer, R., AN INVESTIGATION OF HELICOPTER TRANSMISSION NOISE REDUCTION BY VIBRATION ABSORBERS AND DAMPING, Boeing Vertol Company; USAAMRDL Technical Report 72-34, Eustis Directorate, U.S. Army Air Mobility Research and Development Laboratory, Ft. Eustis, Virginia, August 1972, AD 752 579.

9. Hartman, R. M., and Badgley, R. H., MODEL 301 H1H/ATC TRANSMISSION NOISE REDUCTION PROGRAM-TEST RESULT REPORT, The Boeing Vertol Company, USAAMRDL Technical Report (Not Yet Issued), U.S. Army Air Mobility Research and Development Laboratory, Fort Eustis, Virginia.

10. Badgley, R. H., and Hartman, R. M., GEARBOX NOISE REDUCTION: PREDICTION AND MEASUREMENT OF MESH-FREQUENCY VIBRATIONS WITHIN AN OPERATING HELICOPTER ROTOR-DRIVE GEARBOX, ASME Paper No. 73-DET-31, presented at the ASME Design Engineering Technical Conference, Cincinnati, Ohio, September 9-12, 1973.

11. Hartman, R. M., A DYNAMICS APPROACH TO HELICOPTER TRANSMISSION NOISE REDUCTION AND IMPROVED RELIABILITY, presented at the 29th Annual National Forum of the American Helicopter Society, Washington, D.C., May 1973.

12. Bendet, S. J., and Piersol, A. G., MEASUREMENT AND ANALYSIS OF RANDOM DATA, John Wiley & Sons, 1966.

13. Buckingham, Earle, ANALYTICAL MECHANICS OF GEARS, Dover Publications, Inc., New York, 1963, p 324.

APPENDIX I
CALCULATION OF POWER SPECTRAL DENSITY FUNCTION

The method of calculation presented herein follows that given in [12]. Let n be the number of calculation points in one tooth mesh cycle. The time interval between data points is

$$\Delta t = \frac{1}{n \, f_M} \tag{25}$$

where f_M is the mesh frequency. The cutoff frequency is defined as

$$f_c = \frac{n \, f_M}{2} \tag{26}$$

The total time of record is defined as

$$T_r = n_M \cdot n \cdot \Delta t$$

$$= \frac{n_M}{f_M} \tag{27}$$

where n_M is the number of mesh cycles over which tooth deflection data is recorded.

The autocorrelation function is, by definition,

$$R(\tau) = \lim_{T \to \infty} \frac{1}{T} \int_0^T x(t) \, x(t + \tau) \, dt \tag{28}$$

where x is the tooth deflection and t is the time. The power spectral density function is related to $R(\tau)$ by

$$G(f) = 4 \int_0^\infty R(\tau) \cos 2\pi \, f\tau \, d\tau \tag{29}$$

where f is frequency.

Tooth deflection x is known numerically at discrete points separated by Δt. Let

$$x_i = x(i \, \Delta t) \qquad i = 1, 2, \ldots, nn_M \tag{30}$$

The autocorrelation function at displacement $r \, \Delta t$ may be estimated by

49

$$\widetilde{R}_r \, (r \, \Delta t) \;=\; \frac{1}{nn_M - r} \sum_{i=1}^{nn_M - r} x_i \, x_{i+r} \tag{31}$$

$$r \;=\; 0, \, 1, \, 2, \, \ldots, \, m$$

where r is the lag number and m the maximum lag number. This maximum lag number determines the maximum displacement and the equivalent resolution bandwidth for power spectral calculation as follows:

$$\tau_{max} \;=\; m \, \Delta t \;=\; \frac{m}{n \, f_M} \tag{32}$$

$$B_e \;=\; \frac{1}{\tau_{max}} \;=\; \frac{n \, f_M}{m} \tag{33}$$

It is desirable to keep τ_{max} less than one-tenth of the time of record T_r. This will avoid certain instabilities that can occur in autocorrelation function estimates. In the calculation, τ_{max} is set to be about 1/20 of T_r.

m is then determined by

$$m \;\leq\; \frac{n \, n_M}{20} \tag{34}$$

In other words, m is set equal to the integer part of the right-hand side.

The numerical approximation of Equation (29) is

$$\widetilde{G} \, (f) \;=\; 2 \, \Delta t \left[\widetilde{R}_o + 2 \sum_{r=1}^{m-1} \widetilde{R}_r \cos\left(\frac{\pi r \, f}{f_c} \right) + \widetilde{R}_m \cos\left(\frac{\pi m \, f}{f_c} \right) \right] \tag{35}$$

The numerical estimate of the power spectral function should be calculated only at the m+1 special discrete frequencies where

$$f \;=\; \frac{k \, f_c}{m} \qquad k \;=\; 0, \, 1, \, 2, \, \ldots \, m \tag{36}$$

This will provide m/2 independent spectral estimates since the bandwidth B_e is $\frac{2 \, f_c}{m}$. At these discrete frequencies,

$$\widetilde{G}_k \;=\; \frac{2}{n \, f_M} \left[\widetilde{R}_o + 2 \sum_{r=1}^{m-1} \widetilde{R}_r \cos\left(\frac{\pi r \, k}{m} \right) + (-1)^k \, \widetilde{R}_m \right] \tag{37}$$

50

The index k is called the harmonic number. $\tilde{G}_k$ is the "raw" estimate of the power spectral density function at harmonic k. The "smooth" estimate G_k at harmonic k is

$$G_o = 0.5 \, \tilde{G}_o + 0.5 \, \tilde{G}_1$$

$$G_k = 0.25 \, \tilde{G}_{k-1} + 0.5 \, \tilde{G}_k + 0.25 \, \tilde{G}_{k+1} \qquad k = 1, 2, \ldots m-1 \qquad (38)$$

$$G_m = 0.5 \, \tilde{G}_{m-1} + 0.5 \, \tilde{G}_m$$

The ratio of the frequency at harmonic k to mesh frequency is

$$\frac{f_k}{f_M} = \frac{kn}{2m} \qquad (39)$$

where m is given by Equation (34). The frequency interval is approximately

$$\Delta f_k \sim \frac{10 \, f_M}{n_M} \qquad (40)$$

The above method of calculation has been programmed in subroutine SPECT. This subroutine has been tested successfully by using a simple sine function over a hundred cycles of time. A sharp peak was clearly seen at the single frequency of the sine function. In the application to the gear mesh induced vibration, Equation (40) indicates that n_M should be set

equal to about a hundred times the minimum number of cycles to complete a base period of tooth deflection variation. Therefore, for periodic tooth deflection variation, Fourier analysis (subroutine FOUR) is more economical to use to extract the frequency content of the induced vibration, since it requires the tooth deflection data over only the minimum number of mesh cycles to cover one base period. However, for random variation of gear parameters, only subroutine SPECT can be used to obtain the frequency spectrum of the induced vibration.

51

APPENDIX II
COMPUTER PROGRAM FOR PREDICTION OF GEAR MESH EXCITATION SPECTRA

Input Variables, Format, and Instructions

Card 1   Title, columns 2 through 72.

Card 2   Control numbers.   Format (7I5)

     a.   NMC   Number of mesh cycles.

                  Place the last digit of this number in column 5.

     b.   INT   Identification as to whether this control card represents the last complete set of input data being submitted.
If more sets of input data follow, use 0.
If this is the last set, use 1.

                  Place this digit in column 10.

     c.   MN   Classification of the types of spur gears to be considered.
If both the driving and the driven gears are external gears, use 1.
If the driving gear is an external gear and if the driven gear is an internal (ring) gear, use 0.
(The program will not run properly if the internal gear is submitted as the driving gear.)

                  Place this digit in column 15.

     d.   MMM   Number of initial terms of the Fourier analysis for which coefficients will be printed, beyond the coefficient for the constant term. This number cannot exceed (FI x NMC + NMC/2), where FI is the input variable submitted on card 4.

                  Place the last digit of this number in column 20.

     e.   IPLT   Instruction as to whether the calculated tooth meshing error is to be plotted.
If tooth meshing error is to be plotted, use 1.
If plotting is to be bypassed, use 0.

                  Place this digit in column 25.

     f.   IFOUR   Instruction as to whether Fourier analysis of the tooth meshing error is to be performed.
If it is to be performed, use 1.
If it is to be bypassed, use 0.

                  Place this digit in column 30.

g. ISPECT Instruction as to whether power spectral density function for the tooth meshing error is to be calculated.
If it is to be calculated, use 1.
If it is to be bypassed, use 0.

Card 3 Gear design data. Format (6E 13.5)

a. FN1 Number of teeth in the driving gear.

Use columns 1 through 13. (Do not omit decimal point.)

b. FN2 Number of teeth in the driven gear.

Use columns 14 through 26. (Do not omit decimal point.)

c. RB1 Base circle radius of driving gear, in.

Use columns 27 through 39.

d. RØ1 Radius to the outside diameter of the driving gear, in. This should be reduced by any radial loss in working surface at the tip of the teeth, as from tip rounding or chamfering.

Use columns 40 through 52.

e. RØ2 Radius to the outside diameter of the driven gear, or R12 if external, and to the inside diameter, if internal, in. This should be corrected for any radial loss in working surface at the tip of the teeth, as from tip rounding or chamfering. In the case of an internal gear, this radius must be equal to or greater than the base circle radius. No check for this is provided.

Use columns 53 through 65.

Card 4 Gear design data, continued. Format (6E 13.5)

a. RT1 Radius to the beginning (near the base of the tooth) of the involute profile on the driving gear, in.

This is used in the program only in a design check as to whether adequate length of involute has been provided for contact on the teeth of the mating gear up to its tip. If this radius is not specified in the gear design data, this check may be bypassed by substituting the root circle radius.

Use columns 1 through 13.

53

b. RT2   Radius to the beginning (near the base of the tooth) of the involute profile on the driven gear, in. See above for substitute when not specified.

Use columns 14 through 26.

c. RM1   Radius to the root circle of the driving gear, in. If the radius submitted is smaller than the computed base circle radius, this is noted in the output, and the input value of root radius is used at some points in the program. If the root radius is sufficiently smaller than the base circle radius so that the root fillet center lies inside the base circle, the tooth outline between the base circle and the fillet is assumed to be a radial line by the program.

Use columns 27 through 39.

d. RM2   Radius to the root circle of the driven gear, in. For the case of an external gear, the same comments as above apply.

Use columns 40 through 52.

e. FI   Number which indirectly establishes the number of calculation points. The number of these points will equal one plus twice the value of FI. The calculation points may be viewed as selected contact points on the true involute profile, extended where necessary. These contact points with the mating involute are associated with specific angular positions taken by the gear as it is rotated, where the angular positions correspond to uniform subdivisions of the tooth spacing angle. A greater number of these points will give more closely spaced point-by-point output data. A greater number will also give more accurate calculations of tooth deflections and Fourier coefficients. A value of FI equal to 12 giving 25 calculation points has been found to be convenient.

Use columns 52 through 65. (Do not omit decimal point.)

f. T1   Circular tooth thickness at the pitch circle of the driving gear, in. The radius of the pitch circle is as defined in card 3. If not specified in the gear design data, it may be estimated as one-half of the difference between the actual circular pitch and the working backlash.

Use columns 66 through 78.

54

Card 5   Gear design data, continued. Format (5E 13.5)

    a. T2   Circular tooth thickness at the pitch circle of the
        driven gear, in. The comments for Tl also apply
        here.

        Use columns 1 through 13.

    b. Fl   Effective tooth face width of the driving gear, in.
        Where the face widths of the two gears are similar,
        use the actual face width without any reduction for
        normal end chamfering or rounding. Where one tooth
        is much wider, use as its effective face width an
        amount suitably larger than the narrower width to
        allow for the limited additional support that the
        greater width provides.

        Use columns 14 through 26.

    c. F2   Effective tooth face width of the driven gear, in.
        The comments for Fl also apply here.

        Use columns 27 through 39.

    d. RF1   Fillet radius on the driving gear, in.

        Use columns 40 through 52.

    e. RF2   Fillet radius on the driven gear, in.

        Use columns 53 through 65.

Card 6   Gear material properties. Format (6E 13.5)

    a. YE1   Young's modulus (in bending) for the material of
        the driving gear, $lb/in.^2$

        Use columns 1 through 13.

    b. YE2   Young's modulus (in bending) for the material of
        the driven gear, $lb/in.^2$

        Use columns 14 through 26.

    c. GE1   Shear modulus for the material of the driving gear,
        $lb/in.^2$

        Use columns 27 through 39.

    d. GE2   Shear modulus for the material of the driven gear,
        $lb/in.^2$

        Use columns 40 through 52.

55

e. PØS1   Poisson's ratio for the material of the driving
          gear. Since this ratio is used only in the allow-
          ance for the "wide beam effect," it should be re-
          duced for the cases where tooth face width is not
          much greater than tooth thickness, with a limiting
          value of zero when the teeth have a width smaller
          than the thickness.

          Use columns 53 through 65.

f. PØS2   Poisson's ratio for the material of the driven
          gear. Comments for PØS1 also apply here.

          Use columns 66 through 78.

There are NMC sets of the following Card 7 and Card 8. Each set supplies
center distance, tooth spacing errors, tooth profile errors, tooth support
compliances and tangential load for one mesh cycle.

Card 7   Center distance and tooth spacing error data. Format (3E 13.5)

a. CL   Center distance, in.
          This must be the actual center distance, including
          any substantial spreading under load.

          Use columns 1 through 13.

b. VPT1   Tooth spacing error on the driving gear, in. This
          error is based on the distance between the pitch
          points of successive teeth, but the error is ad-
          justed to apply to the direction of the line of
          action. This adjustment is accomplished by multi-
          plying the pitch line error by the cosine of the
          pressure angle. The error is positive if the
          measured spacing is smaller than the desired
          spacing.

          Use columns 14 through 26.

c. VPT2   Tooth spacing error on the driven gear, in. The
          comments under VPT1 also apply here.

          Use columns 27 through 39.

Cards 8-1 to 8-2N   Point-by-point data. Format (5E 13.5)

          Total number of cards equal to twice the number of
          calculation points (N_J) between pitch points of
          adjacent teeth, or the same as two plus four times
          the value of F1 (see card 4). This specifies that
          cards must be introduced even if it is known that
          there is no contact at the particular calculation

56

point or even if the tooth profile does not actually extend to the calculation point. As explained below, a blank card may be used for these points.

For the driving gear, the first card is for the calculation point located (N_J-1) points preceding the pitch point (or inside the pitch circle); the (N_J)th card is for the pitch point; the last or $(2N_J)$th card is for the calculation point located (N_J) points after the pitch point (or outside the pitch circle). The last point may also be described as the point of contact on one meshing tooth when the pitch point is the point of contact on the next meshing tooth.

For the driven gear which is an external gear, the first card is for the calculation point located (N_J) points before the pitch point (or inside the pitch circle); the (N_J+1)th card is for the pitch point; the last or $(2N_J)$th card is for the calculation point located (N_J-1) points after the pitch point (or outside the pitch circle). The point for the first card may also be described as the point of contact on one meshing tooth when the pitch point is the point of contact on the previous meshing tooth.

For the driven gear which is an internal gear, the first card is for the calculation point located (N_J) points following the pitch point (or outside the pitch circle); the (N_J+1)th card is for the pitch point; the last or $(2N_J)$th card is for the calculation point located (N_J-1) points before the pitch point (or inside the pitch circle). The point for the first card may also be described as the point of contact on the meshing tooth when the pitch point is the point of contact on the next meshing tooth.

a. ZJ1   Deviation of the point on the actual tooth profile on the driving gear from the true involute (as defined by the gear design data), in. This true involute is positioned relative to the actual profile so that its deviation at the pitch point is zero. Where the deviation represents material added to the true involute, it is positive; where it represents material subtracted, it is negative. The deviation is measured normal to the involute profile. If the profile does not extend to the particular calculation point or if it is known that the mating gear will not contact at this point, the deviation may be noted as zero.

Use columns 1 through 13.

57

b. UJ1   Tooth support compliance, or any compliance supple-
            mentary to the tooth compliance included in the
            analysis, on the driving gear, in./lb. This com-
            pliance is the deflection under unit load at the
            calculation point on the profile in the direction
            of the load (or normal to the profile). A uniform
            compliance for all calculation points, such as
            would result from a uniform gear shaft compliance,
            would not affect the final results as far as motion
            irregularities or load transfer is concerned; it
            would only increase the mean deviation in transmit-
            ted motion.

            Use columns 14 through 26.

c. ZJ2   Deviation of the point on the actual tooth profile
            on the driven gear from the true involute, in. The
            comments under ZJ1 also apply here.

            Use columns 27 through 39.

d. UJ2   Tooth support compliance, etc., on the driven gear,
            in./lb. The comments under UJ1 also apply here.

            Use columns 40 through 52.

e. WT   Total load, tangent to the pitch circle, transmitted
            by the gear teeth, lb.

            In the first N card 8s, WT should be left blank.
            WT in the second N card 8s represents the loads at
            the N calculation points in one gear mesh.

            Use columns 53 through 65.

Card 9 Gear Speed. Format (I5,E 13.5)

a. NWS   Identification as to whether the input speed is the
            speed of driving or driven gear.
            If driving gear speed is inputted, use 1.
            If driven gear speed is inputted, use 2.

            Place this digit in column 5.

b. WS   Driving or driven gear speed, rpm.

            Use columns 6 through 18.

Output Variables and Explanations

1. Title

2. Control numbers — NMC, INT, NMZ, MMM, as in input card 2.

3. Design — FI(=I), FN1(=N1), RB1, RO1, TR1, RM1
    BLANK, FN2(=N2), BLANK, RO2 or RI2, RT2, RM2
    T1, F1, RF1, YE1, GE1, PØS1
    T2, F2, RF2, YE2, GE2, PØS2
    all as in input cards 3 through 6.

Items 4-11 are printed for every mesh cycle, totally NMC cycles.

4. Mesh cycle identification and center distance.

5. Input listing of profile error and supplementary compliance — ZJ1, UJ1, ZJ2, UJ2 as in input card 8.

6. Pressure angle, degrees.

7. Incidental data — RP1, RB1, BA1, BR1, AT1
                      RP2, RB2, BA2, BR2, AT2

   where: RPL   pitch circle radius of driving gear, in.

           RP2   pitch circle radius of driven gear, in.

           RB1   base circle radius of driving gear, in.

           RB2   base circle radius of driven gear, in.

           BA1   arc of approach of driving gear, rad.

           BA2   arc of approach of driven gear, rad (negative on internal gears).

           BR1   arc of recess of driven gear, rad.

           BR2   arc of recess of driving gear, rad (negative on internal gears).

           AT1   angle of rotation of driving gear from the position at which the line of action intersects the involute at the start of the involute profile to the position at which the line of action intersects the involute at the pitch point, rad.

           AT2   similar angle of rotation of driven gear, rad.

   Check statement when part of the profile extends within the base circle.

   Program will continue in any case, and, where necessary, the root radius will be set equal to the base circle radius. However, in calculating the tooth profile and the tooth deflections, the

original root circle radius will be used with the specified fillet radius. If the root circle lies inside the base circle by more than this fillet radius, a radial line is assumed to connect fillet and involute.

8. Driving gear data — J1, CJ1, AJ1, QJ1ABC, XJ1, YJ1, XME1(=X), YME1(=Y), J1, QJ1A, QJ1B, QJ1C

   where: J1   identification number for calculation points (see under F1 of card 4 in the input data). Listed for values of (-2I) to (2I+1).

   CJ1   condition of engagement if equal to one and no engagement if equal to zero.

   AJ1   angle of rotation from the position of contact at the pitch point to the position of contact at the calculation point - negative for points inside the pitch circle, rad.

   XJ1   coordinates of the calculation point on the involute
   and   profile with the origin at the gear center and with
   YJ1   the X-axis as the centerline of the tooth, given only for the points at which contact will take place with the mating gear, in.

   XME1   coordinates of the point on the root circle midway
   and   between the tangent point of the fillet radius and
   YME1   the involute profile extended (and radial inside the base circle), in. This point is considered to be the end of the effective base of the tooth for deflection purposes.

   QJ1A   elastic compliance of the gear tooth acting as a cantilever beam in bending only, normal to the profile at the calculation point, in./lb.

   QJ1B   elastic compliance of the gear tooth as a cantilever beam in shear only; otherwise as above.

   QJ1C   elastic compliance of the gear tooth as a rigid member rotating in its supporting structure; otherwise as above.

   QJ1ABC combined compliance of the three above, in./lb.

9. Driven gear data — J2, BLANK, AJ2, QJ2ABC, XJ2, YJ2, XME2, YME2, J2, QJ2A, QJ2B, QJ2C

   where: J2   identification number for the calculation points. For external gears, J2 is listed for values of (-2I-1) to (2I). For this case, contact takes

60

place between points of the two gears for which J1 = -J2. For internal gears, J2 is listed for values of (2I+1) to (-2I). For this case, contact takes place between points of the two gears for which J1 = J2.

All other variables are similar to their counterparts for the driving gear.

10. Input tooth spacing error data — VPT1, VPT2

    as in input card 7.

11. Tooth meshing errors, loads and contact compliance — JC1, AJC1, EJT, WTC, WTD, WN, WT, QJD

    where: JC1   identification number for the calculation point on the first tooth of the driving gear, starting with the first point after the pitch point and ending with the point corresponding to the pitch point of the next tooth.

    AJC1   angle of rotation of the driving gear from the position with contact at the pitch point of the first mesh cycle to the position with contact at the calculation point, rad. The last angle in the first mesh cycle is the tooth spacing angle.

    EJT   tooth meshing error or deviation from pure conjugate action, as a pitch-line linear measurement of the motion of the driven gear leading the driving gear, in. A negative value indicates that the driven gear is lagging the driving gear, as might be caused by deflection of the teeth.

    WTC   tangential load carried by the first pair of teeth, lb.

    WTD   tangential load carried by the second pair of teeth, lb.

    WN   total normal load transmitted by the teeth, lb.

    WT   input tangential tooth load, lb.

    QJD   contact or Hertzian compliance combined for both teeth at the contact point, in./lb.

12. List of tooth meshing error over NMC mesh cycles — JC1, AJC1, EJT

    where: JC1   identification number for the calculation point. The last value should be equal to (NMCxN).

61

AJC1   same as AJC1 in item 11.

EJT   same as EJT in item 11.

13. Plot of tooth meshing error.
    Appears only if IPLT in input card 2 is set to be 1.

14. Fourier coefficients — I, A, B, C, KM

    where: I   order of the harmonic to which the coefficients
                   apply. The zero order refers to the constant
                   component.

           A   the Fourier coefficient of the consine or real
                   component for that harmonic of the meshing error,
                   in. The value for $I = 0$ is twice the constant
                   component or mean value of the meshing error.

           B   the Fourier coefficient of the sine or imaginary
                   component for that harmonic of the meshing error,
                   in.

           C   square root of $(A^2 + B^2)$. Appears only if IFOUR
                   in input card 2 is set to be 1.

           KM   ratio of frequency to tooth mesh frequency.

The following output is concerned with the power spectral density function
of the tooth meshing error. Appears only if ISPECT in input card 2 is set
to be 1.

15. Mesh frequency, cps

16. Incidental data — FC, FO, BE, H, TR, TMAX, SM

    where: FC   cutoff frequency, cps.

           FO   fundamental frequency, cps.

           BE   equivalent resolution bandwidth, cps.

           H   sampling interval, cps.

           TR   total record time, sec.

           TMAX   maximum displacement, sec.

           SM   maximum lag number.

17. Power spectral density function — K, FR, GK, GKK, KM

    where: K   harmonic number, from 0 to SM.

62

FR   frequency, cps.

GK   "raw" power spectral density function, in.^{2}

GKK   "smooth" power spectral density function, in.^{2}

KM   ratio of frequency to tooth mesh frequency.

```
             PROGRAM GGEAR(INPUT,OUTPUT,TAPE5=INPUT,TAPE6=OUTPUT,TAPE22)    GGEAR    2
000003       COMMON/YY/UJC1(25),UJD1(25),UJ2(25),UJC2(25),UJD2(25),ZJ1(50)  CZIG     1
         1,ZJC1(25),ZJD1(25),ZJ2(50),ZJC2(25),ZJD2(25),QJ1(50),QJC1(25),QJD1 GGEAR   4
         2(25),QJ2(50),QJC2(25),                 FJ1(50),UJ1(50),    CJC1(2  GGEAR   5
         35),CJD1(25),            AJ1(50),AJ2(50),QJC(50),QJD(50),ZJC(50),ZJD(50  GGEAR  6
         4),VJ(50),EJ1(56),FJ2(50),AJC1(25),AJC2(25),FJC1(27),QJD2(25),ZM2(  GGEAR   7
         550),UM2(50),WTC(27)                                                GGEAR    8
000003       COMMON PJ(50),CJ(50),QJ(50),AJ(50),XJ(50),YJ(50))              GGEAR    9
         1A(1500),B(1500),G(3000)                                           MAY11    1
000003       COMMON DD,BR,BA,FJ,CC,YM,NN,N,FNJ,EP,TAN,RB,GM,F,XM,MN,II,M     ALG      1
000003       COMMON QA(50),QB(50),QC(50),QA1(50),QB1(50),QC1(50),QA2(50),QB2(50  GGEAR 12
         1),QC2(50)  ,IH,IP                                                 GGEAR   13
000003       COMMON WT(50),HEAD1(6),HEAD2(6)                                GGEAR   14
000003       COMMON/GU/NMC,INT,MMM,IPLT,FN1,FN2,RB1,RO1,RO2,RT1,RT2,RM1,RM2,FI,  ALG    2
         1T1,T2,F1,F2,RF1,RF2,YE1,YE2,GE1,GE2,POS1,POS2,ANG                 ALG      3
000003       DIMENSION GGG(3000),WTCC(3000),FJCC1(3000),AANG(3000)          MAY11    2
000003       NR=5                                                           GGEAR   18
000004       NW=6                                                           GGEAR   19
000005   198 READ(NR,100) (HEAD1(I),I=1,4),(HEAD2(I),I=1,4)                 GGEAR   20
000025       READ(NR,117) NMC,INT,MN,MMM,IPLT,IFOUR,ISPECT                  MAY9     1
000047       READ(NR,112)FN1,FN2,RB1,RO1,RO2                               GGEAR   22
000065       READ(NR,112)RT1,RT2,RM1,RM2,FI,T1                              GGEAR   23
000105       READ(NR,112)T2,F1,F2,RF1,RF2                                   GGEAR   24
000123       READ(NR,112)YE1,YE2,GE1,GE2,POS1,POS2                          GGEAR   25
000143       WRITE(NW,100) (HEAD1(I),I=1,4),(HEAD2(I),I=1,4)                GGEAR   26
000163       WRITE(NW,101)                                                  GGEAR   27
000167       WRITE(NW,108)                                                  GGEAR   28
000173       WRITE(NW,109) NMC,INT,MN,MMM                                   GGEAR   29
000207       WRITE(NW,104)                                                  GGEAR   30
000213       WRITE(NW,102) FI,FN1,RB1,RO1,RT1,RM1                           GGEAR   31
000233       IF(MN) 511,510,511                                             GGEAR   32
000236   510 WRITE(NW,103)                                                  GGEAR   33
000240       GO TO 512                                                      GGEAR   34
000241   511 WRITE(NW,160)                                                  GGEAR   35
000245   512 WRITE(NW,158)THETP,FN2,RO2,RT2,RM2                             GGEAR   36
000263       WRITE(NW,105)                                                  GGEAR   37
000267       WRITE(NW,102)T1,F1,RF1,YE1,GE1,POS1                            GGEAR   38
000307       WRITE(NW,107)                                                  GGEAR   39
000313       WRITE(NW,102)T2,F2,RF2,YE2,GE2,POS2                            GGEAR   40
000333       WRITE(NW,164)                                                  GGEAR   41
000337       ANG=0.                                                         GGEAR   42
000340       IMC=1.                                                         GGEAR   43
000342       N=2.*FI+1.                                                     GGEAR   44
000345       NN=N+N                                                         GGEAR   45
000346       IF(MN.EQ.0) T2=-T2                                             JUNE14   1
000351   150 WRITE(NW,1500)                                                 MAY3     2
000355       READ(NR,112)CL,VPT1,VPT2                                       ATT1     1
000367       WRITE(NW,1000) IMC,CL                                          GGEAR   47
000377       WRITE(NW,110)                                                  FINAL    1
000403       L=NN                                                           CZIG     2
000405       DO 209 I=1,NN                                                  GGEAR   48
000406       READ(NR,112)ZJ1(I),UJ1(I),ZJ2(I),UJ2(I),WT(I)                  GGEAR   49
000423       WRITE(NW,102)ZJ1(I),UJ1(I),ZJ2(I),UJ2(I)                       GGEAR   50
000437       ZM2(L)=ZJ2(I)                                                  GGEAR   51
```

64

```
000442          UM2(L)=UJ2(I)                                          GGEAR   52
000444          IF(L-1) 209,209,225                                    GGEAR   53
000446      225 L=L-1                                                  GGEAR   54
000450      209 CONTINUE                                               GGEAR   55
000453          CALL GEARO(CL,VPT1,VPT2)                               GGEAR   56
000455          NNN=IMC*N                                              GGEAR   57
000460          DO 200 I=1,N                                           GGEAR   58
000461          JJ=NNN+I-N                                             GU       1
000463          AANG(JJ)=AJC1(I)                                       MAY3     3
000466          GGG(JJ)=EJ1(I)                                         GGEAR   60
000470          G(JJ)=GGG(JJ)                                          GGEAR   61
000472          WTCC(JJ)=WTC(I)                                        GGEAR   62
000474      200 FJCC1(JJ)=JJ                                          MAY2     1
000500          IMC=IMC+1                                              GGEAR   64
000501          IF(IMC.LE.NMC) GO TO 150                              GGEAR   65
000503          WRITE(NW,1500)                                         MAY3     4
000507          WRITE(NW,2000)                                         MAY3     5
000513          DO 2500 I=1,NNN                                        MAY3     6
000515     2500 WRITE(NW,102)FJCC1(I),AANG(I),GGG(I)                  MAY3     7
000531          IF(IPLT.EQ.1) CALL PLT(FJCC1,GGG,WTCC,NNN)            GGEAR   66
000536          M=FI                                                   GU       3
000540          IF(IFOUR.NE.1) GO TO 3000                             MAY9     2
000542          WRITE(NW,128)                                          ALG      4
000546          CALL FOUR                                             GGEAR   67
000547          LL=MMM+1                                               GGEAR   68
000551          DO 250 I=1,LL                                          GGEAR   69
000553          LP=I-1                                                 GGEAR   70
000554          SMK=1.*LP/NMC                                          JUNE7    1
000560          RESLT=SQRT(A(I)**2+B(I)**2)                            GGEAR   71
000566      250 WRITE(NW,129)LP,A(I),B(I),RESLT,SMK                   JUNE7    2
000606     3000 IF(ISPECT.NE.1) GO TO 3500                            MAY9     3
000610          CALL SPECT                                            MAY9     4
000611     3500 CONTINUE                                              MAY9     5
000611          IF(INT)300,198,300                                    GGEAR   73
000612      300 CALL EXIT                                            GGEAR   74
000613      100 FORMAT(8A10)                                          GGEAR   75
000613      101 FORMAT(72H0   PN0335=COMPUTATIONS OF GEAR TOOTH MESHING ERRORS  GGEAR   76
                1   3-22-1966        )                                GGEAR   77
000613      102 FORMAT(7E13.5)                                        MAY9     6
000613      103 FORMAT(12H0   PRE.ANGLE7X2HN224X3HRI210X3HRT210X3HRM2)  GGEAR   79
000613      104 FORMAT(/7X1H111X2HN111X3HRB110X3HRO110X3HRT110X3HRM1)  GGEAR   00
000613      105 FORMAT(/6X2HT111X2HF111X3HRF15X12HYOUNGS MOD-12X41HSHEAR MOD-12X11  GGEAR   81
                1HPOS.RATIO-1)                                        GGEAR   82
000613      107 FORMAT(/6X2HT211X2HF211X3HRF25X12HYOUNGS MOD-22X11HSHEAR MOD-22X11  GGEAR   83
                1HPOS.RATIO-2)                                        GGEAR   84
000613      108 FORMAT(50H0 MESH CYCLES     INPUT,    DIFF.GEAR N+OF HARMONIC)  GGEAR   85
000613      109 FORMAT(4X I4,4(8X I4))                                GGEAR   86
000613      110 FORMAT(60H0INPUT LISTING OF PROFILE ERROR AND SUPPLEMENTARY COMPLI  FINAL    2
                1ANCE/6X2HZ111X2HU111X2HZ211X2HU2)                    FINAL    3
000613      112 FORMAT(6E13.5)                                        GGEAR   87
000613      117 FORMAT(8I5)                                           MAY9     7
000613      128 FORMAT(43H0CALCULATED FOURIER COEFFICIENTS FOR ERRORS//7H       19X ALG    5
                15HA(I) 13X4HB(I)14X1HC14X2HKM)                       JUNE7    3
000613      129 FORMAT(I7.3(4X  E14.7),F14.7)                         JUNE7    4
000613      158 FORMAT(2E13.5,13X,3E13.5)                             GGEAR   90


000613      160 FORMAT(12H0            7X2HN224X3HRO210X3HRT210X3HRM2)  GGEAR   91
000613      164 FORMAT(//16H CALCULATED DATA)                         GGEAR   92
000613     1000 FORMAT(16H MESH CYCLE NO.=,I3,20H,    CENTER DISTANCE=,E13.6)  MAY14    1
000613     1500 FORMAT(/6X 20(H*3X)/)                                 MAY3     8
000613     2000 FORMAT(5X 3HJC19X4HAJC16X11HTANG. ERPOR)             MAY3     9
000613          STOP                                                 GGEAR   94
000615          END                                                  GGEAR   95
```

```
               SUBROUTINE GEARO(CL,VPT1,VPT2)                             JUN13      1
  000006        COMMON/YY/UJC1(25),UJD1(25),UJ2(25),UJC2(25),UJD2(25),ZJ1(50)  CZIG       3
               1,ZJC1(25),ZJD1(25),ZJ2(50),ZJC2(25),ZJD2(25),QJ1(50),QJC1(25),QJD1  GEARO      4
               2(25),QJ2(50),QJC2(25),            FJ1(50),UJ1(50),     CJC1(2 GEARO      5
               35),CJD1(25),         AJ1(50),AJ2(50),QJC(50),QJD(50),ZJC(50),ZJD(50 GEARO      6
               4),VJ(50),EJ1(56),FJ2(50),AJC1(25),AJC2(25),FJC1(27),QJD2(25),ZM2(  GEARO      7
               550),UM2(50),WTC(27)                                      GEARO      8
  000006       COMMON PJ(50),CJ(50),QJ(50),AJ(50),XJ(50),YJ(50),         GEARO      9
               1A(1500),B(1500),G(3000)                                  MAY11      3
  000006       COMMON DD,BR,BA,FJ,CC,YM,NN,N,FNJ,EP,TAN,RB,GM,F,XM,MN,II,M  ALG        7
  000006       COMMON QA(50),QB(50),QC(50),QA1(50),QB1(50),QC1(50),QA2(50),QB2(50 GEARO     12
               1),QC2(50) ,IH,IP                                         GEARO     13
  000006       COMMON WT(50),HEAD1(6),HEAD2(6)                           GEARO     14
  000006       COMMON/GU/NMC,INT,MMM,IPLT,FN1,FN2,RB1,RO1,RO2,RT1,RT2,RM1,RM2,FI,  ALG        8
               1T1,T2,F1,F2,RF1,RF2,YE1,YE2,GE1,GE2,POS1,POS2,ANG        ALG        9
       C SPECIFY AND INITIALIZE   READING AND WRITING UNITS FOR IBM 1800 GEARO     17
  000006       NR=5                                                      GEARO     18
  000006       NW=6                                                      GEARO     19
  000010   198 CONTINUE                                                  GEARO     20
  000010       RP1=CL*FN1/(FN1+FN2)                                      APR30      1
  000013       IF(MN.EQ.0)RP1=CL*FN1/(FN2-FN1)                          JUNE7      5
  000017       CTT=RB1/RP1                                               GEARO     22
  000021       TTT=SQRT(1.-CTT**2)/CTT                                   GEARO     23
  000026       THETP=ATAN(TTT)                                          JUNE5      1
  000030       THETPP=THETP*180./3.1415927                              JUNE5      2
  000033       WRITE(NW,112)                                            YUNG       1
  000036       WRITE(NW,102) THETPP                                     JUNE5      3
  000044       IF(F1-F2) 320,320,321                                    GEARO     25
  000051   321 FF2=F2                                                    GEARO     26
  000053       GO TO 322                                                 GEARO     27
  000053   320 FF2=F1                                                    GEARO     28
  000055   322 FF2=FF2**0.8                                              GEARO     29
  000061   304 DD1=-T1/2.0/RP1+THETP                                     GEARO     33
  000065       F12=FN1/FN2                                               GEARO     34
  000067       RP2=RP1/F12                                               GEARO     35
  000070       DD2=-T2/2.0/RP2+THETP                                     GEARO     36
  000074       FNJ=2.0*FI+1.0                                            GEARO     37
  000077       N=FNJ                                                     GEARO     38
  000101       NN=N+N                                                    GEARO     39
  000102       CS=CTT                                                    JUNE6      1
  000104       TAN=TTT                                                   JUNE5      4
  000105       EP1=1.0-POS1*POS1                                         GEARO     43
  000107       EP1=YE1/EP1                                               GEARO     44
  000111       EP2=1.0-POS2*POS2                                         GEARO     45
  000114       EP2=YE2/EP2                                               GEARO     46
  000115       EP12=(1.0/EP1+1.0/EP2)*0.5                                GEARO     47
  000121       EP12=EP12**0.9                                            GEARO     48
  000125       RB2=RB1/F12                                               JUNE5      5
  000127       C1=RO1/RB1                                                GEARO     51
  000130       C2=RO2/RB2                                                GEARO     52
  000132       BR2=(SQRT (C2*C2-1.0)-TAN)                                GEARO     53
  000140       BR1=(SQRT (C1*C1-1.0)-TAN)                                GEARO     54
  000146       C3=TAN/F12                                                GEARO     55
  000147       IF(BR1-C3) 403,403,404                                    GEARO     56
```

66

```
000154      404 BR1=C3                                              GEARO   57
000156          WRITE(NW,126)BR1                                    GEARO   58
000163      403 BA1=BR2/F12                                         GEARO   59
000165          BA2=BR1*F12                                         GEARO   60
000166          IF(MN) 440,450,440                                  GEARO   61
000172      450 BA1=-BA1                                            GEARO   62
000173          BA2=-BA2                                            GEARO   63
000175      440 IF(BA1-TAN) 401,401,402                             GEARO   64
000200      402 BA1=TAN                                             GEAFO   65
000202          WRITE(NW,125)BA1                                    GEARU   66
000207      401 C1=6.2831845/FN1                                    GEARO   67
000211          IF(BA1-C1) 213,213,611                              GEARO   68
000216      611 WRITE(NW,174)                                       GEARO   69
000222      213 IF(BR1-C1) 215,612,612                              GEARO   70
000227      612 WRITE(NW,175)                                       GEARO   71
000233      215 C1=RT1/RB1                                          GEARO   72
000235          C2=RT2/RB2                                          GEARO   73
000237          C1 =SQRT (C1*C1-1.0)-TAN                            GEARO   74
000245          AT1=ABS (C1)                                        GEARO   75
000246          C2 =SQRT (C2*C2-1.0)-TAN                            GEARO   76
000255          AT2=ABS (C2)                                        GEARO   77
000257          WRITE(NW,122)                                       GEARO   78
000262          WRITE(NW,102)RP1,RB1,BA1,BR1,AT1                    FINAL    6
000300          WRITE(NW,162)                                       GEARO   80
000304          WRITE(NW,102)RP2,RB2,BA2,BR2,AT2                    GEARO   81
000322          NMZ=1                                               JUN13    2
000323          NUZ=1                                               JUN13    3
000324          IF(AT1-BA1) 311,216,216                             GEARO   84
000331      311 WRITE(NW,176)                                       GEARO   85
000335      216 IF(AT2-BA2) 309,217,217                             GEARO   86
000342      309 IF(MN) 620,621,620                                  GEARO   87
000343      621 WRITE(NW,178)                                       GEARO   88
000347          GO TO 217                                           GEARO   89
000352      620 WRITE(NW,179)                                       GEARO   90
000356      217 IF(RM1-RB1) 191,192,192                             GEARO   91
000363      191 AM1=1.0                                             GEARO   92
000365          WRITE(NW,118)                                       GEARO   93
000370          GO TO 1920                                          GEARO   94
000373      192 AM1=RM1/RB1                                         GEARO   95
000375     1920 C1=AM1                                              GEARO   96
000376          AM1=SQRT (AM1*AM1-1.0)-TAN                          GEARO   97
000404          C2=RF1/RB1                                          GEARO   98
000406          PF1=C2                                              GEARO   99
000407          C1=RM1/RB1                                          GEARO  100
000411          C3=(C1+C2)**2-1.0                                   GEARO  101
000414          IF(C3) 406,406,407                                  GEARO  102
000420      406 C3=0.0                                              GEARO  103
000421          WRITE(NW,156)                                       GEARO  104
000425          TPD1=0.0                                            GEARO  105
000426          WRITE(NW,156)PD1                                    GEARO  106
000434          GO TO 408                                           GEARO  107
000437      407 PD1=SQRT (C3)                                       GEARO  108
000441          TPD1=ATAN (PD1)                                     GEARO  109
000444      408 IF(RM2-RB2) 193,194,194                             GEARO  110
000451      193 AM2=1.0                                             GEARO  111
```

67

```
000453          WRITE(NW,119)                     GEARO   112
000456          GO TO 1940                        GEARO   113
000461      194 AM2=RM2/RB2                       GEARO   114
000463     1940 C1=AM2                            GEARO   115
000464          AM2=SQRT (AM2*AM2-1.0)-TAN        GEARO   116
000472          C2=RF2/RB2                        GEARO   117
000474          PF2=C2                            GEARO   118
000475          C1=RM2/RB2                        GEARO   119
000477          IF(MN) 456,455,456                GEARO   120
000502      455 C2=-C2                            GEARO   121
000503      456 C3=(C1+C2)**2-1.0                 GEARO   122
000506          IF(C3) 409,409,410                GEARO   123
000510      409 C3=0.0                            GEARO   124
000511          WRITE(NW,155)                     GEARO   125
000515          TPD2=0.0                          GEARO   126
000516          WRITE(NW,155)PD2                  GEARO   127
000524          GO TO 411                         GEARO   128
000527      410 PD2=SQRT (C3)                     GEARO   129
000531          TPD2=ATAN (PD2)                   GEARO   130
000534      411 K1=1                              GEARO   131
000535          E1=PF1                            GEARO   132
000536          E2=PD1                            GEARO   133
000540          E3=TPD1                           GEARO   134
000541          E4=RM1                            GEARO   135
000543          DD=DD1                            GEARO   136
000544          C1=AM1                            GEARO   137
000546      201 C2=DD+C1                          GEARO   138
000550          C1=ATAN (TAN+C1)                  GEARO   139
000554          C4=C1-C2                          GEARO   140
000556          C3=E3-E2-DD+TAN                   GEARO   141
000562          IF(K1-1) 422,422,425              GEARO   142
000567      425 IF(MN) 422,421,422                GEARO   143
000570      421 C3=-C3                            GEARO   144
000571          C4=-C4                            GEARO   145
000573      422 C1=C3+E1                          GEARO   146
000575          C4=(C1+C4)*0.5                    GEARO   147
000600          Y=E4*SIN (C4)                     GEARO   148
000602          X=E4*COS (C4)                     GEARO   149
000605          IF(K1-1) 202,202,203              GEARO   150
000612      202 XM1=X                             GEARO   151
000613          YM1=Y                             GEARO   152
000615          K1=K1+1                           GEARO   153
000617          DD=DD2                            GEARO   154
000620          C1=AM2                            GEARO   155
000621          E1=PF2                            GEARO   156
000623          E2=PD2                            GEARO   157
000624          E3=TPD2                           GEARO   158
000626          E4=RM2                            GEARO   159
000630          GO TO 201                         GEARO   160
000630      203 XM2=X                             GEARO   161
000631          YM2=Y                             GEARO   162
000633          EE=6.2831854/FNJ                  GEARO   163
000635          CC=EE/FN1                         GEARO   164
000636          FJ =-FNJ+1.0                      GEARO   165
000640          RB=RB1                            GEARO   166
```

68

```
000641          BR=BR1                                      GEARO    167
000643          BA=BA1                                      GEARO    168
000644          OD=DD1                                      GEARO    169
000646          XM=XM1                                      GEARO    170
000647          YM=YM1                                      GEARO    171
000651          GM=GE1                                      GEARO    172
000652          F=F1                                        GEARO    173
000654          II=1                                        CEARO    174
000655          EP=EP1                                      GEARO    175
000657          WRITE(NW,151)                               GEARO    176
000662          CALL AJCDH                                  GEARO    177
000663          DO 221 I=1,NN                               GEARO    178
000667          C1    =XJ(I)                                GEARO    179
000670          C2    =YJ(I)                                GEARO    180
000672          FJ1(I)=PJ(I)                                GEARO    181
000674          C3=CJ(I)                                    GEARO    182
000675          AJ1(I)=AJ(I)                                GEARO    183
000677          CJ1(I)=QJ(I)                                GEARO    184
000701          IH1=IH                                      GEARO    185
006702          IP1=IP                                      GEARO    186
000704          QA1(I)=QA(I)                                GEARO    137
000706          QB1(I)=QB(I)                                GEARO    188
000710          QC1(I)=QC(I)                                GEARO    189
000712          IF(C3) 515,515,516                          GEARO    190
000714      515 WRITE(NW,102)FJ1(I),C3,AJ1(I)               GEARO    191
000726          GO TO 221                                   GEARO    192
000731      516 WRITE(NW,102)FJ1(I),C3,AJ1(I),QJ1(I),C1,C2  GEARO    193
000751      221 CONTINUE                                    GEARO    194
000756          WRITE(NW,120)XM1,YM1                        GEARO    195
000765          WRITE(NW,161)                               GEARO    196
000771          DO 517 I=IH1,IP1                            GEARO    197
000775      517 WRITE(NW,102)FJ1(I),QA1(I),QB1(I),QC1(I)    GEARO    198
001015          DD=DD2                                      GEARO    199
001016          RB=RR2                                      GEARO    200
001017          XM=XM2                                      GEARO    201
001021          YM=YM2                                      GEARO    202
001022          IF(MN) 302,301,302                          GEARO    203
001024      301 FJ=FNJ                                      GEARO    204
001026          GO TO 310                                   GEARO    205
001026      302 FJ=-FNJ                                     GEARO    206
001030      310 F=F2                                        GEARO    207
001031          EP=EP2                                      GEARO    208
001033          GM=GE2                                      GEARO    209
001034          CC=EE/FN2                                   GEARO    210
001036          II=2                                        GEARO    211
001040          WRITE(NW,152)                               GEARO    212
001043          CALL AJCDH                                  GEARO    213
001044          L=NN                                        GEARO    214
001046          DO 222 I=1,NN                               GEARO    215
001051          C4    =XJ(I)                                GEARO    216
001052          C5    =YJ(I)                                GEARO    217
001054          IH2=IH                                      GEARO    218
001055          IP2=IP                                      GEARO    219
001057          QA2(I)=QA(I)                                GEARO    220
001061          QB2(I)=QB(I)                                GEARO    221
```

69

```
001063          QC2(I)=QC(I)                                GEARO    222
001065          FJ2(I)=PJ(I)                                GEARO    223
001067          C1=AJ(I)                                    GEARO    224
001070          AJ2(L)=C1                                   GEARO    225
001073          C2=QJ(I)                                    GEARO    226
001074          QJ2(L)=C2                                   GEARO    227
001076          IF(C2) 519,518,519                          GEARO    228
001076      518 WRITE(NW,132)FJ2(I),C1                      GEARO    229
001106          GO TO 520                                   GEARO    230
001111      519 WRITE(NW,132)FJ2(I),C1,C2,C4,C5             GEARO    231
001127      520 IF(L-1) 222,222,226                         GEARO    232
001133      226 L=L-1                                       GEARO    233
001135      222 CONTINUE                                    GEARO    234
001140          WRITE(NW,120)XM2,YM2                        GEARO    235
001147          WRITE(NW,163)                               GEARO    236
001153          DO 521 I=IH2,IP2                            GEARO    237
001157      521 WRITE(NW,102)FJ2(I),QA2(I),QB2(I),QC2(I)    GEARO    238
001177          DO 251 I=1,N                                GEARO    239
001200          IN=I+N                                      GEARO    240
001201          FJC1(I)=FJ1(IN)                             GEARO    241
001204          AJC1(I)=AJ1(IN)                             GEARO    242
001206          AJC2(I)=AJ2(IN)                             GEARO    243
001210          QJD1(I)=QJ1(I)                              GEARO    244
001212          QJC1(I)=QJ1(IN)                             GEARO    245
001214          QJC2(I)=QJ2(IN)                             GEARO    246
001216          QJD2(I)=QJ2(I)                              GEARO    247
001220          CJD1(I)=CJ (I)                              GEARO    248
001222      251 CJC1(I)=CJ (IN)                             GEARO    249
001226          MUZ=1                                       GEARO    250
001227          MMZ=1                                       GEARO    251
001230      197 CONTINUE                                    MAY1       1
001230          L=NN                                        GEARO    253
001232          DO 415 I=1,N                                GEARO    254
001233          IN=I+N                                      GEARO    255
001234          UJD1(I)=UJ1(I)                              GEARO    256
001236          UJC1(I)=UJ1(IN)                             GEARO    257
001241          UJC2(I)=UM2(IN)                             GEARO    258
001243          UJD2(I)=UM2(I)                              GEARO    259
001245          ZJD1(I)=ZJ1(I)                              GEARO    260
001247          ZJC1(I)=ZJ1(IN)                             GEARO    261
001251          ZJC2(I)=ZM2(IN)                             GEARO    262
001253          ZJD2(I)=ZM2(I)                              GEARO    263
001255          QJC(I)=QJC1(I)+UJC1(I)+QJC2(I)+UJC2(I)      GEARO    264
001263          QJD(I)=QJD1(I)+UJD1(I)+QJD2(I)+UJD2(I)      GFARO    265
001273      415 ZJC(I)=ZJC1(I)+ZJC2(I)                      GEARO    266
001301      199 CONTINUE                                    GEARO    267
001301          WRITE(NW,106)                               GEARO    268
001305          WRITE(NW,102)VPT1,VPT2                      GEARO    269
001317          VP1=VPT1/CS                                 GEARO    270
001322          VP2=VPT2/CS                                 GEARO    271
001324      418 CONTINUE                                    MAY1       2
001324          WRITE(NW,115)                               GEARO    275
001330          DO 501 I=1,N                                GEARO    276
001334          WT(I)=WT(N+I)                               GEARO    277
001337          WN=WT(I)/CS                                 GEARO    278
```

```
001341          IF(WN)214,214,800                                      GEARO   279
001343      800 CONTINUE                                               GEARO   280
001343          C1=WN**.1                                              MAY1      3
001347          QD=1.37/FF2*EP12/C1                                    MAY1      4
001352          ZJD(I)=ZJD1(I)+ZJD2(I)+VP1-VP2                         GEARO   281
001360          CCC  =QJC(I)+QD                                        GEARO   282
001362          DDD  =QJD(I)+QD                                        GEARO   283
001364          C1=CJC1(I)                                             GEARO   284
001366          C2=CJD1(I)                                             GEARO   285
001367          IF(C1) 256,256,257                                     GEARO   286
001371      256 IF(C2) 501,501,258                                     GEARO   287
001373      257 IF(C2) 259,259,260                                     GEARO   288
001375      259 VJ(I)=ZJC(I)-CCC    *WN                               GEARO   289
001401          WTC(I)=WN*CS                                           GEARO   290
001403          WTD=0.0                                                GEARO   291
001404          GO TO 261                                              GEARO   292
001405      258 VJ(I)=ZJD(I)-DDD    *WN                               GEARO   293
001411          WTC(I)=0.0                                             GEARO   294
001412          WTD=WN*CS                                              GEARO   295
001414          GO TO 261                                              GEARO   296
001415      260 C3=CCC    *WN+ZJD(I)-ZJC(I)                           GEARO   297
001422          C4=DDD    *WN+ZJC(I)-ZJD(I)                           GEARO   298
001426          IF(C3) 259,259,262                                     GEARO   299
001430      262 IF(C4) 258,258,263                                     GEARO   300
001432      263 C1=CCC+DDD                                             GEARO   301
001434          C2=CCC    *ZJD(I)+DDD    *ZJC(I)-CCC*DDD*WN           GEARO   302
001442          VJ(I)=C2/C1                                            GEARO   303
001444          C1=CS/C1                                               GEARO   304
001445          WTC(I)=(DDD*WN+ZJC(I)-ZJD(I))*C1                       GEARO   305
001452          WTD=(CCC*WN+ZJD(I)-ZJC(I))*C1                          GEARO   306
001460      261 EJI(I)=VJ(I)/CS                                        GEARO   307
001463          AJC1(I)=ANG+AJC1(I)                                    GEARO   308
001465          WRITE(NW,102)FJC1(I),AJC1(I),EJI(I),WTC(I),WTD,WN,WT(I),QD   MAY1   5
001511      501 CONTINUE                                               GEARO   310
001516          ANG=AJC1(N)                                            GEARO   311
001517       24 IF(NUZ-MUZ) 504,504,502                               GEARO   312
001522      502 MUZ=MUZ+1                                              GEARO   313
001524          GO TO 199                                              GEARO   314
001524      504 MUZ=1                                                  GEARO   315
001525          IF(NMZ-MMZ) 214,214,506                               GEARO   316
001530      506 MMZ=MMZ+1                                              GEARO   317
001532          GO TO 197                                              GEARO   318
001532      214 CONTINUE                                               GEARO   319
001532      503 RETURN                                                 GEARO   320
001533      102 FORMAT(8E13.5)                                         MAY1      6
001533      106 FORMAT(//34H INPUT DATA ON TOOTH SPACING ERROR/6X4HVPT19X4HVPT2)   GEARO   322
001533      110 FORMAT(60H0INPUT LISTING OF PROFILE ERROR AND SUPPLEMENTARY COMPLI  GE-NO   323
                 1ANCE/6X2HZ111X2HU111X2HZ211X2HU2)                    GEARO   324
001533      112 FORMAT(16H0PRES.ANGLE(DEG))                            FINAL     7
001533      115 FORMAT(42H0CALCULATED TOOTH MESHING ERRORS AND LOADS//6X3HJC19X4HA  GEARO   325
                 1JC16X11HTANG. ERROR6X3HWTC10X3HWTD11X2HWN11X2HWT10X3HQJD)   MAY1   7
001533      118 FORMAT(74H0DRIVING GEAR INPUT ROOT RADIUS SMALLER THAN BASE CIRCLE  GEARO   327
                 1 RADIUS                    )                         GEARO   328
001533      119 FORMAT(74H0DRIVEN  GEAR INPUT ROOT RADIUS SMALLER THAN BASE CIRCLE  GEARO   329
                 1 RADIUS                    )                         GEARO   330
```

71

```
001533      120 FORMAT(48H0COOD. OF EFFECTIVE TOOTH PROFILE AT ROOT CIRCLE11X1HX13 GEARO    331
                1X1HY/52X,2E13.6)                                                  GEARO    332
001533      122 FORMAT(/6X3HRP110X3HRB110X3HBA110X3HBR110X3HAT1)                    ALG       10
001533      125 FORMAT(66H0 DRIVEN GEAR TEETH ENGAGE UNDER CUT PORTION OF DRIVING   GEARO    334
                1GEAR TEETH//6H  BA1=,  E13.6)                                      GEARO    335
001533    . 126 FORMAT(66H0 DRIVING GEAR TEETH ENGAGE UNDER CUT PORTION OF DRIVEN   GEARO    336
                1GEAR TEETH//6H  BR1=,  E13.6)                                      GEARO    337
001533      132 FORMAT(  E13.5,13X,4E13.5)                                          GEARO    338
001533      151 FORMAT(/6X2HJ111X3HCJ110X3HAJ18X6HQJ1ABC9X3HXJ110X3HYJ1)           GEARO    339
001533      152 FORMAT(/6X2HJ224X3HAJ28X6HQJ2ABC9X3HXJ210X3HYJ2)                   GEARO    340
001533      155 FORMAT(63H0DRIVEN  GEAR INPUT RADIUS TO FILLET CENTER INSIDE BASE   GEARO    341
                1CIRCLE./42H0PROGRAM CONTINUES WITH CORRECT TREATMENT.)             GEARO    342
001533      156 FORMAT(63H0DRIVING GEAR INPUT RADIUS TO FILLET CENTER INSIDE BASE   GEARO    343
                1CIRCLE./42H0PROGRAM CONTINUES WITH CORRECT TREATMENT.)             GEARO    344
001533      159 FORMAT(13X,4E13.5)                                                 GEARO    345
001533      161 FORMAT(/6X2HJ110X4HQJ1A9X4HQJ1B9X4HQJ1C)                           GEARO    346
001533      162 FORMAT(/6X3HRP210X3HRB210X3HBA210X3HBR210X3HAT2)                   GEARO    347
001533      163 FORMAT(/6X2HJ210X4HQJ2A9X4HQJ2B9X4HQJ2C)                           GEARO    348
001533      170 FORMAT(43H0CALCULATED TOTAL CONTACT COMPLIANCE  QJD=,E13.6)         GEARO    349
001533      171 FORMAT(23H0CALCULATED NORMAL  WN=,  E13.6)                          GEARO    350
001533      174 FORMAT(80H0 ANGLE OF APPROACH ON DRIVING GEAR IS GREATER THAN TOOT  GEARO    351
                1H SPACING ANGLE. PROGRAM/25HCONTINUED WITHOUT OVERLAP)             GEARO    352
001533      175 FORMAT(75H0 ANGLE OF RECESS ON DRIVING GEAR IS NOT SMALLER THAN TO  GEARO    353
                1OTH SPACING ANGLE. /34H PROGRAM CONTINUED WITHOUT OVERLAP)         GEARO    354
001533      176 FORMAT(80H0 DRIVING GEAR TEETH MESHING ON PROFILE INSIDE OF TIF DI  GEARO    355
                1AMETER. PROGRAM CONTINU-/21HED WITHOUT CORRECTION)                 GEARO    356
001533      178 FORMAT(80H0 DRIVEN  GEAR TEETH MESHING ON PROFILE OUTSIDE OF TIF D  GEARO    357
                1IAMETER. PROGRAM CONTIN-/22HUED WITHOUT CORRECTION)                GEARO    358
001533      179 FORMAT(80H0 DRIVEN  GEAR TEETH MESHING ON PROFILE INSIDE OF TIF DI  GEARO    359
                1AMETER. PROGRAM CONTINU-/21HED WITHOUT CORRECTION)                 GEARO    360
001533          END                                                                GEARO    361
```

```
                 SUBROUTINE AJCDH                                          AJCDH      2
000002           DIMENSION SD(50),CD(50),BIK(50),AIK(50),FLK(50) ,CDC(50)  AJCDH      3
000002           COMMON PJ(50),CJ(50),QJ(50),AJ(50),XJ(50),YJ(50),         MAY11      4
                1A(1500),B(1500),G(3000)                                   MAY11      5
000002           COMMON DD,BR,BA,FJ,CC,YM,NN,N,FNJ,EP,TAN,RB,GM,F,XM,MN,II, AJCDH      5
000002           COMMON QA(50),QB(50),QC(50),QA1(50),QB1(50),QC1(50),QA2(5  QB2(50 AJCDH  6
                1),QC2(50),IM,IP                                           AJCDH      7
000003           DO 106 I=1,NN                                             AJCDH      8
000004           QA(I)=0.0                                                 AJCDH      9
000005           QB(I)=0.0                                                 AJCDH     10
000006           QC(I)=0.0                                                 AJCDH     11
000007           QJ(I)=0.0                                                 AJCDH     12
000010           XJ(I)=0.0                                                 AJCDH     13
000011       106 YJ(I)=0.0                                                 AJCDH     14
000014           IF(II-1) 405,405,403                                      AJCDH     15
000017       405 MM=1.0                                                    AJCDH     16
000021           GO TO 404                                                 AJCDH     17
000022       403 MM=MN                                                     AJCDH     18
000024       404 K=1                                                       AJCDH     19
000025           DO 501 I=1,NN                                             AJCDH     20
000027           AJ(I)=FJ*CC                                               AJCDH     21
000031           PJ(I)=FJ                                                  AJCDH     22
000032           IF(II-1) 412,412,413                                      AJCDH     23
000035       412 CALL CALCJ(AJ(I),BR,BA,XY)                                AJCDH     24
000042           CJ(I)=XY                                                  AJCDH     25
000044           GO TO 414                                                 AJCDH     26
000045       413 XY=CDC(I)                                                 AJCDH     27
000047       414 IF(XY) 503,503,101                                        AJCDH     28
000051       101 IF(K-1) 102,102,103                                       AJCDH     29
000054       102 IM=I                                                      AJCDH     30
000056       103 AX=AJ(I)                                                  AJCDH     31
000060           DJ=DD*AX                                                  AJCDH     32
000062           SD(I)=SIN (DJ)                                            AJCDH     33
000066           CD(I)=COS (DJ)                                            AJCDH     34
000072           C1=ATAN (TAN*AX)                                          AJCDH     35
000076           C3=COS (C1)                                               AJCDH     36
000100           C4=C1-DJ                                                  AJCDH     37
000102           IF(MM) 402,401,402                                        AJCDH     38
000104       401 C4=-C4                                                    AJCDH     39
000105       402 C5=SIN (C4)                                               AJCDH     40
000107           C6=COS (C4)                                               AJCDH     41
000111           C1=RB/C3                                                  AJCDH     42
000113           XJ(I)=C1*C6                                               AJCDH     43
000116           YJ(I)=C1*C5                                               AJCDH     44
000120           IF(K-1) 242,242,243                                       AJCDH     45
000122       242 BIK(I)=(YJ(I)**3-YM**3)/3.0*F                             AJCDH     46
000130           AIK(I)=(YJ(I)+YM)*F                                       AJCDH     47
000133           FLK(I)=XJ(I)-XM                                           AJCDH     48
000136           GO TO 504                                                 AJCDH     49
000136       243 BIK(I)=(YJ(I)**3-YJ(I-1)**3)/3.0*F                        AJCDH     50
000144           AIK(I)=(YJ(I)+YJ(I-1))*F                                  AJCDH     51
000147           FLK(I)=XJ(I)-XJ(I-1)                                      AJCDH     52
000152       504 K=K+1                                                     AJCDH     53
000154       503 IF(I-NN) 502,501,501                                      AJCDH     54
```

73

```
000157      502 IF(MM) 506,505,506                    AJCDH    55
000160      505 FJ=FJ-1.                              AJCDH    56
000162          GO TO 501                             AJCDH    57
000163      506 FJ=FJ+1.0                             AJCDH    58
000165      501 CONTINUE                              AJCDH    59
000170          IF(II-1) 301,301,302                  AJCDH    60
000172      301 IF(MM) 601,302,601                    AJCDH    61
000173      601 LL=NN                                 AJCDH    62
000175          DO 303 I=1,NN                         AJCDH    63
000176          COC(I)=CJ(LL)                         AJCDH    64
000200          IF(LL-1) 303,303,305                  AJCDH    65
000203      305 LL=LL-1                               AJCDH    66
000205      303 CONTINUE                              AJCDH    67
000210      302 IP=K+IH-2                             AJCDH    68
000213      410 DO 246 L=IH,IP                        AJCDH    69
000215          E1=0.0                                AJCDH    70
000216          E2=0.0                                AJCDH    71
000216          E3=0.0                                AJCDH    72
000217          E4=0.0                                AJCDH    73
000220          EE=XJ(L)-XM                           AJCDH    74
000223          IM=L                                  AJCDH    75
000223          IF(MM) 202,203,202                    AJCDH    76
000225      203 EE=-EE                                AJCDH    77
000226      202 DO 245 I=IM,IM                        AJCDH    78
000230          C1      =XJ(L)-XJ(I)                  AJCDH    79
000233          C5=FLK(I)                             AJCDH    80
000234          IF(MM) 207,208,207                    AJCDH    81
000236      208 C1=-C1                                AJCDH    82
000237          C5=-C5                                AJCDH    83
000241      207 C2=C5/BIK(I)                          AJCDH    84
000243          C3=(C5+3.0*C1)*C5+3.0*C1*C1           AJCDH    85
000251          E4=E4+C2                              AJCDH    86
000253          C4=2.0*C1+C5                          AJCDH    87
000255          E1=E1+C3*C2                           AJCDH    88
000260          E2=E2+C4*C2                           AJCDH    89
000263      245 E3=E3+C5/AIK(I)                       AJCDH    90
000271          IF(MM) 206,205,206                    AJCDH    91
000272      205 IM=IM-1                               AJCDH    92
000274      206 C1=CD(L)*CD(L)                        AJCDH    93
000276          C2=SD(L)*YJ(L)                        AJCDH    94
000300          QA(L) =C1/3.0*E1/EP+(C2*E4-CD(L)*E2)/EP*C2   AJCDH    95
000312          QB(L) =C1/GM*E3*1.2                   AJCDH    96
000317          C1=(EE*CD(L)-YJ(L)*SD(L))/YM          AJCDH    97
000323          QC(L)=C1/EP*1.327/F*C1                AJCDH    98
000330      246 QJ(L)=QA(L)+QB(L)+QC(L)               AJCDH    99
000336          RETURN                                AJCDH    100
000337          END                                   AJCDH    101
```

74

```
          SUBROUTINE FOUR                                         FOUR      2
       C  REQUIRES 2*N+1 POINTS  F(I)                             FOUR      3
       C  POINTS CORRESPOND TO THETA=2*PI/(2*N+1),....,2*PI       FOUR      4
       C  OUTPUT  A(I),B(I)   REFER TO COSINE AND SINE OF (I-1)*THETA  FOUR  5
000002    COMMON PJ(50),CJ(50),QJ(50),AJ(50),XJ(50),YJ(50),      FOUR      6
          1A(1500),B(1500),G(3000)                               MAY11     6
000002    COMMON DD,BR,BA,FJ,CC,YM,NN,N,FNJ,EP,TAN,RB,GM,F,XM,MN,II,M  FOUR   8
000002    COMMON/GU/NMC,INT,MMM,IPLT,FN1,FN2,RB1,RO1,RO2,RT1,RT2,RM1,RM2,FI,  MAY9  8
          1T1,T2,F1,F2,RF1,RF2,YE1,YE2,GE1,GE2,POS1,POS2,ANU     MAY9      9
000002    C=1.0                                                  FOUR      9
000003    S=0.0                                                  FOUR     10
000004    M=IFIX(FI)*NMC+NMC/2                                   MAY9     10
000010    N1=M+1                                                 FOUR     11
000012    NA=N*NMC                                               MAY9     11
000014    N2=NA-1                                                MAY9     12
000015    T1=2./NA                                               MAY9     13
000020    T2=T1*3.1415927                                        FOUR     15
000021    C1=COS (T2)                                            FOUR     16
000023    S1=SIN (T2)                                            FOUR     17
000026    DO 7 IP=1,N1                                           FOUR     18
000027    U1=0.0                                                 FOUR     19
000030    U2=0.0                                                 FOUR     20
000031    DO 3 I=1,N2                                            FOUR     21
000032    J=N2-I+2                                               FOUR     22
000034    U3=G(J)+2.0*C*U1-U2                                    FOUR     23
000042    U2=U1                                                  FOUR     24
000043  3 U1=U3                                                  FOUR     25
000047    A(IP)=T1*(G(1)+C*U1-U2)                                FOUR     26
000054    B(IP)=T1*S*U1                                          FOUR     27
000056    AA=A(IP)*C-B(IP)*S                                     FOUR     28
000062    BB=A(IP)*S+B(IP)*C                                     FOUR     29
000065    A(IP)=AA                                               FOUR     30
000067    B(IP)=BB                                               FOUR     31
000071    Q=C1*C-S1*S                                            FOUR     32
000074    S=C1*S+S1*C                                            FOUR     33
000077  7 C=Q                                                    FOUR     34
000103    RETURN                                                 FOUR     35
000103    END                                                    FOUR     36


          SUBROUTINE CALCJ(C1,C2,C3,C4)                          CALCJ     2
000007    IF(C3) 240,231,241                                     CALCJ     3
000011    DATA EHEAD3/4H LB./                                    CALCJ     4
000011 241 IF(C1) 230,218,218                                    CALCJ     5
000013 230 IF(ABS (C1)-C3) 220,220,219                           CALCJ     6
000017 231 IF(C1) 219,218,218                                    CALCJ     7
000021 240 IF(C1) 219,219,242                                    CALCJ     8
000023 242 C3=-C3                                                CALCJ     9
000024    IF(C1-C3) 219,218,218                                  CALCJ    10
000026 218 IF(C2-C1) 219,220,220                                 CALCJ    11
000030 220 C4=1.0                                                CALCJ    12
000031    GO TO 221                                              CALCJ    13
000032 219 C4=0.0                                                CALCJ    14
000033 221 RETURN                                                CALCJ    15
000034    END                                                    CALOJ    16
```

75

```
              SUBROUTINE PLT(X,Y,Z,NPTS)                                    PLT      2
000007        DIMENSION Y(3000),X(3000),Z(3000),AXX(4),AYY(4),AZZ(4),ILABX(5),  MAY11    7
        1            ILABY(5),HEAD3(3)                                      PLT      4
000007        COMMON PJ(50),CJ(50),QJ(50),AJ(50),XJ(50),YJ(50),            MAY11    8
        1A(1500),B(1500),G(3000)                                           MAY11    9
000007        COMMON DD,BR,BA,FJ,CC,YM,NN,N,FNJ,EP,TAN,RB,GM,F,XM,MN,II,M   PLT      6
000007        COMMON QA(50),QB(50),QC(50),QA1(50),QB1(50),QC1(50),QA2(50),QB2(50  PLT      7
        1),QC2(50),IH,IP                                                   PLT      8
000007        COMMON WT(50),HEAD1(6),HEAD2(6)                              MAY1     11
000007        DATA (ILABX(J),J=1,3)/10H    CALCUL,10HATION POIN,2HT /       PLT     10
000007        DATA (ILABY(J),J=1,3)/10HTANGENTIAL,10H ERROR (IN,2H.)/       PLT     11
000007        DATA ILABZ/10HLOAD (LB.)/                                     PLT     12
000007        DATA (HEAD3(I),I=1,2)/10HTANG. FORC,4HE = /                   PLT     13
000007        IN=5                                                          PLT     14
000007        IO=6                                                          PLT     15
000010        ICAL=22                                                       PLT     16
000012        CALL PLOTS(IBUF,4000,ICAL)                                    PLT     17
000014        CALL PLOT(4.,4.5,-3)                                          PLT     18
000017        CALL PLOT(-2.,-4.,3)                                          PLT     19
000022        CALL DASHPT(-2.,6.,.25)                                       PLT     20
000025        CALL SCALE(X,5.,NPTS,+1)                                      PLT     21
000032        Y(NPTS+1)=0.                                                  PLT     22
000036        DO 10 K=1,NPTS                                                PLT     23
000040     10 Y(K)=-Y(K)                                                    PLT     24
000043        CALL SCALE(Y,4.,NPTS+1,+1)                                    PLT     25
000050        Y(NPTS+2)=Y(NPTS+3)                                           PLT     26
000056        CALL SCALE(Z,3.,NPTS,+1)                                      PLT     27
000061        AXX(1)=X(NPTS+1)                                              PLT     28
000065        AXX(2)=X(NPTS+2)                                              PLT     29
000067        AYY(1)=Y(NPTS+1)                                              PLT     30
000071        AYY(2)=Y(NPTS+2)                                              PLT     31
000073        AZZ(1)=Z(NPTS+1)                                              PLT     32
000074        AZZ(2)=Z(NPTS+2)                                              PLT     33
000077        CALL AXIS(0.,0.,ILABX,-22,5.,0.,AXX(1),AXX(2))               PLT     34
000106        CALL AXIS(0.,0.,ILABY,22,4.,90.,0.,AYY(2))                   PLT     35
000116        CALL FLINE(X,Y,-NPTS,1,1,3)                                   PLT     36
000125        CALL PLOT(0.,-4.,-3)                                          PLT     37
000130        CALL AXIS(0.,0.,ILABX,-22, 5.,0.,AXX(1),AXX(2))              PLT     38
000140        CALL AXIS(0.,0.,ILABZ,10,3.,90.,AZZ(1),AZZ(2))               PLT     39
000150        CALL FLINE(X,Z,-NPTS,1,1,11)                                  PLT     40
000157        CALL PLOT(.5,9.5,-3)                                          PLT     41
000162        CALL SYMBOL(0.,0.,.14,HEAD1,0.,40)                           PLT     42
000166        CALL SYMBOL(0.,-.25,.14,HEAD2,0.,40)                         PLT     43
000172        CALL SYMBOL(0.,-.5,.14,HEAD3,0.,14)                          PLT     44
000176        CALL NUMBER(999.,999.,.14,WT,0.,2)                           PLT     45
000202        CALL SYMBOL(999.,999.,.14,EHEAD3,0.,4)                       PLT     46
000206        CALL PLOT(6.,-9.,-3)                                          PLT     47
000211        CALL DASHPT(0.,9.,.25)                                        PLT     48
000214        CALL PLOT(0.,0.,999)                                          PLT     49
000217        DO 20 K=1,NPTS                                                PLT     50
000223     20 Y(K)=-Y(K)                                                    PLT     51
000226        RETURN                                                        PLT     52
000227        END                                                          PLT     53
```

76

```
                    SUBROUTINE SPECT                                              MAY9    14
                    DIMENSION GN(3000),RR(3000),FR(200),GK(200),KK(200),GKK(200)  MAY11   10
 .000002            COMMON PJ(50),CJ(50),QJ(50),AJ(50),XJ(50),YJ(50),             MAY11   11
 000002            1A(1500),B(1500),G(3000)                                        MAY11   12
                    COMMON DD,BR,BA,FJ,CC,YM,NN,N,FNJ,EP,TAN,RB,GM,F,XM,MN,II,M    GEARC    1
 000002             COMMON/GU/NMC,INT,MMM,IPLT,FN1,FN2,RA1,RO1,RO2,KT1,RT2,RM1,RM2,FI,  MAY11  14
 000002            1T1,T2,F1,F2,RF1,RF2,YE1,YE2,GE1,GE2,POS1,POS2,ANG             MAY11   15
                                                                                  MAY11   16
 000002             NR=5                                                          MAY11   17
 000003             NW=6                                                          MAY11   18
                  C NWS=1,WS=SPEED OF DRIVING GEAR IN RPM                         MAY11   19
                  C NWS=2,WS=SPEED OF DRIVEN GEAR IN RPM                          MAY11   20
 000004             READ(NR,100) NWS,WS                                           MAY11   21
 000014             WS=WS*6.28/60.                                                MAY11   22
 000016             FM=FN1*WS/6.28                                                MAY11   23
 000020             IF(NWS.EQ.2) FM=FN2*WS/6.28                                   MAY11   24
 000024             WRITE(NW,110) FM                                              MAY11   25
 000032             FC=FM*N/2.                                                    MAY11   26
 000035             NT=N*NMC                                                      MAY11   27
 000037             TR=NMC/FM                                                     MAY11   28
 000041             H=1./FM/N                                                     MAY11   29
 000044.            FO=1./TR                                                      MAY11   30
 000046             M=NT/20                                                       MAY11   31
 000051             SM=M                                                          MAY11   32
 000052             TMAX=M*H                                                      MAY11   33
 000055             BE=1./TMAX                                                    MAY11   34
 000057             WRITE(NW,115)                                                 MAY11   35
 000062             WRITE(NW,120) FC,FO,BE                                        MAY11   36
 000074             WRITE(NW,125)                                                 MAY11   37
 000100             WRITE(NW,120) H,TR,TMAX,SM                                    MAY11   38
 000114             SUM=0.                                                        MAY11   39
 000115             DO 10 I=1,NT                                                  MAY11   40
 000117          10 SUM=SUM+G(I)                                                  MAY11   41
 000123             SA=SUM/NT                                                     MAY11   42
 000125             DO 20 I=1,NT                                                  MAY11   43
 000127             GN(I)=G(I)-SA                                                 MAY11   44
 000132          20 CONTINUE                                                      MAY11   45
 000134             MM=M+1                                                        MAY11   46
 000136             DO 30 I=1,MM                                                  MAY11   47
 000137             IR=I-1                                                        MAY11   48
 000140             FR(I)=IR*FC/SM                                                MAY11   49
 000144             CC=1./(NT-IR)                                                 MAY11   50
 000147             RR(I)=0.                                                      MAY11   51
 000151             DO 25 J=1,NY                                                  MAY11   52
                  C RR(I)=R(I-1)                                                  MAY11   53
                    IF((J+IR).GT.NT) GO TO 30                                     MAY11   54
 000153          25 RR(I)=GN(J)*GN(J+IR)+RR(I)                                    MAY11   55
 000157          30 RR(I)=RR(I)*CC                                                MAY11   56
 000165             MS=M-1                                                        MAY11   57
 000172             DO 40 K=1,MM                                                  MAY11   58
 000174             KK(K)=K-1                                                     MAY11   59
 000175             GK(K)=RR(1)+RR(MM)*(-1.)**KK(K)                               MAY11   60
 000177             SSS=0.                                                        MAY14    2
 000206             DO 35 JK=1,MS                                                 MAY14    3
 000207             JJ=JK+1
 000211
```

77

```
000212          AA=3.1416*JK*KK(K)/SM                                    MAY11    62
000217       35 SSS=SSS+2.*RR(JJ)*COS(AA)                               MAY11    63
000230       40 GK(K)=(GK(K)+SSS)*2.*M                                  MAY11    64
000236          GKK(1)=.5*GK(1)+.5*GK(2)                                MAY11    65
000241          GKK(MM)=.5*GK(M)+.5*GK(MM)                              MAY11    66
000246          DO 50 LL=2,M                                            MAY11    67
000247          GKK(LL)=.25*GK(LL-1)+.5*GK(LL)+.25*GK(LL+1)             MAY11    68
000255       50 CONTINUE                                                MAY11    69
000260          WRITE(NW,130)                                           MAY11    70
000264          WRITE(NW,140)                                           MAY11    71
000270          DO 60 I=1,MM                                            MAY11    72
000272          SKM=KK(I)*N/(2.*SM)                                     JUNE7     6
000277          WRITE(NW,150)KK(I),FR(I),GK(I),GKK(I),SKM               JUNE7     7
000314       60 CONTINUE                                                MAY11    74
000317      100 FORMAT(I5,E13.5)                                        MAY11    75
000317      110 FORMAT(/1X26HMESHING FREQUENCY IN CPS =,E13.5)          MAY11    76
000317      115 FORMAT(/7X2HFC11X2HF011X2HBE)                           MAY11    77
000317      120 FORMAT(8E13.5)                                          MAY11    78
000317      125 FORMAT(/7X1HH12X2HTR11X4HTMAX9X2HSM)                    MAY11    79
000317      130 FORMAT(/1X31HPOWER SPECTRAL DENSITY FUNCTION)           MAY11    80
000317      140 FORMAT(/6X,1HK6X2HFR11X2HGK11X3HGKK10X2HKM)             JUNE7     8
000317      150 FORMAT(I7,3E13.5,F13.5)                                 JUNE7     9
000317          RETURN                                                  MAY11    83
000317          END                                                     MAY11    84
```